

AD-A249 872



ITATION PAGE

Form Approved

OMB No 0704-0188

ed to average 1 hour per response, including the time for reviewing instructions, searching existing data sources, reviewing the collection of information. Send comments regarding this burden estimate or any other aspect of this collection of information, including suggestions for reducing this burden, to Washington Headquarters Services, Directorate for Information Operations and Reports, 1215 Jefferson Davis Highway, Suite 1204, Arlington, VA 22202-4302, and to the Office of Management and Budget, Paperwork Reduction Project (0704-0188), Washington, DC 20503.

| | | | | |
|---|--|---|---|--|
| 1. AGENCY USE ONLY (Leave blank) | | 2. REPORT DATE | 3. REPORT TYPE AND DATES COVERED THESIS/DISSERTATION | |
| 4. TITLE AND SUBTITLE Impulsive Magnetic Perturbations of the High Latitude, Dayside Ionosphere | | | 5. FUNDING NUMBERS | |
| 6. AUTHOR(S) Michael D. Krajnak, Captain | | | | |
| 7. PERFORMING ORGANIZATION NAME(S) AND ADDRESS(ES) AFIT Student Attending: University of California | | | 8. PERFORMING ORGANIZATION REPORT NUMBER AFIT/CI/CIA- 91-110 | |
| 9. SPONSORING/MONITORING AGENCY NAME(S) AND ADDRESS(ES) AFIT/CI Wright-Patterson AFB OH 45433-6583 | | | 10. SPONSORING/MONITORING AGENCY REPORT NUMBER | |
| 11. SUPPLEMENTARY NOTES | | | | |
| 12a. DISTRIBUTION/AVAILABILITY STATEMENT Approved for Public Release IAW 190-1 Distributed Unlimited ERNEST A. HAYGOOD, Captain, USAF Executive Officer | | | 12b. DISTRIBUTION CODE | |
| 13. ABSTRACT (Maximum 200 words) <div data-bbox="295 1379 768 1633" data-label="Text"><p>DISTRIBUTION STATEMENT A Approved for public release; Distribution Unlimited</p></div> <div data-bbox="1020 1352 1410 1661" data-label="Text"><p>DTIC ELECTE MAY 11 1992 S B D</p></div> | | | | |
| 14. SUBJECT TERMS | | | 15. NUMBER OF PAGES 92 | |
| | | | 16. PRICE CODE | |
| 17. SECURITY CLASSIFICATION OF REPORT | 18. SECURITY CLASSIFICATION OF THIS PAGE | 19. SECURITY CLASSIFICATION OF ABSTRACT | 20. LIMITATION OF ABSTRACT | |

UNIVERSITY OF CALIFORNIA

Los Angeles

**Impulsive Magnetic Perturbations
of the High Latitude, Dayside Ionosphere**

**A thesis submitted in partial satisfaction of the
requirements for the degree Master of Science
in Geophysics and Space Physics**

by

Michael Dismas Krajnak

1991

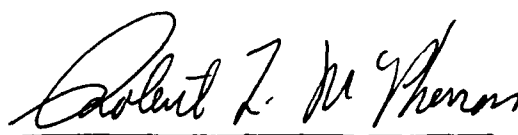
92 5 01 033

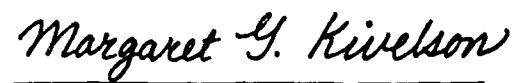
92-11937



The thesis of Michael Dismas Krajnak is approved.


Paul J. Coleman

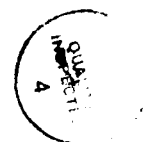

Robert L. McPherron


Margret G. Kivelson, Committee Chair

| | |
|--------------------|--|
| Accession For | |
| NTIS GRA&I | <input checked="checked" type="checkbox"/> |
| DTIC TAB | <input type="checkbox"/> |
| Unannounced | <input type="checkbox"/> |
| Justification | |
| By | |
| Distribution/ | |
| Availability Codes | |
| Dist | Avail and/or Special |
| A-1 | |

University of California, Los Angeles

1991



Dedication

To Mary, my wife, and the kids, Jonathon, Mary Karen, and Bryan. They have enriched my life far more then any program of academic study could.

Contents

| | |
|------------------------|----|
| List of Figures | v |
| List of Tables | ix |
| Acknowledgments | x |
| Abstract of the Thesis | xi |

| | |
|------------------------------|-------------|
| <u>Chapter</u> | <u>Page</u> |
| 1. Introduction | 1 |
| 2. Basic Theory and Concepts | 10 |
| 3. Observations | 29 |
| 4. Analysis | 49 |
| 5. Discussion | 75 |
| 6. Conclusions | 84 |
| Bibliography | 87 |

List of Figures

| <u>Figure</u> | <u>Page</u> |
|---|-------------|
| 1-1 The ionospheric equivalent current vectors as plotted by Friis-Christensen (1988a) showing the vortex structures associated with the field-aligned currents. | 7 |
| 2-1 Wave polarizations for the intermediate (Alfven) and fast modes in a uniform cold plasma. | 11 |
| 2-2 A Russell-Elphic FTE showing a flux tube in the magnetosphere connected through the magnetopause to the IMF. | 13 |
| 2-3 The closure currents (Pedersen) and ionospheric plasma convection for a pair of field-aligned currents in the northern hemisphere. | 15 |
| 2-4 A schematic of the field-aligned currents generated at the magnetopause by a sudden compression according to the Glaßmeier-Heppner model. | 17 |
| 2-5 The perturbations of the H, D, and V components of the magnetic field in the HD (horizontal) plane due to an ionospheric Hall current loop plotted by Lanzerotti et al. (1986). | 19 |
| 2-6 A schematic of a coaxial type Saunders-Lee FTE which closes in the ionosphere with a Pedersen current with return currents in a cylindrical shell around the central current. | 21 |
| 2-7 A schematic diagram of the compressed magnetosphere showing the form and locations of the transition regions. | 22 |
| 2-8 The field-aligned currents and the sense of the ionospheric plasma convection associated with the various. Closure currents are not shown. Where pertinent the direction of travel has been shown with an arrow pointing up indicating poleward and right, tailward. | 25 |
| 2-9 The global distribution of FACs predicted by the various models. For simplicity we do not show the return currents of the Saunders-Lee FTE systems since the exact nature of these currents is less well understood and since in any case it is the central primary current which is expected to generate the ground signature. | 26 |

- 3-1 The locations of the satellites used in this study in the GSM XY plane. 32
- 3-2 A time series plot of eight hours of data of the GSM components of the IMF and the total field measured at IMP-8. Minor tic marks on the time axis are every 5 minutes, major tics are every two hours and labeled under the last time axis. 33
- 3-3 The plasma parameters, number density, bulk velocity, dynamic, and total (dynamic plus thermal) pressure for the same eight hour time interval as figure 3-2. 34
- 3-4 One hour of magnetic field data from SCATHA showing the total field and the components in HDV coordinates. Time tics are every minute with major tic marks (and labels) every 15 minutes. 35
- 3-5 Magnetic field data from GOES-5 presented in the same format as figure 3-4. 38
- 3-6 Magnetic field data from AMPTE/CCE covering the same time period as GOES-5 and SCATHA, but presented in GSM coordinates. 39
- 3-7 A comparison of the increase in the total magnetic field seen by SCATHA, GOES-5, and AMPTE/CCE. The baselines have been adjusted to allow the relative heights of the increases to be compared. 40
- 3-8a,b,c Stack plots of the filtered X, Y, and Z magnetic field components for one hour worth of ground data presented in the same format as the space measurements. The vertical scale for each plot ranges from -50.0 to 100.0 nT. The northernmost station is plotted at the top (SOR) and lower stations are farther south, with PEL being the furthest south. 42-44
- 3-9 A plot of the filtered H, D, and Z components of the magnetic field at Rovaiemi, just south of the EISCAT magnetometer cross. 45
- 3-10 The HDZ magnetic field components for the one hour interval around the event for the two conjugate stations Iqaluit (IQA, top panel) and South Pole (SPA). 46
- 3-11 The AE index presented of the same time interval (1000-1800 UT) as the IMP-8 data. 48
- 4-1 Power spectra for the magnetic field HDZ components and the total field taken at Ivalo for the one hour interval (1200-1300 UT) with the event (3600 data points) on a log-log plot. The bottom scales covers 0.5 to 50.0 milliHertz and the vertical scale shows

the power (nT^2) from 1 to 10^6

50

4-2 Power spectra for the IMF measurements taken from IMP-8. Here the GSM components of the magnetic field are used and plotted over a slightly different range than the previous plot, 0.5 to 100 mHz on the horizontal scale and 0.1 to 10^3 nT^2

52

4-3 A comparison of the dynamic pressure at IMP-8 with the increase in the magnetic field measured at SCATHA. The vertical scales have been adjusted so that the amplitude of the main increase is about the same. Both traces are plotted on the same time scale with one minute tick marks. It is easy to see that the two occur much more closely together than the seven minutes required to travel from IMP-8 to SCATHA at the solar wind velocity.

54

4-4 A comparison of the changes in the total magnetic field measured at SCATHA and a conjugate ground station (Narsarsuaq, NAQ). The data is unfiltered. This plot shows the delay between the satellite and ground station. The vertical scale is the same for both traces, but the data has been offset to allow the comparison.

55

4-5 This figure illustrates the connection between the solar wind dynamic pressure and the ground magnetic perturbations. The same eight hours presented in the earlier IMP-figures are covered here. The top panel shows the dynamic pressure observed at IMP-8 the next two panels show the filtered horizontal (X and Y) components of the magnetic field at Thule (THL) and the bottom panel shows the magnitude of the horizontal perturbation.

57

4-6 This figure is a contour plot of the magnitude of the horizontal ground magnetic perturbation over the northern hemisphere in geomagnetic coordinates at 1210 UT. The asterisks mark the locations of the stations used to compile this data. The dashed circles are the 60° and 75° magnetic latitudes. The vertical line is the magnetic meridian which passes through the earth-sun line. The sunward side is on the top and dawn to the right. Contour labels are in nT. Magnetic activity before the event can be seen in the tail although the fourth and final onset has not occurred yet.

58

4-7a..g These figures show a series of contour plots structured like figure 4-6 covering the time of the event (the event maximum at EISCAT occurred at 12:35, figure 4-7e). For clarity in some cases the highest contours in the night side have been cut off. At all times the substorm effects seem to be confined to the nightside hemisphere around the midnight meridian.

59-66

4-8 The top three panels show a one hour section of the X magnetic component from 1200-1300 UT following the convection of figure 3-8. These stations span 150° of

magnetic longitude across the dayside hemisphere. The top panel shows, Murmansk (MMK) in the dusk hemisphere, the next panel shows Eskadalemuir (ESK) which is within 10° of the noon meridian, and the third is St. Johns (STJ). The next three panels show the Y component for these stations, and the last three show the magnitude of the horizontal perturbation. Especially noteworthy is the change in the signal shape and amplitude from dusk to dawn. 67

4-9 These plots show a series of stations spanning 30° of magnetic longitude from Thule (THL) in the north and proceeding southward through Godhaven (GDH) and Narssarssuaq (NAQ) to St. Johns. The scales and arrangement for this figure is similar to figure 4-8 using four stations north-south instead of three east-west. Note that we expect GDH and NAQ to bracket the position of the auroral oval. 69

4-10 This schematically illustrates the arrangement assumed (a plane phase front moving parallel to its normal) would be fitted to the data for the three high resolution stations. The scales in this diagram are not exact. 72

4-11 The equivalent current pattern derived from the EISCAT stations from 1230 to 1253 UT. Vectors are plotted every 20 seconds with time decreasing to the left corresponding to a physical displacement of 400 km for a stable structure convecting over the stations. 74

5-1 This figure shows the expected field line geometry for the near radial IMF during the event including the effects of the bow shock and magnetosheath. For this event we believe that the phase front of the pressure front is organized by the magnetic field and follows the same form. 76

List of Tables

| Table | Page |
|--|------|
| 2-1 Predicted characteristics of the ground signatures of the FAC systems associated with the various models in the post-noon, north hemisphere. A positive pressure increase and negative IMF B_y have been assumed where relevant. | 28 |
| 3-1 Data from CDAW-9 used in this study. | 29 |
| 3-2 Locations in GSM coordinates of the satellites used in this paper. | 31 |
| 3-3 Ground magnetometer stations, resolution and location, used in this study. | 37 |
| 5-1 Summary of observations versus predicted characteristics expected from the various models for this event. | 83 |

Acknowledgements

I want to thank Dr. Kivelson and Dr. McPherron, their encouragement and ideas were essential in completing this thesis.

I also want to thank all of the graduate students I have met and worked with during my assignment at UCLA, their friendship and help provided me with an education that cannot be found at any university.

ABSTRACT OF THE THESIS

Impulsive Magnetic Perturbations of the High Latitude, Dayside Ionosphere

by

Michael Dismas Krajnak

Master of Science in Geophysics and Space Physics

University of California, Los Angeles, 1991

Professor Margaret G. Kivelson, Chair

Recently interest has grown in the study of dayside magnetic impulse events observed at high latitude ground stations. These signals may be signatures of dayside magnetopause processes in the ionosphere. Successful identification of the ground signature of any process means that its contribution to the magnetospheric environment can be monitored with ground stations. Recent work has focused on signals that are expected to accompany mesoscale field-aligned currents moving through the ionosphere. The actual source of these currents remains controversial, with Flux Transfer Events (FTEs) and solar wind pressure enhancements being the primary candidates. We use a data set from the Ninth Coordinated Data Analysis Workshop which includes observations of the type that have been associated with dayside magnetic impulse events. We focus on the morphology and dynamics of this event which appear unique. For example, the inferred velocity across a chain of stations near 1400 local time is two to ten times faster than reported near the

terminator. We compare solar wind plasma and magnetic field parameters with models that relate the impulsive events to solar wind pressure perturbations or FTEs. There is an increase of the dynamic pressure prior to the event and the solar wind magnetic field is southward throughout the entire interval. ~~We find that~~ the event is well correlated to the dynamic pressure change, but the theories reviewed do not satisfactorily explain all of the observed features, possibly because a pressure increase and an FTE are both present, or because of incomplete station coverage.

Chapter 1: Introduction.

Since the early days of magnetospheric physics, the solar wind has been accepted as the fundamental driver for magnetospheric phenomena. However, the question of exactly how solar wind-magnetospheric coupling takes place is still unanswered. A number of mechanisms have been postulated based on initial observations and theories. Definitive proof of any one process has been difficult because of the complexity of isolating fundamental processes from the intricacy of the magnetospheric system. Recently a great deal of interest has been generated about the idea of using high latitude ground data to study coupling processes occurring at the magnetopause. Isolating and understanding the processes involved has been particularly difficult because of the remote sensing aspects of the measurements and the complications introduced as signals propagate through the ionosphere. This study is an attempt to isolate and understand the high latitude dayside impulsive magnetic ground signals associated with a large amplitude pressure pulse in the solar wind. We will use multipoint measurements throughout the magnetospheric environment to help interpret the ground measurements. Often attempts to isolate and study one process can lead to insights concerning others. The latest impetus given to the study of the ground signatures of coupling processes can be traced to the excitement surrounding the discovery of flux transfer events (FTEs) by Russell and Elphic (1978). FTEs are one method of coupling the solar wind to the magnetosphere and ionosphere. Early attempts to study and discover the implications of FTEs led to much of the work that underlies this thesis. FTEs are a form of reconnection which may have a significant role in transferring flux from the solar wind to the magnetosphere. Reconnection as a quasi-steady phenomena may be traced back to Dungey (1961). Despite initial resistance,

evidence accumulated early that pointed towards reconnection being a dominant mode of solar wind interaction with the magnetosphere (Cowley, 1982). However, in situ observations of reconnection were missing or ambiguous (Russell, 1984). FTEs may represent the "missing" flux transfer mechanism that quasi-steady reconnection does not appear to provide. After the initial discovery, scientists looked for new ways to observe and study FTEs. Several researchers suggested that FTEs should produce recognizable ground signals (Saunders et al., 1984; Cowley, 1984). If true, the large number of ground instruments already in place could be used to search for FTE signatures. Additionally, the established methods for working with ground data would speed up the initial analysis. Several researchers developed preliminary theories based on the field-aligned current (FAC) systems that they expected to be driven by an FTE (Southwood, 1985; Goertz et al., 1985; Lee, 1986). Since FTE's are essentially a magnetopause process they map to the high latitude ionosphere. Several tentative FTE signatures were identified in ground-based radar and magnetometer data (Goertz et al., 1985; Lanzerotti et al., 1986; Todd et al. 1986). These first tentative identifications led to an effort to make better observations. McHenry and Clauer (1987) suggested that data from high resolution magnetometer arrays would be needed to distinguish between the different models' signatures. Friis-Christensen et al. (1988a) conducted such a study with the Greenland Magnetometer Array. Their conclusions dramatically changed the questions that were being asked about the magnetic transients. Friis-Christensen et al. observed signals similar to those already reported; however, additional information derived from the magnetometer network led them to conclude that the magnetic signal was caused by pressure perturbations in the solar wind. Several other papers soon supported this conclusion (Friis-Christensen et al., 1988b; Farrugia et al., 1988, 1989; Glaßmeier et al., 1989; Glaßmeier and Heppner,

1990). The basic question being asked had changed from "where are the FTE signatures" to "what is the source of the observed transients?".

Theoretical Work

The basic process that is associated with all modes of solar wind momentum transfer is field-aligned current (FAC) flow (Southwood and Hughes, 1983). Models for FTE current systems have been based on observations (Russell and Elphic, 1978; Saunders et al., 1984), models of possible generation mechanisms (Lee and Fu, 1985; Southwood et al., 1988; Scholer, 1988), and theoretical MHD considerations (Southwood, 1985; Sonnerup, 1987). FTE models that involve a single FAC are sometimes referred to as Saunders-Lee systems, dipolar currents are called Southwood systems (McHenry and Clauer, 1987). In addition to the structure of the FTE, its path through the ionosphere also reveals useful information. When an FTE forms, it is expected to be accelerated by the magnetic tension of the kinked field line in the reconnection region. Once the FTE motion reaches steady state the reconnected flux tubes should be carried antisunward by global convection (Goertz, 1985; Sonnerup, 1987). Identifying signals that propagate in this fashion would be an important first step in finding FTE signatures in the ionosphere. Later, observations made with magnetometer arrays led to the suggestion that the magnetic signals being studied as FTE signatures could also be due to solar wind pressure perturbations (Friis-Christensen et al., 1988a). Several papers give qualitative descriptions based on pressure pulses (Elphic, 1988; Sibeck et al., 1989a; Sibeck, 1990a). Papers which focused on quantitative issues have tried to describe how a pressure change can generate a FAC. Proposed mechanisms include divergence of magnetopause currents (Glaßmeier and Heppner, 1990), coupling of compressional pulses to field-aligned currents due to plasma nonuniformities (Southwood and Kivelson, 1990a), and by shears in plasma flows (Kivelson and Southwood, 1991a).

Observed vortices have been classified into single, dipolar, and multiple vortices by Friis-Christensen et al. (1988a). The models of Lee (1986) and Glaßmeier and Heppner (1990) lead naturally to single vortices; other classes of signals could be reproduced by a more highly structured pressure pulse. Kivelson and Southwood (1991a) predict dipolar and higher order structures. They state that a highly asymmetric pulse could produce a structure that appeared to be a single vortex because one vortex might be distorted to the point that it could not be recognized, but they felt that it would be an unusual occurrence (see also Kivelson and Southwood 1990c). When field-aligned currents couple to the ionosphere they drive horizontal Pedersen and Hall currents. It is the Hall current loop around the vertical current that is expected to produce the ground magnetic signal and be associated with a vortex-like convection pattern in the ionosphere. The effects on the ground of the Pedersen and vertical currents are expected to cancel (ref. McHenry and Clauer, 1987) at high latitudes where the background magnetic field is approximately vertical. When field-aligned currents are generated at the magnetopause they map to the poleward edge of the auroral oval

Observations

Three basic types of sensors have been employed in the search for FTE signals: optical, radar, and ground-based magnetometers. In general, optical signatures were not considered in this study (Some introductory material regarding optical signatures is included in Sandholt et al., 1986; Lockwood et al., 1989; Mende and Rairden, 1990). Spacecraft observations are sometimes considered in conjunction with ground data to determine the characteristics of the global environment in which these processes take place. The first reports of possible FTE signatures were given by Goertz et al. (1985) using STARE (Scandinavian Twin Auroral Radar Experiment) incoherent scatter radar

data. This radar is capable of characterizing bulk flows in the ionosphere from the Doppler shift of the radar echo (Hargreaves, 1978). Goertz, in agreement with Saunders et al. (1984), estimated the scale size of the FTE signature in the ionosphere to be on the order of 200 km. Since FTEs originate near the magnetopause, the ground signal is expected to map to the polar convection reversal boundary (CB). However, the CB is rarely in the field of view of the STARE system, so the study was limited to two events which occurred when the CB was in the field of view. In both events, evidence for the Hall current vortex was found. The ground track of the observed disturbance generally followed that predicted for an FTE. There was an isolated region of flow moving sporadically poleward across the CB. Poleward of the CB the flow was antisunward, sometimes with a component northward. The size scale (50 to 300 km) observed was also roughly in agreement with that predicted for FTEs. Similar evidence was reported by Todd et al. (1986). The first attempts to study ground magnetometer data used single or widely spaced magnetometers. Lanzerotti et al. (1986, 1987) described the magnetic perturbations expected for a single stationary Hall current loop, emphasizing the unipolar appearance of the vertical component. Magnetometer records were searched for impulsive signatures that could be due to an ionospheric Hall current loop. Several events were found and described in the paper. The 1987 paper expanded this work by using magnetically conjugate stations. However, the work still only considered the effects of a single current loop and relied on assumptions about the current structure and dynamics. Bering et al. (1988) tried to determine more about the structure using electric field data from balloon electrometers and obtained results that did not fully agree with either the Saunders-Lee or Southwood current systems. Subsequent studies followed a suggestion by McHenry and Clauer (1987) and primarily used magnetometer

arrays. The first report of this kind was made by Friis-Christensen et al. (1988a) which contained some interesting conclusions. For one event observed near 07 LT the phase differences between various stations showed that the signal was moving tailward at 3-5 km/s. Friis-Christensen was able to reproduce the two dimensional pattern of equivalent currents by assuming that the current structure was fairly stable and that the ionospheric conductivity was uniform. Figure 1-1 dramatically reveals the twin vortex pattern that was observed. Friis-Christensen et al. found the overall motion and structure inconsistent with the expected signatures for FTEs. In particular, the velocities were much higher than expected for FTEs which would be moving at roughly the ionospheric sound speed, 1 km/sec (Farrugia et al., 1989). As a result Friis-Christensen et al. sought an alternative explanation for their data. They associated the perturbation with a sudden change in the solar wind dynamic pressure shown in IMP-8 data. Similar studies soon followed which showed similar convection patterns and motion and also correlated events to changes in the solar wind (Friis-Christensen et al., 1988b; Farrugia et al., 1988, 1989; Glaßmeier et al. 1989; Glaßmeier and Heppner, 1990). Sibeck et al. (1989a and c) have demonstrated additional evidence for pressure perturbations as a source of these events as well as showing that some events initially interpreted as being due to FTEs could be linked to variations in the solar wind dynamic pressure.

Current Work

Some of the recent work done on this problem has concentrated on distinguishing between the two primary theories that have been put forth to explain the various observations. Three papers, one by Lanzerotti (1989) the others by Sibeck et al. (1989a and b), contain a good review of some of the problems up until that time. Sibeck felt that Lanzerotti's observations (Lanzerotti et al., 1986, 1987; Lanzerotti, 1988; Lanzerotti and

*Ionospheric convection vortices observed by
Friis-Christensen et al.*

GREENLAND CHAIN MAGNETIC PERTURBATIONS
PLOTTED AS EQUIVALENT CONVECTION

28 JUNE 1986
10:06-10:21 UT

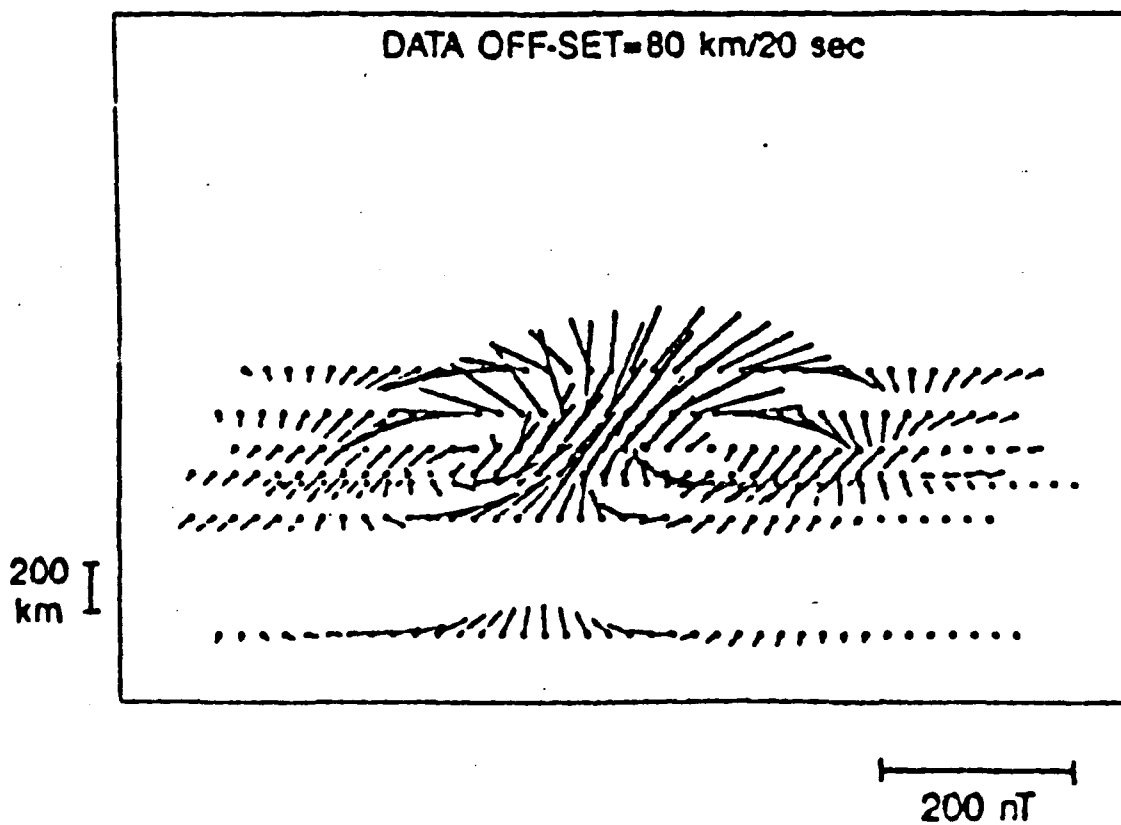


figure 1-1

MacLennan, 1988) could be correlated to changes of the solar wind dynamic pressure. Lanzerotti pointed out that the existence of pressure variations did not preclude the occurrence of FTEs. Sibeck showed that there was little or no southward component of the IMF present during many events described by Lanzerotti (1986, 1987) and Todd (1986). Since FTEs are highly correlated to a southward IMF the chance of an FTE being the cause is reduced. Lanzerotti replied that the chance was still finite. He felt that other processes that might influence FTE formation could not be ruled out. Both authors mentioned that the bow shock can have a considerable effect on solar wind parameters (following Fairfield et al., 1990), including IMF orientation and dynamic pressure, which relate to the signal generation process. Other authors have been involved in this debate. For example, Bering et al. (1990) show a significant number of impulsive events that were preceded by little or no dynamic pressure change. Other papers have mentioned the fact that the exact path of an FTE cannot be predicted. By variations (Goertz et al., 1985), magnetic field topology (Lanzerotti et al., 1986; Crooker and Siscoe, 1990; Crooker, 1990), and details of the flux transport process (Southwood, 1987) are some of the reasons why an FTE might not follow a straightforward path.

Summary

Research on dayside magnetic impulse events has been very active in recent years. The first papers which began the renewed interest on this topic were those that speculated on the ground signature of FTEs. Initial observations have raised a number of questions about the possible sources for these signals. Further studies are needed to help refine our understanding of the impulsive signals seen at high latitudes and how they relate to solar wind coupling. In particular, there is a need to characterize the structure, scale sizes, scale times, and locations for better classification and defining the processes

involved. Additionally, identifying the global characteristics under which these impulsive perturbations can occur can help identify the possible sources and how they influence or interact with other magnetospheric processes. The purpose of this paper is to make an thorough study of a single case where we believe pressure pulse effects dominate. By studying an extreme case of the pressure pulse type of event we hope to clarify some of the features and dynamics of this process. Comparisons to existing models and previous reports will be made and we will try to define criteria which distinguish a pressure pulse response from FTE types of events.

Chapter 2: Basic Theory and Concepts.

In the magnetosphere field-aligned currents serve the purpose of transmitting mechanical forces along flux tubes. The creation of FACs can be discussed in terms of applied stresses; however, the morphology of the resulting current structures can strongly depend on the exact generation mechanism. It is also possible to discuss the general characteristics of the ground signature of a FAC, but the actual dynamics of the current moving through the ionosphere depends on the source.

Generating Field-Aligned Currents

Any dynamic process which transfers solar wind momentum to the magnetosphere will involve changes to the stress balance along the magnetopause. The transverse and compressional signals which propagate surface stresses through an elastic body, have as their counterparts in the magnetosphere, hydromagnetic waves. The magnetic field which threads the plasma defines a preferential direction of propagation, more so for the Alfvén and slow mode waves which cannot propagate across field lines. Changes in the stress balance along a magnetic flux tube requires the propagation of Alfvén waves (Southwood and Hughes, 1983). Alfvén waves generated at or just inside the magnetopause map to the edge of the polar cap or just equatorward of it. In MHD for a uniform plasma it is Alfvén waves which carry field-aligned currents. In figure 2-1 the polarization relationships for Alfvén and fast mode waves are shown for a cold, uniform plasma (after Kivelson, 1991). The diagram illustrates that only for the Alfvén mode is $\mathbf{j} \cdot \mathbf{B} \neq 0$.

Field-Aligned Currents and Flux Transfer Events

Reconnection is widely accepted as a major contributor to solar wind - magnetospheric interaction, especially when B_z is southward (Cowley, 1982). Recent interest has

Polarization relations for Fast and Alfven modes

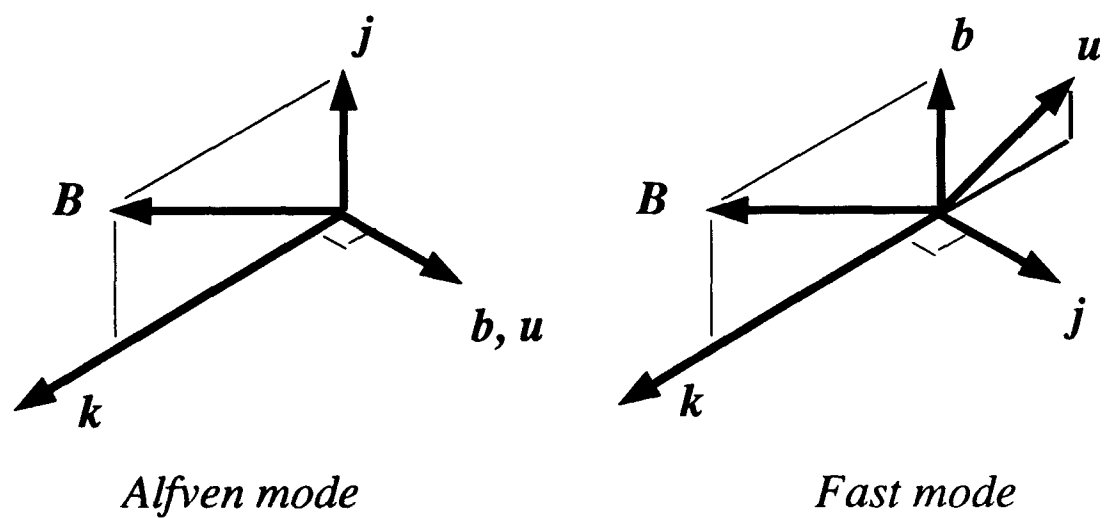


figure 2-1

focused on the role of Flux Transfer Events (FTEs). FTEs are a form of reconnection observed at the Earth's magnetopause that occur on limited spatial and temporal scales (Russell and Elphic, 1978, 1979). The earliest model of an FTE is shown in figure 2-2.

The FTE is shown as a flux tube in the magnetosheath connected to the magnetosphere through a hole in the magnetopause. Magnetopause field lines are shown draped over the FTE (Russell and Elphic, 1979). FACs were connected to FTEs observationally, when it was noted (Saunders et al., 1984) that the field lines around the FTE had a helical twist, indicating the presence of current flowing in the flux tube. This twisting of the field lines is not an intrinsic characteristic of the early Russell-Elphic model. Several subsequent models were proposed for the formation of FTEs, all of which included features that could explain the presence of a FAC flowing through an FTE. Lee and Fu (1985) proposed that FTE structures were formed by a multiple X-line reconnection (MXR) process. The shear in the magnetic field from the magnetosheath with $B_y \neq 0$ to the magnetosphere with $B_y = 0$ is responsible for giving a helical twist to the FTE field. Later, Southwood et al. (1988) and Scholer (1988) suggested that FTEs could be formed by time dependent or bursty single X-line reconnection (SXR). The tube like structure of an FTE was reproduced by an impulsive change in the reconnection rate which formed a plasma bubble. As with the Lee and Fu model, the magnetosheath B_y component was responsible for adding a helical twist to the FTE field. Southwood et al. pointed out that shears in the plasma flow across the magnetopause could add to the field twist. Finally, we note that Sonnerup (1987) was able to reconcile the idea of a core field-aligned current with the Russell-Elphic paradigm. He noted that the stresses that build up as an FTE is initially propelled away from the reconnection site by magnetic tension require the formation of a current that passes through the FTE. Besides a central FTE current inferred from satellite

Russell-Elphic FTE model

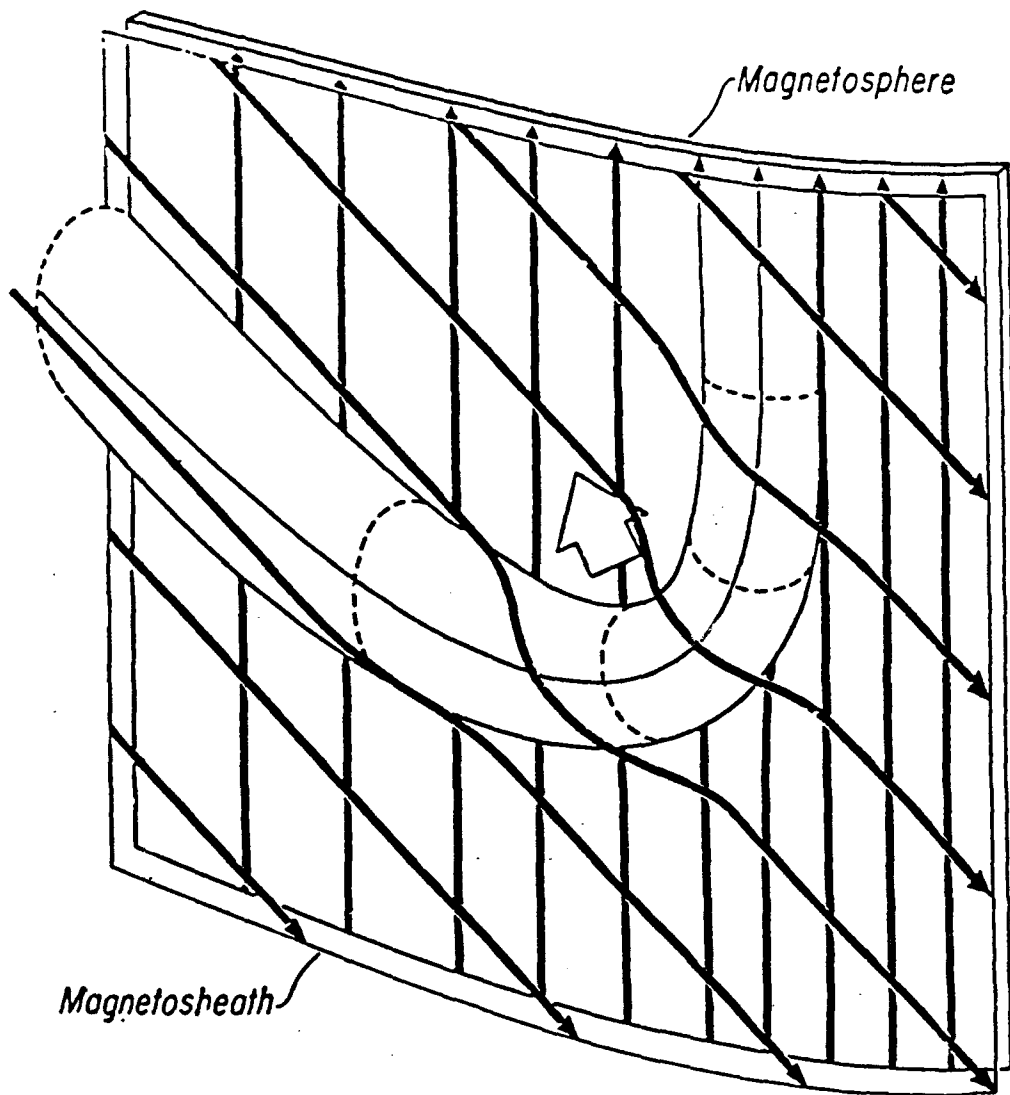


figure 2-2

observations, other currents are expected to develop as a result of the drag exerted on the flux tube by the ionosphere. Southwood (1985) pointed out that the stresses which tow the ionospheric end of the flux tube will set up vortical flows on the flanks of the structure. In the ionosphere it is fairly simple to show that vorticity relates directly to field-aligned currents (for example see Kivelson and Southwood, 1991b) by the expression,

$$j_{\parallel}/\Sigma_P = -\Omega \cdot \mathbf{B}$$

where Σ_P is the height integrated Pedersen conductivity and Ω is the vorticity. Figure 2-3 shows a pair of vortices due to flux tube motion, the field-aligned currents associated with them, and a closure current (Pedersen) perpendicular to the direction of motion. One can view the closure currents as providing the $\mathbf{j} \times \mathbf{B}$ force which drives the flux tube through the ionosphere.

Pressure Pulses and Field-Aligned Currents

Pressure fluctuations can also change the stress balance at the magnetopause. A number of steps in this process are basic to almost all descriptions that have been given so far. They include a sharp change in the solar wind pressure, which may be due to changes in solar wind composition, density, or velocity. The pressure front will move over the magnetosphere at speeds typical of magnetosheath velocities (200 km/s). In the interior of the magnetosphere the pressure perturbation launches a fast mode wave. The fast mode speed in the magnetosphere is typically greater than magnetosheath speeds. The velocity is on the order of 2000 km/s just inside the magnetopause compared to 200 km/s in the magnetosheath. The fast mode wave speed increases radially inward until it encounters a sudden minimum at the plasmopause of 150 km/s, and then increases again (Nishida, 1978; Moore et al., 1987). Since the wave speed in the magnetosphere is typically greater than the speeds in the magnetosheath the pressure in the magnetosphere increases ahead

Twin Convection Vortex

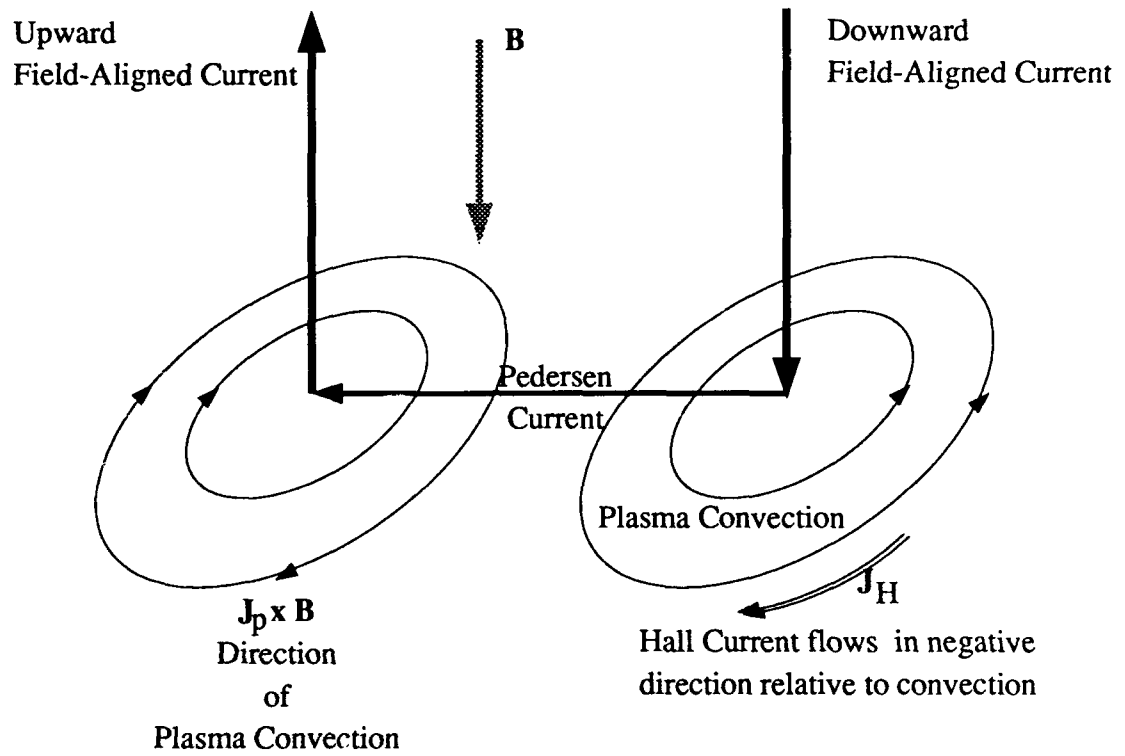


figure 2-3

of the sheath pressure front and should cause an outward bulge ahead of the surface wave (Nishida, 1978). A number of authors have attempted to explain the detailed processes that allow the perturbation to couple to the ionosphere. Elphic (1988) recognizes the role that FACs play in communicating stresses, but describes the ionospheric coupling effects in terms of fluctuations in the magnetopause location. Inward/outward motions of the magnetopause map to equatorward/poleward motions of the polar cap boundary and forces tailward/sunward motion of ionospheric plasma resulting in vortex convection patterns. Glaßmeier and Heppner (1990) present a model in which FACs result from a divergence in the magnetopause currents which must change to come into equilibrium with the change in solar wind pressure. Figure 2-4 shows a schematic of the Glaßmeier-Heppner model with a pair of field-aligned currents bracketing the region of the pressure change. These currents would map to the polar cap boundary like the process described by Elphic. The concept of a compressional perturbation closing through field-aligned currents has been challenged by Kivelson and Southwood, 1991a and b. Southwood and Kivelson (1990) show that a nonuniform plasma distribution leads to coupling between the fast and intermediate modes. Thus the fast mode signal generates field-aligned currents throughout the magnetosphere as it propagates through the magnetospheric cavity. This effect is most important near L-shells where the driving frequencies match the resonant frequencies of the field line. The field aligned currents generated occur in balanced dipoles with equal amounts of upward and downward current (for more discussion see Southwood and Hughes, 1983). Kivelson and Southwood (1991a) discuss another mechanism for coupling the two MHD modes, one that is more likely to produce signals at higher latitudes. They draw attention to the shear in the azimuthal flow near the boundary due to the pressure pulse passing over the magnetopause. These shears result in parallel

Glassmeier-Heppner Model

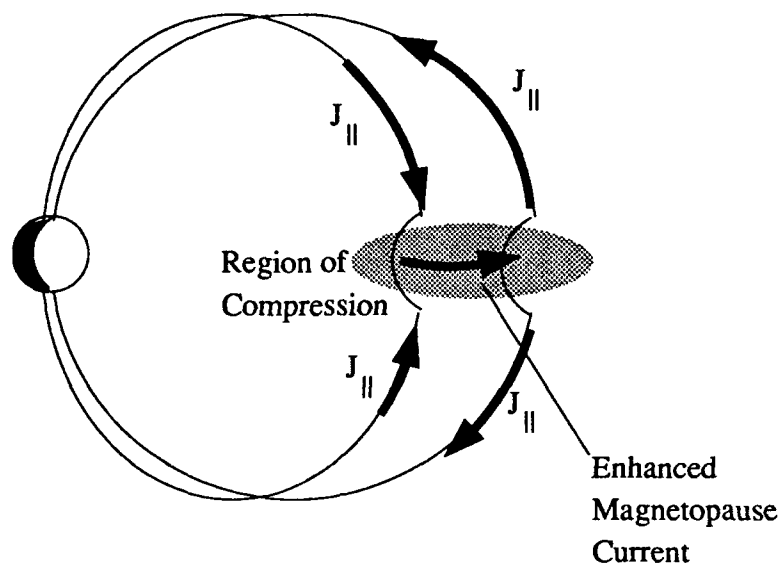


figure 2-4

plasma vorticity, which in MHD is linked to FACs. As the pressure pulse passes the direction of the shears changes and the associated field-aligned current changes direction. As in the previous model FACs occur in balanced pairs. However, the source region for the parallel currents in this case is near the magnetopause instead of near a resonant L-shell in the magnetosphere, which means they map to higher latitudes in the ionosphere near the polar convection reversal boundary like the processes described by Glaßmeier and Heppner or Elphic.

Ground Signatures

The basic ideas behind the ionospheric/ground response to a single field-aligned current are well laid out. When a FAC contacts the ionosphere it drives horizontal Pedersen currents in the direction of the applied electric field. Collisional effects in the ionosphere result in the formation of Hall currents perpendicular to the Pedersen currents. In a uniform ionosphere Hall currents close on themselves, forming loops around the incident FAC. The ground magnetic signature of the vertical and Pedersen currents cancel under the conditions of a vertical magnetic field and a uniformly conducting flat ionosphere. The signal is solely generated by the ionospheric Hall current loop (McHenry and Clauer, 1987). Figure 2-5 taken from Lanzerotti (1986) shows the ground signature of a single current loop in HDZ coordinates (station centered cartesian coordinates with H towards the magnetic north, D east, Z vertically down). The signature is characterized by a bipolar signature in H and D and a unipolar signature in Z. The FAC structures and dynamics proposed by various models can be built up by summing together the effects of an appropriate set of current loops. FTE models which map a single core of field-aligned current to the ionosphere (e. g., Saunders et al., 1984), generally follow Lee (1986) and close the circuit with a return current flowing back in a thin cylindrical shell

*Magnetic field perturbations for an ionospheric
Hall current loop
calculated by Lanzrotti*

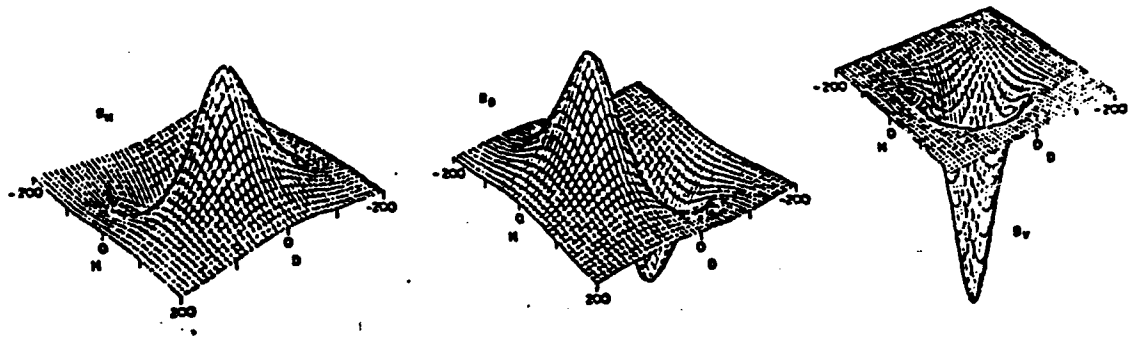


figure 2-5

around the FTE (figure 2-6). To first order the motion of the FTE at the magnetopause is initially controlled by magnetic tension present in the field line kink where the flux tube passes through the magnetopause. After the flux tube straightens the FTE convects with the magnetosheath flow (Goertz et al., 1985; Sonnerup, 1987). In the ionosphere this maps to poleward motion, with modifications due to IMF B_y , followed by tailward motion. In the northern hemisphere the center current is into the ionosphere for IMF $B_y > 0$ and out of the ionosphere for $B_y < 0$ (Lee, 1986; Sonnerup, 1987). The field-aligned current system predicted by Southwood (1985) results in the formation of a pair of Hall current loops in the ionosphere (figure 2-3). The effects of two current loops must be added to yield a magnetic footprint which will sweep over a ground station. The vortex structures are on the flanks of the FTE so the line connecting the current loops, which defines the orientation of the magnetic footprint, is perpendicular to the direction of motion. The ground track of the FTE with respect to the station and the orientation of the footprint determine the actual perturbations measured by the station. Southwood (1987) discusses the factors which control the FTE motion, including magnetic tension and convection discussed before. He also considers how as flux tubes are added to the polar cap some will be drawn around the flanks resulting in tailward motion along the polar cap boundary. In both cases, the FTE motion is associated with the physical dragging of the entire flux tube, we can then expect velocities in the ionosphere to be limited to the ionospheric sound velocity, on the order of 1 km/sec (Farrugia et al., 1989). In the case of pressure pulse generated FACs, the number of currents generated for a step function pressure increase or decrease depends on the coupling mechanism suggested. Figure 2-7 shows a schematic of a partially compressed magnetopause. On each flank is an uncompressed region and a transition region with the compressed

Cylindrical FTE Model

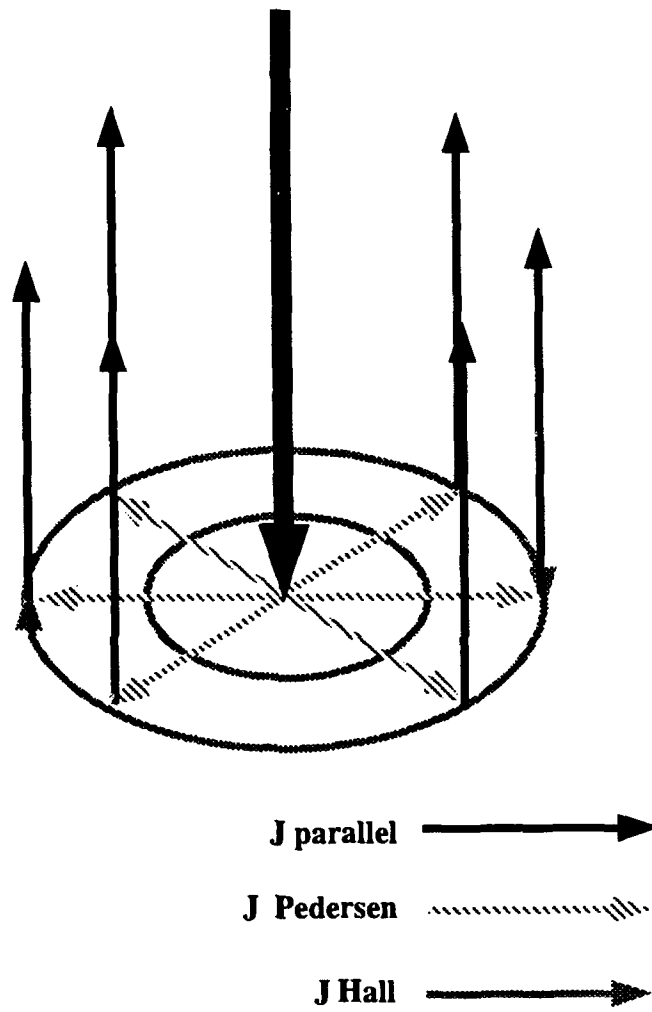


figure 2-6

Compressed Magnetopause

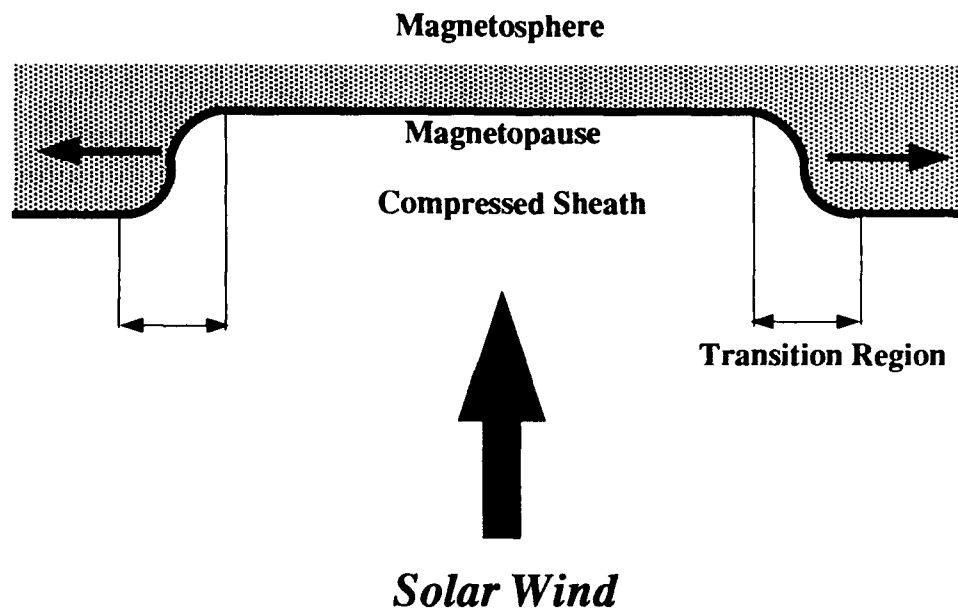


figure 2-7

magnetopause between them. The transition region is the critical area associated with the generation of field aligned currents. With the Kivelson and Southwood (1991a) or Southwood and Kivelson (1990) processes two field aligned currents arise from vortical flow perturbations driven by the passing front in each transition region. If the pressure change in the solar wind has some unusual structure it could produce a highly asymmetric transition region with one clearly defined current and a poorly defined current so only a single convection vortex could be resolved on the ground (Kivelson and Southwood, 1991a). For a positive pressure pulse the leading FAC is parallel to the background field (in towards the ionosphere for the northern hemisphere) on the dusk flank with a return current of the opposite sense. On the dawn flank the direction of these currents is reversed (Kivelson and Southwood, 1991b). All other mechanisms discussed so far associate only one FAC per transition region. It is fairly easy to see that in the Glaßmeier-Heppner model a compression generates current into the ionosphere on the dusk flank and out of the ionosphere on the dawn flank in the north and south hemispheres. Multiple pressure fluctuations can generate a variety of structures. As the transition region moves along the flanks the ionospheric convection vortices are seen moving tailward. Multiple vortices form vortex "trains" aligned with the direction of motion. Because there is no physical dragging of flux tubes through the ionosphere, the ionospheric velocities are not limited as in the case of FTEs.

Summary of Models

In table 2-1 we summarize the local characteristics of the current models as they apply to the event E in the CDAW data base, $B_y < 0$ and a step-like pressure increase. In the table we cover the Saunders-Lee FTE (SLF), Southwood FTE (SF), Glaßmeier-Heppner pressure pulse (GHP), and Kivelson-Southwood pressure pulse (KSP). The

ground signature of the Southwood-Kivelson resonance model is qualitatively similar to the KSP at the resonant L-shell. To our knowledge no discussion has appeared in the literature about any special features of the ground signature for an FTE generated by bursty reconnection. We characterize the models in terms of speed, direction, local flow pattern, scale size, and the sense (into or out of the ionosphere) of the FAC system for the post-noon, north quadrant of the dayside hemisphere. The local flow pattern is sometimes difficult to visualize so the flow pattern associated with each model is shown in figure 2-8. We break down the possible flow patterns observed locally into three types: monopolar (MP), parallel dipole (DP_{\parallel}), and perpendicular dipole (DP_{\perp}). The line joining the vortex centers is parallel to the direction of motion for DP_{\parallel} and perpendicular for DP_{\perp} . This classification scheme focuses attention on the number and structure of the field-aligned currents near the ground station and ignores some other details of these processes. The global pattern of currents may be very different as we will shortly discuss. The sense of the FAC system for a single current is just the sense of the current in the post-noon north quadrant. For multiple current systems the sense is determined by the FAC whose signature would first be encountered by a ground station directly in its path. This may give an undefined result in some cases. We also list the controlling parameter which influences the direction of the currents (into, out of the ionosphere). In figure 2-9 we depict the global distribution of FACs for a positive pressure pulse and negative IMF B_y . An important feature is that the pressure pulse theories predict FACs in all four quadrants of the dayside hemisphere versus two quadrants for the FTE theories. In trying to compare the magnetic footprints of the various systems it is important to note that a single upward current in the northern hemisphere has the same magnetic footprint (ref. figure 2-5) as a downward current in the southern hemisphere. A particularly useful

***Local form of FAC systems for
positive pressure perturbation, negative IMF By,
in the post-noon, northern hemisphere***

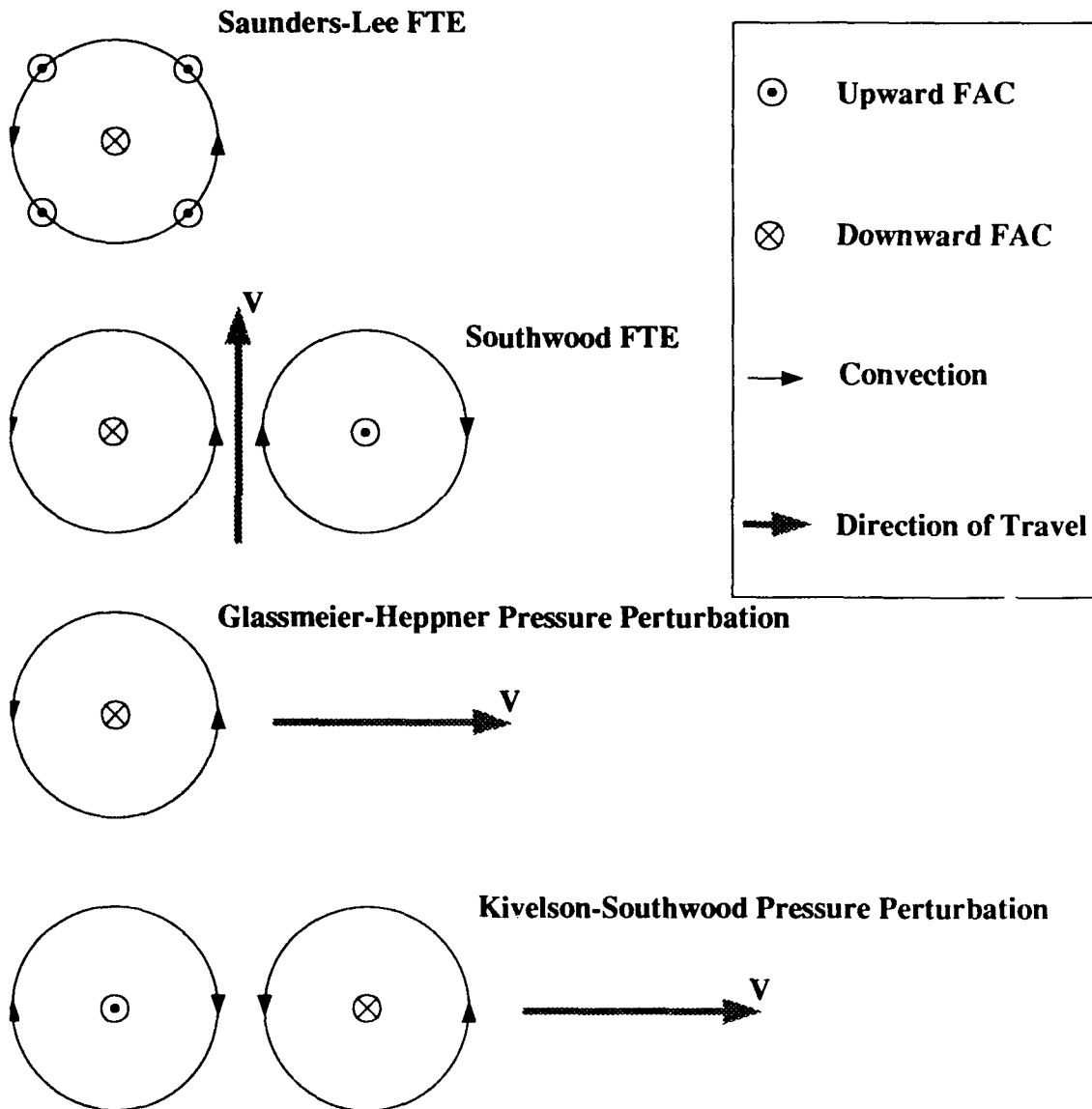


figure 2-8

***Global Distribution of FACs
for postive pressure enhancement, negative IMF By***

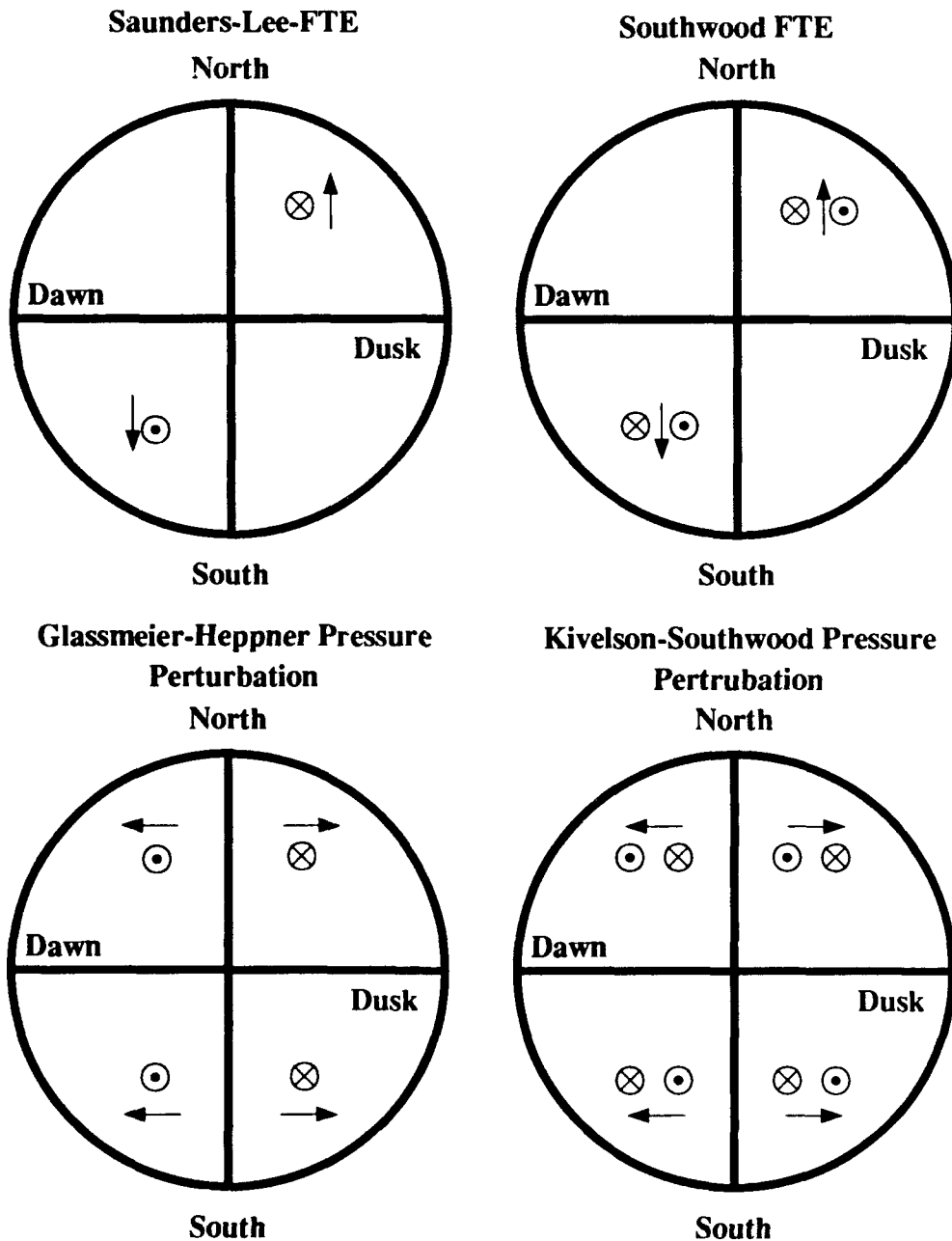


figure 2-9

feature for distinguishing between FTE and pressure pulse related perturbations is the ionospheric velocity of the signal. The two different FTE and pressure pulse models differ in their prediction of monopolar or dipolar ionospheric convection vortices.

TABLE 2-1: Predicted Characteristics of High Latitude (near the CB) Ionospheric Signatures in the Post-Noon Section of the Northern Hemisphere.

A positive pressure pulse and IMF By < 0 has been assumed where relevant.

| Model - | <u>SLF</u> | <u>SF</u> | <u>GHP</u> | <u>KSP</u> |
|------------------------|----------------------------|---|-----------------------------------|-----------------|
| Speed | ~1 km/s | ~1 km/s | ~1-10 km/s | ~1-10 km/s |
| Direction | Poleward then anti-sunward | | Tailward | Tailward |
| Local Flow Pattern | MP | DP | Quasi-MP ¹ | DP _⊥ |
| Scale Sizes | ~200 km | ~200 km | ~200-2000 km | ~200-2000 km |
| Sense of FAC system | Downward | Undefined | Downward | Downward |
| Leading FAC depends on | IMF By | Direction (Initially determined by By) | Pressure increasing or decreasing | |

Table of expected characteristics predicted for Saunders-Lee FTE model (SLF), Southwood FTE model (SF), Glaßmeier-Heppner pressure pulse (GHP), and Kivelson-Southwood pressure pulse (KSP).

¹We prefer to use the term quasi-monopolar for the GHP system since it is monopolar on a local scale and bipolar on a global scale for a dynamic pressure enhancement.

Chapter 3: Observations.

All of the data for this study were taken from the Ninth Coordinated Data Analysis Workshop (CDAW-9) online data base maintained by the National Space Science Data Center (NSSDC). Each CDAW is organized for the purpose of studying a specific problem in space physics. The method used is to identify interesting periods of activity and pool a variety of data from different sources into a computer format easily shared by many researchers. The resulting data base contains detailed observations covering short time periods; this makes it extremely useful for conducting case studies. Not all of the data base was used; a brief description of the data employed in this study is given in table 3-1. The data are given in a variety of coordinate systems which we briefly review here. In space GSM and HVD coordinates are used. GSM coordinates are earth

Table 3-1: Data taken from CDAW-9 used in this study.

| Data | Resolution | Source |
|--------------------------------------|------------|----------|
| | | |
| AMPTE/CCE Magnetic Field | 68 seconds | Nylund |
| GOES-5 Magnetic Field | 60 seconds | Nagai |
| IMP-8 Magnetic Field | 15 seconds | Lepping |
| IMP-8 Plasma Parameters | 60 seconds | Lazarus |
| SCATHA Magnetic Field | 16 seconds | Fennel |
| | | |
| AE Index | 60 seconds | Kroehl |
| | | |
| EISCAT Magnetometers | 20 seconds | Luehr |
| High Resolution Ground Magnetometers | 1 second | Bosinger |
| FMI Magnetometers | 60 seconds | Koskinen |

centered cartesian coordinates with the X axis towards the sun, the Z axis northward in the plane containing the X axis and the earth's dipole, and the Y axis completing the right-handed system. HDV coordinates are also a right-handed, earth-centered system with H northward, V radially outward, and D eastward. On the ground, station-centered XYZ and HDZ coordinates are used. In both cases Z is always radially inward. XYZ coordinates are "geographic" with X towards the rotation pole and Y eastward completing the system. HDZ are "magnetic" coordinates with H towards the magnetic north and D towards the magnetic east.

Event Selection

For the CDAW event to be useful for our study it had to satisfy two criteria. One, the ground magnetometer data had to contain signals similar to those studied by Lanzerotti, Friis-Christenson, Glaißmeier, and others. These signals are impulsive with magnitudes from tens of nanotesla up to a hundred or more nanotesla. The vertical signal may be unipolar or bipolar. The east-west signal looks roughly like the negative derivative of the north-south signal (Lanzerotti et al., 1986; Glameier et al., 1989). The second criterion is that there was a large pressure pulse observable in the solar wind.

Satellite Data

Four satellites were used in this study: IMP-8, SCATHA, AMPTE/CCE, and GOES-5. Table 3-2 lists the GSM coordinates of each satellite at 12:30 UT. Figure 3-1 shows the locations of these satellites in the XY plane. It also shows the magnetopause location based on an elliptical fit for the dayside magnetopause and scaled to a magnetopause nose distance of 9 Re. This distance is based on pressure balance with the pre-event solar wind conditions following Nishida (1978).

Table 3-2: Locations in GSM coordinates of the satellites used in this paper and the time resolution of the onboard magnetometer.

| Satellite | GSM X | GSM Y | GSM Z | Resolution |
|-----------|-------|-------|-------|------------|
| AMPTE/CCE | 2.34 | -7.82 | 1.20 | 68 seconds |
| GEOS-5 | 1.37 | -6.49 | 0.00 | 60 seconds |
| IMP-8 | 37.33 | 3.09 | -1.47 | 15 seconds |
| SCATHA | 5.98 | -3.04 | -1.66 | 16 seconds |

IMP-8 is 37 Re from the center of the earth almost directly upstream from earth. Figure 3-2 shows the magnitude of the solar wind magnetic field and its components in GSM coordinates from 1000 UT to 1800 UT on May 8, 1986. Figure 3-3 shows the solar wind plasma parameters. At 11:12 UT all three components of B reverse sign from positive to negative. This inclines the field lines more than 45 degrees to the normal Parker spiral angle, making it nearly radial. Bz is now southward and remains so throughout the rest of the study period. At 12:22 UT there is an 2 nT decrease in the total magnetic field down to 4 nT. At the same time the particle density increases from 9 to 15 cm⁻³. Pressure is approximately balanced across this interface. The solar wind velocity is more or less uniform throughout this period at 425 km/sec. As a consequence of the density increase the dynamic pressure also increases. From 12:22 to 14:01 the magnetic field and pressure continue to fluctuate out of phase. At 14:01 the magnetic field experiences an increase and there is a decrease in the solar wind density.

Magnetospheric Satellites: SCATHA, AMPTE/CCE, GOES-5

SCATHA is the satellite located closest to the nose of the magnetopause, near 10LT. Figure 3-4 shows the magnetic field at SCATHA in HDV coordinates and the total

Satellites' Positions in GSM XY plane

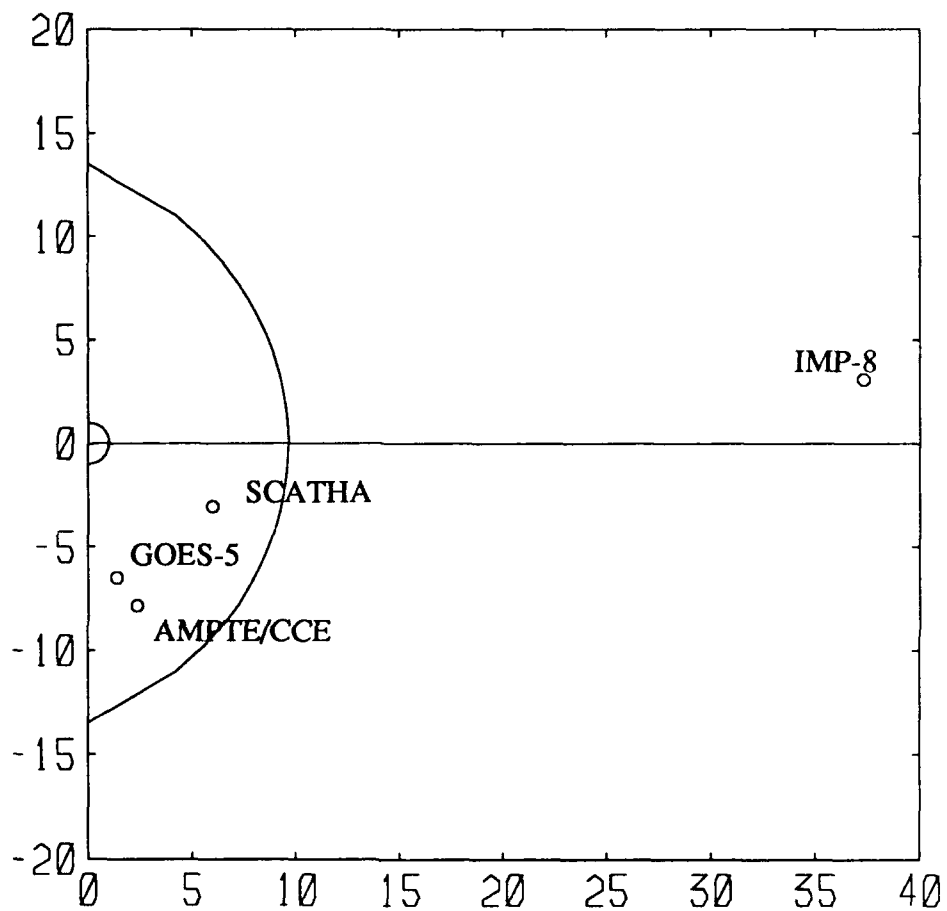


figure 3-1

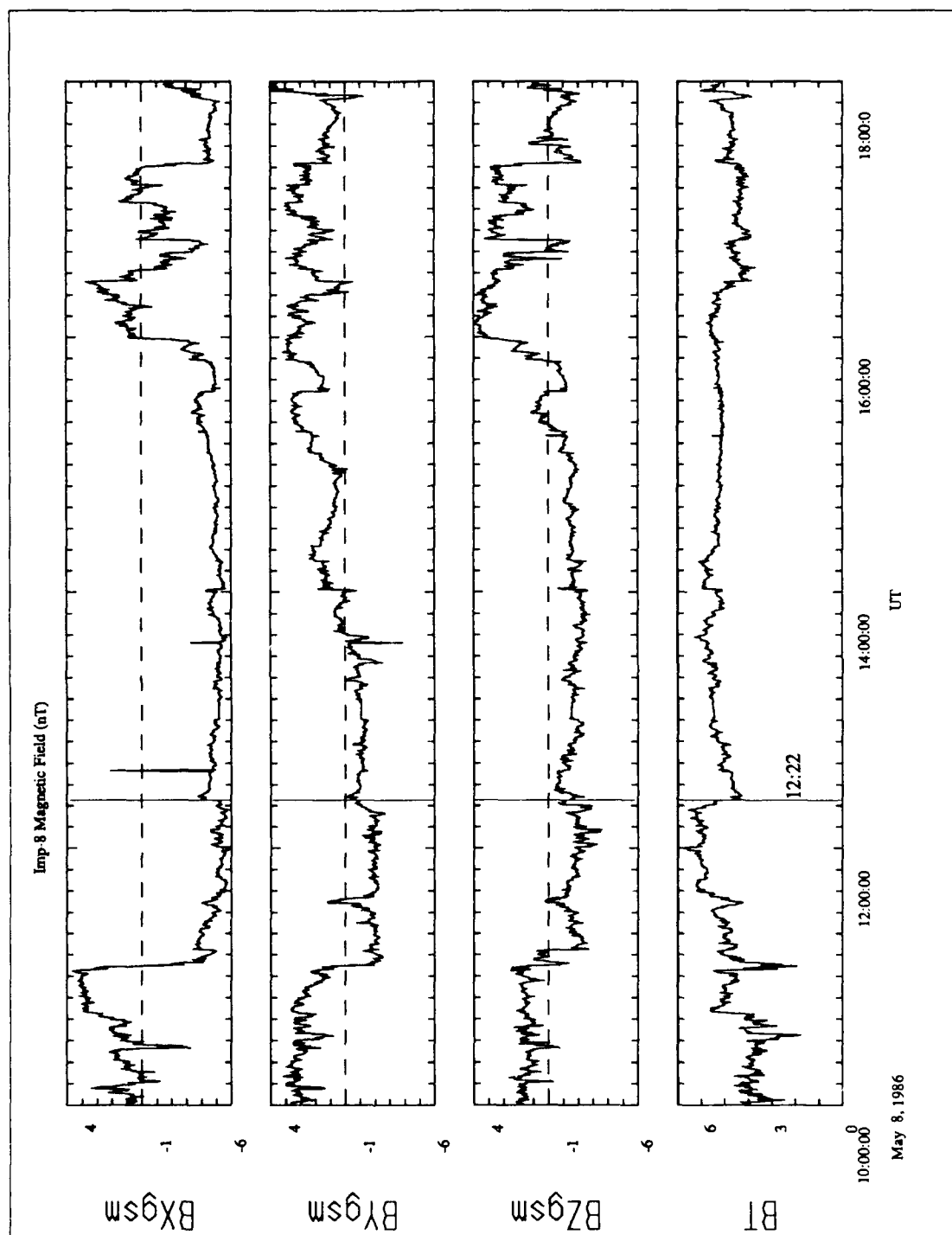


figure 3-2

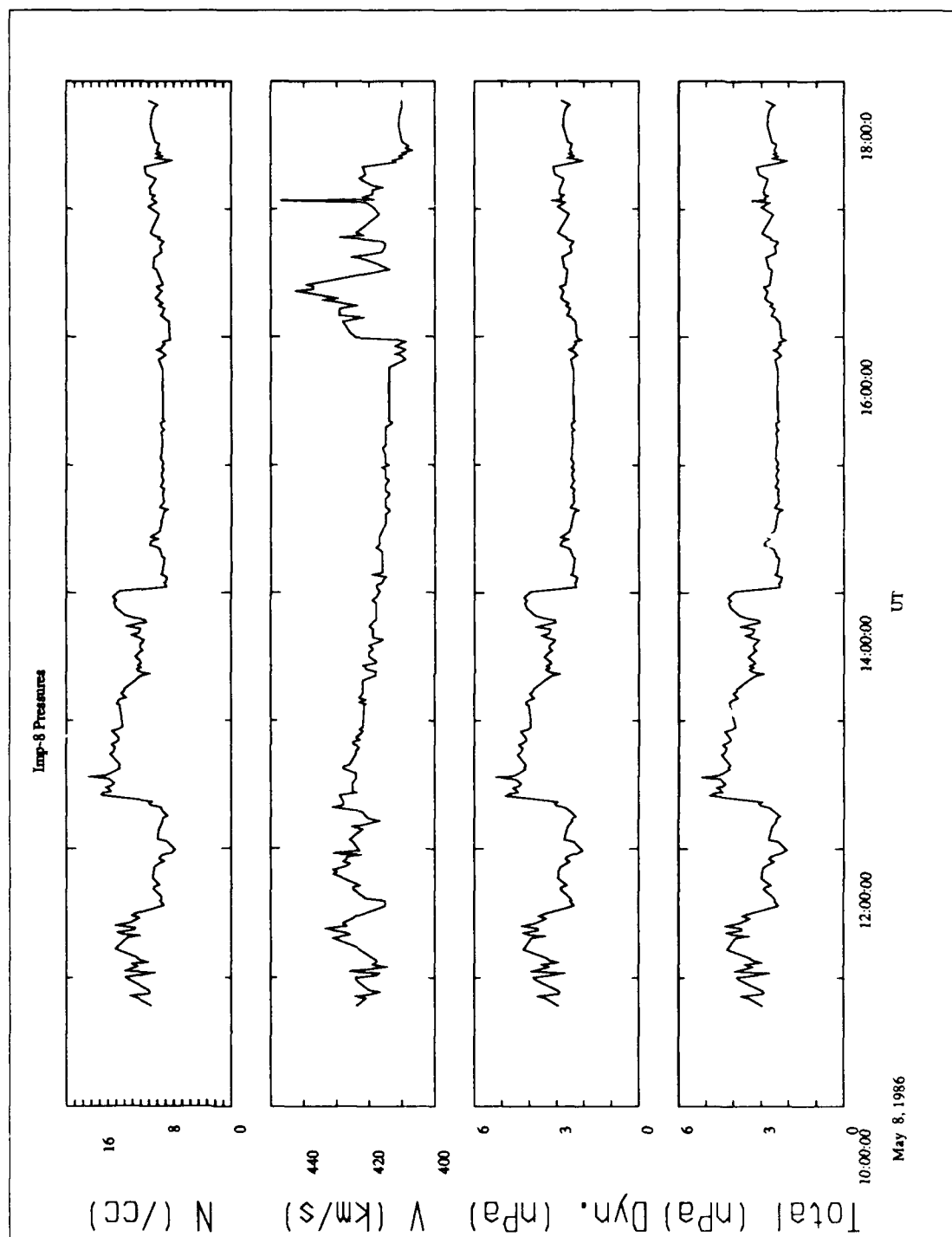


figure 3-3

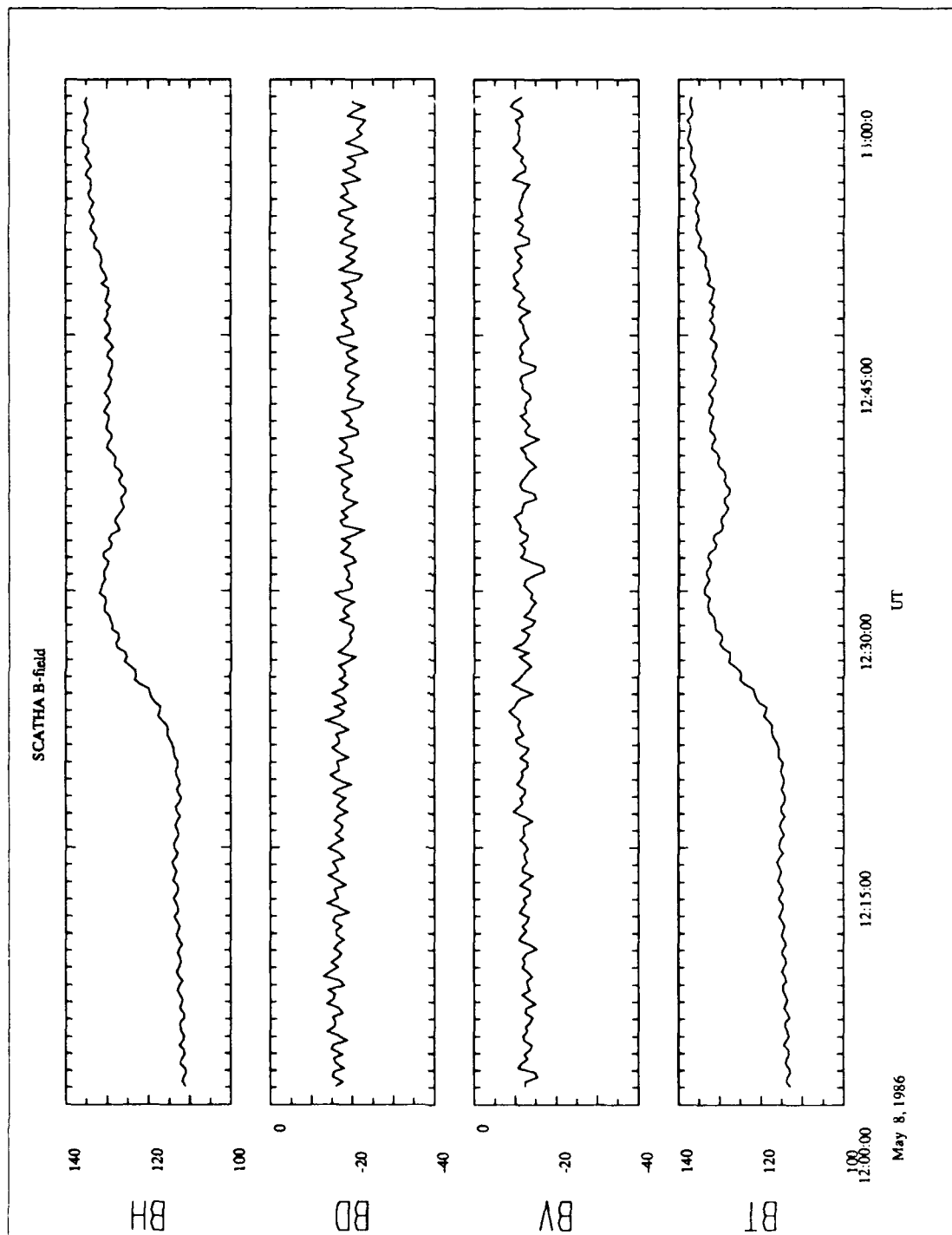


figure 3-4

field. The H direction is almost field-aligned so it shows perturbations similar to the total field. The high frequency component (1 minute) of the signal is a result of problems correcting for the spacecraft's spin (J. Fennel, personal communication). However, the compressional enhancement of the field beginning at 12:20 is clearly evident. This is typical of satellite signatures for SI/SSC types of events associated with pressure pulses. Figure 3-5 shows the GOES-5 magnetic field data also in HDV coordinates. The signal is clearly similar to the SCATHA data. Note that because of the low resolution of the data, it is not possible to time the signal from SCATHA to GOES, even though GOES is three hours dawnward of SCATHA. AMPTE/CCE is near the same local time as GOES, displaced 1.6 Re radially outward. The AMPTE data in figure 3-6 is in GSM coordinates so that the Z direction corresponds closely to the field-aligned component. This signal shows the same compression of the magnetic field as the other satellites. Figure 3-7 shows the total field from all three satellites. Notice that the amplitude of the compressional increase decreases with distance tailward (5.2 Re from SCATHA to GOES) and radially inward (1.6 Re from AMPTE to GOES) from the nose.

Ground Data

Table 3-3 shows a list of all of the ground stations used in this study. They fall into four categories: EISCAT magnetometers, high resolution Finnish magnetometers, world ground magnetometers of the Finnish Meteorological Institute (FMI), which we will sometimes refer to as "synoptic" magnetometers, and miscellaneous stations. The EISCAT magnetometer cross consists of five stations spanning 3.5° of magnetic latitude (63.69° to 67.19° degrees), with two stations placed as "outriggers" near the center of the north-south array forming a three station crossbar from 117.84 to 123.46 degrees (5.62 degrees east-west). The EISCAT data in the CDAW data base is in XYZ coordinates. The

Table 3-3:

| Stations | ID | Res | Glat | Glom | Mlat | Mlong |
|----------|----|-----|------|------|------|-------|
|----------|----|-----|------|------|------|-------|

EISCAT:

| | | | | | | |
|-------------|-----|-----|-------|-------|-------|--------|
| Soroya | SOR | 20s | 70.50 | 22.22 | 67.19 | 120.71 |
| Alta | ALT | 20s | 69.90 | 22.96 | 66.55 | 120.53 |
| Kautoleino | KAU | 20s | 69.00 | 23.05 | 65.74 | 119.55 |
| Muonio | MUO | 20s | 68.00 | 23.53 | 64.77 | 118.84 |
| Pello | PEL | 20s | 66.90 | 24.08 | 63.69 | 118.16 |
| Kilpisjarvi | KIL | 20s | 69.10 | 20.70 | 66.22 | 117.84 |
| Kevo | KEV | 20s | 69.80 | 27.01 | 65.80 | 123.46 |

High Resolution Stations:

| | | | | | | |
|-------------|-----|----|-------|-------|-------|--------|
| Ivalo | IVA | 1s | 68.60 | 27.48 | 64.66 | 122.52 |
| Kilpisjarvi | KIL | 1s | 69.02 | 20.87 | 66.12 | 117.88 |
| Rovaniemi | ROV | 1s | 66.77 | 25.94 | 63.26 | 119.52 |

FMI World Magnetometers:

| | | | | | | |
|----------------|-----|----|-------|---------|-------|---------|
| Baker Lake | BLC | 1m | 64.33 | -96.03 | 73.67 | -39.85 |
| Barrow | BRW | 1m | 71.30 | -156.75 | 69.10 | -116.33 |
| Cambridge Bay | CBB | 1m | 69.10 | -105.00 | 76.77 | -60.87 |
| College | COL | 1m | 64.87 | -147.83 | 65.10 | -100.77 |
| Cape Schmidt | CPS | 1m | 68.92 | -179.48 | 63.38 | -130.46 |
| Eskdalemuir | ESK | 1m | 55.32 | -3.20 | 58.05 | 84.07 |
| Fort Churchill | FCC | 1m | 58.80 | -94.10 | 67.28 | -70.60 |
| Godhaven | GDH | 1m | 69.32 | -53.52 | 79.25 | 34.62 |
| Glenlea | GLL | 1m | 49.53 | 262.87 | 59.19 | -33.94 |
| Mould Bay | MBC | 1m | 76.30 | -119.40 | 79.62 | -100.11 |
| Murmansk | MMK | 1m | 68.25 | 33.08 | 63.46 | 126.43 |
| Narssarssuaq | NAQ | 1m | 61.20 | -45.40 | 70.60 | 38.66 |
| Ottawa | OTT | 1m | 45.40 | -75.55 | 56.37 | -5.89 |
| Poste-de-la-B | PDB | 1m | 55.20 | -77.70 | 66.31 | -2.62 |
| Resolute | RES | 1m | 64.70 | -94.90 | 83.14 | -64.02 |
| Sitka | SIK | 1m | 57.10 | -135.30 | 60.31 | -81.88 |
| Sodankyla | SOD | 1m | 67.37 | -26.63 | 63.68 | 120.64 |
| St. Johns | STJ | 1m | 47.60 | -52.60 | 57.91 | 23.39 |
| Thule | THL | 1m | 77.48 | -69.17 | 88.46 | 14.10 |
| Victoria | VIC | 1m | 48.50 | -123.40 | 54.33 | -64.34 |
| Yellowknife | YEK | 1m | 62.43 | -114.40 | 69.14 | -63.44 |

Miscellaneous Stations:

| | | | | | | |
|------------|-----|-----|--------|--------|--------|------|
| Iqaluit | IQA | 10s | 63.80 | 291.50 | 74.77 | 3.97 |
| South Pole | SPA | 10s | -90.00 | 0.00 | -78.98 | 0.00 |

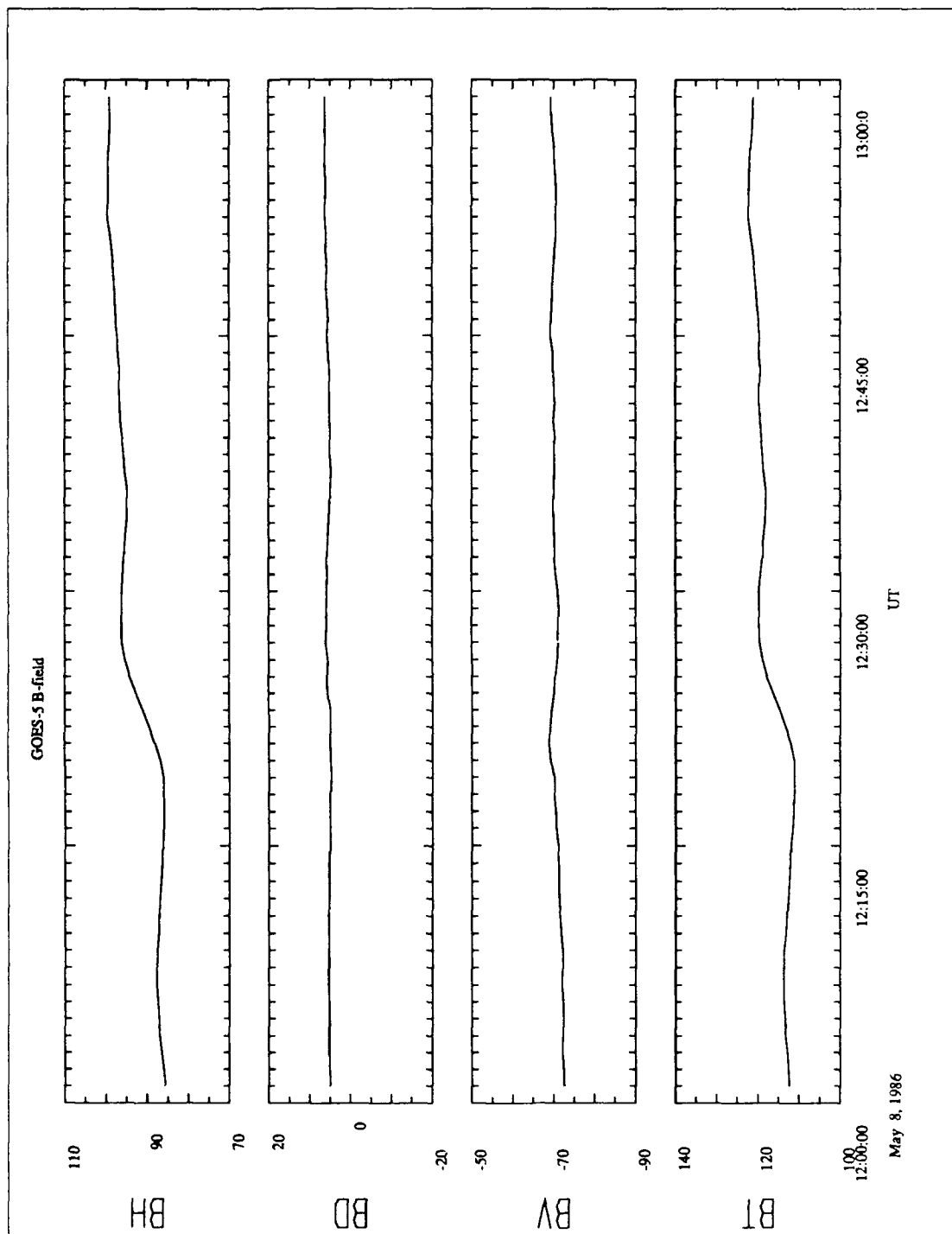


figure 3-5

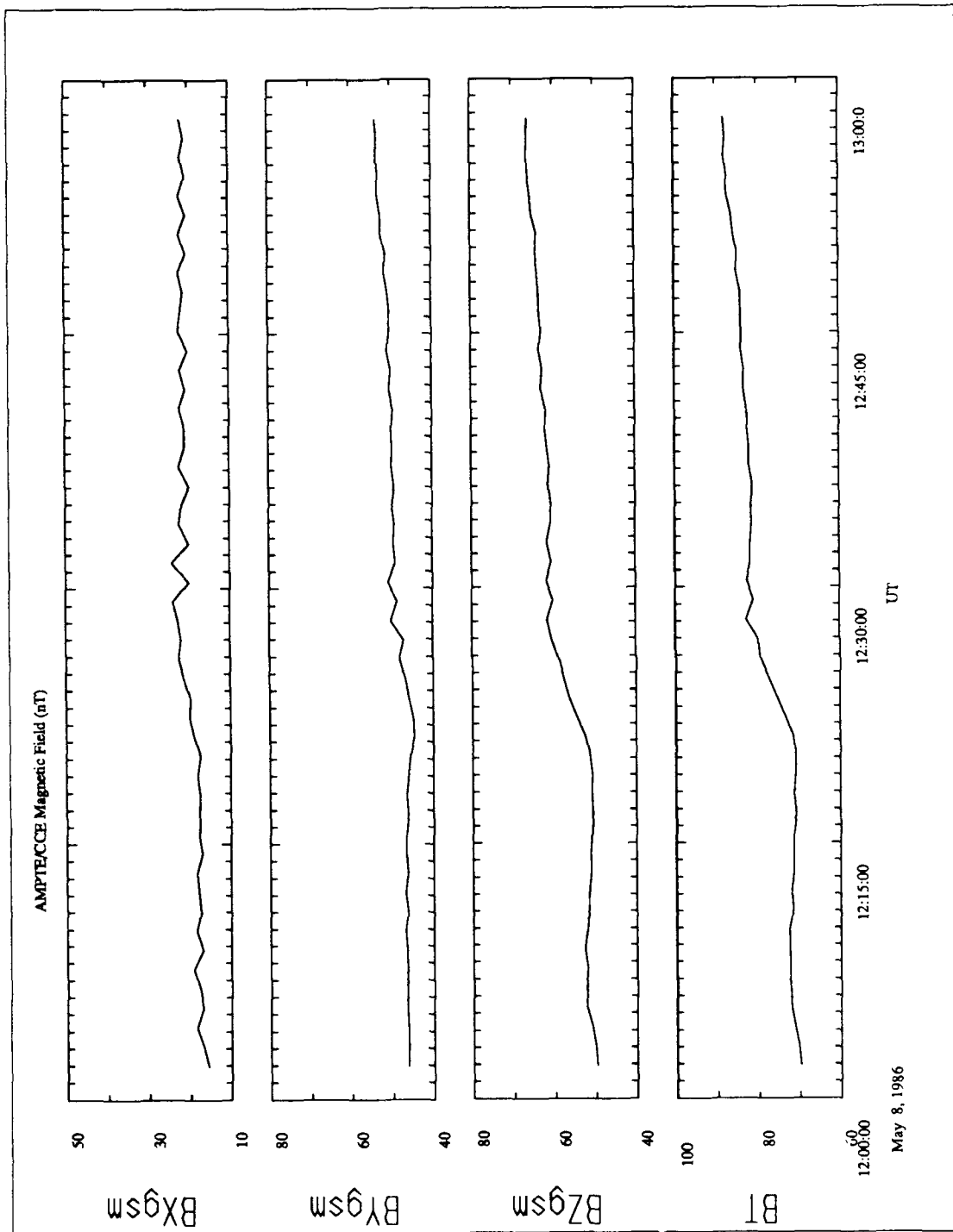


figure 3-6

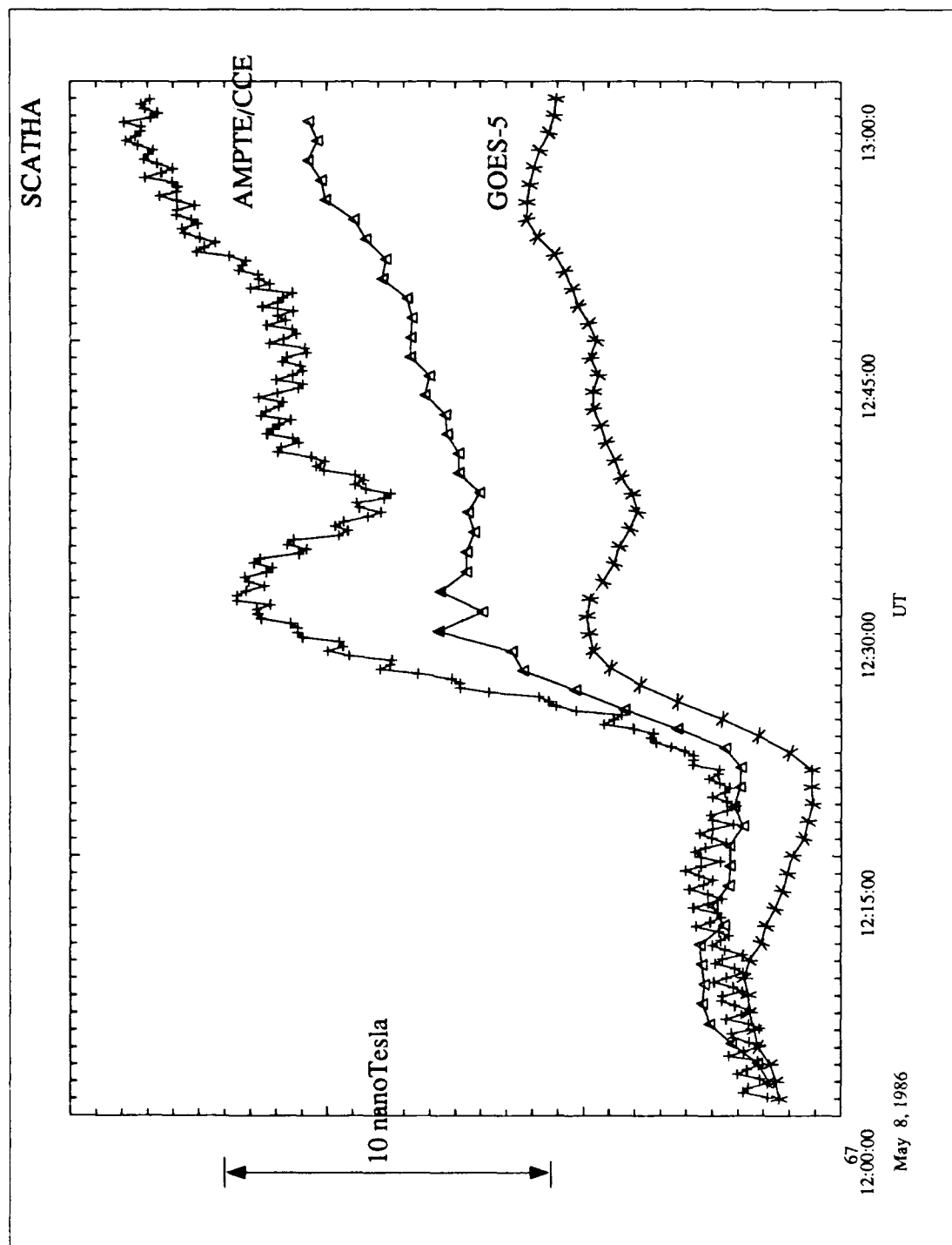


figure 3-7

X-axis is displaced 5.5° from the geomagnetic north (H. Luehr, personal communication). Figure 3-8(a-c) shows stack plots from the north-south portion of the array for each component. The northern most station is at the top of each plot. These signals have been high-passed filtered by subtracting a 20 minute running average in order to remove background trends. These plots show the impulsive character of the event, which matches the basic event selection criteria already discussed. The event appears to consist of a large impulse beginning around 12:32 UT, followed by two or three smaller waves. The total duration of the event is approximately 20 minutes. Roughly colocated with the EISCAT stations are three high resolution stations: Ivalo, Kilpisjarvi, and Rovaniemi. The induction coil magnetometers at these stations are capable of 0.1 second resolution. The data in the CDAW data base consists of 1 second averages. This makes this set of ground stations much better suited for timing signal propagation. The data from these stations is in HDZ coordinates. Figure 3-9 shows the three components of the magnetic perturbation at Rovaniemi, which are characteristic of all three stations. The signals closely resemble the EISCAT data, with the addition of a small high frequency component. Following Lanzerotti et al. (1988) we will also be examining the data from a set of conjugate stations, Iqaluit and South Pole station. The magnetometer data from these stations have a 10 second resolution and are given in HDZ coordinates. Figure 3-10 shows the basic (filtered) data from these two stations. The Iqaluit data show a strong positive deflection of all three components beginning at 12:21 that increases more or less uniformly until 12:26, and decays back over 6 to 10 minutes. This general trend can be seen in the South Pole data, somewhat attenuated, and the D and Z perturbations are negative. Also in the South pole data is evidence for a higher frequency pulsation at 12:26 with a period of 2-3 minutes. This signal in turn is reflected at Iqaluit as small deflections on the more

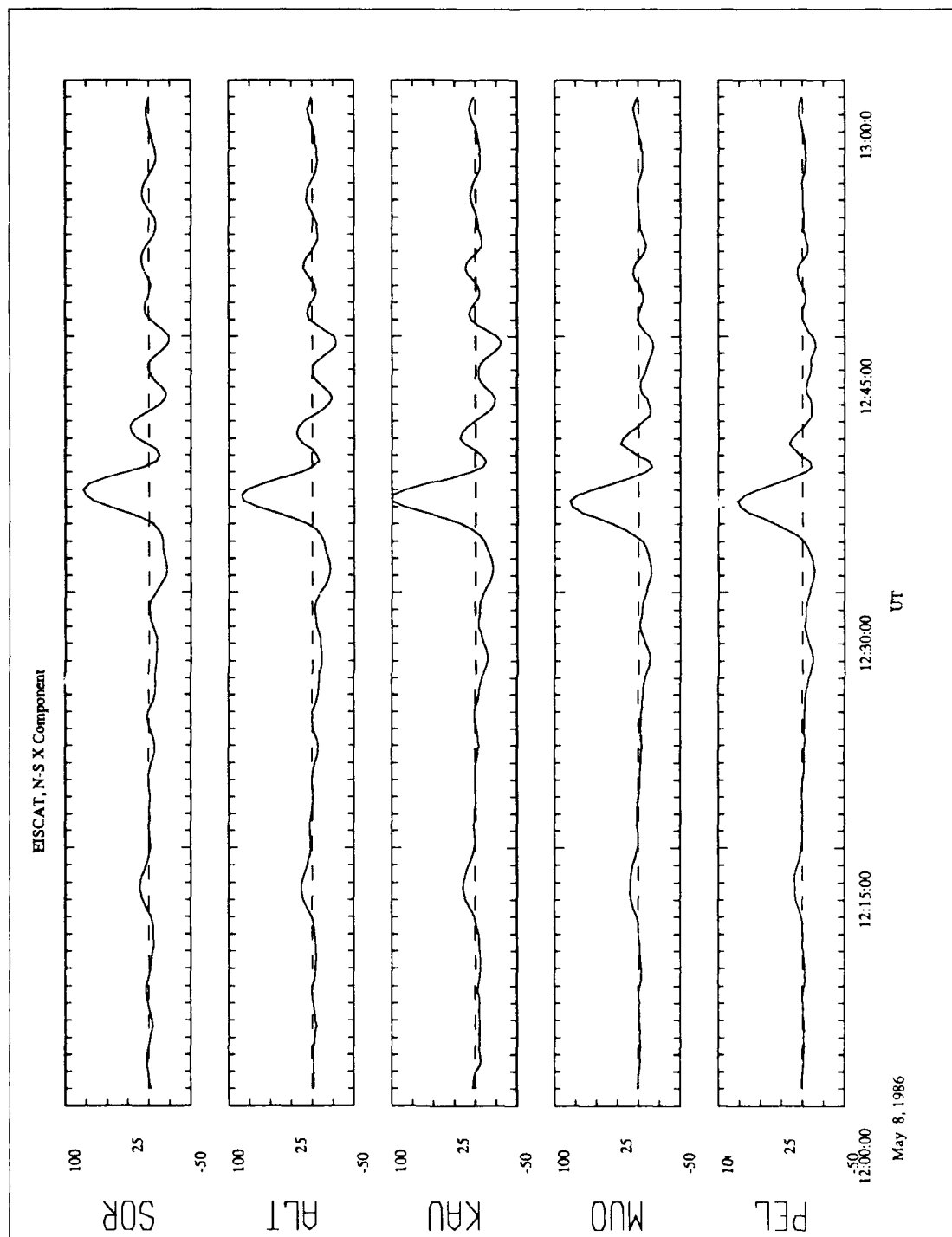


figure 3-8a

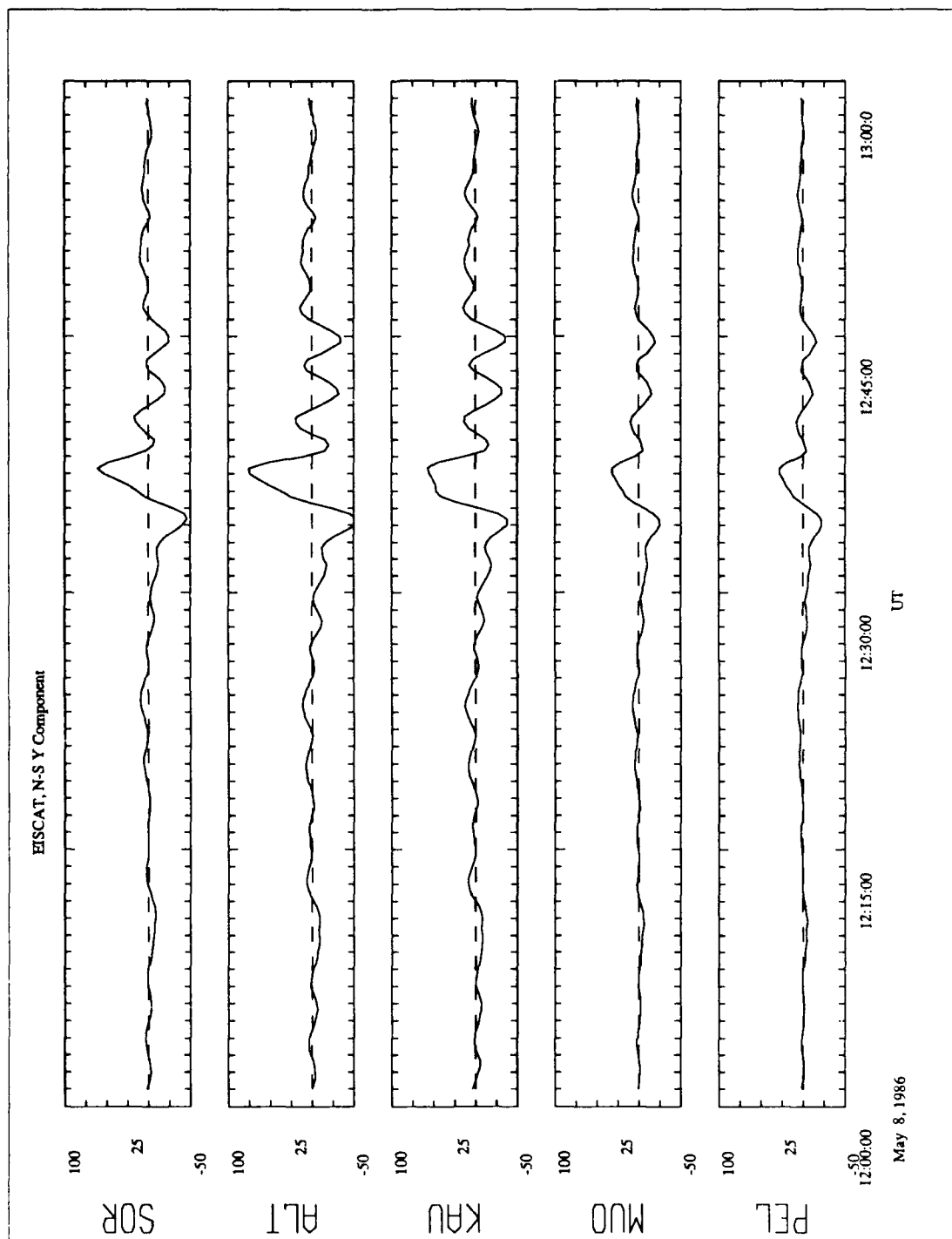


figure 3-8b

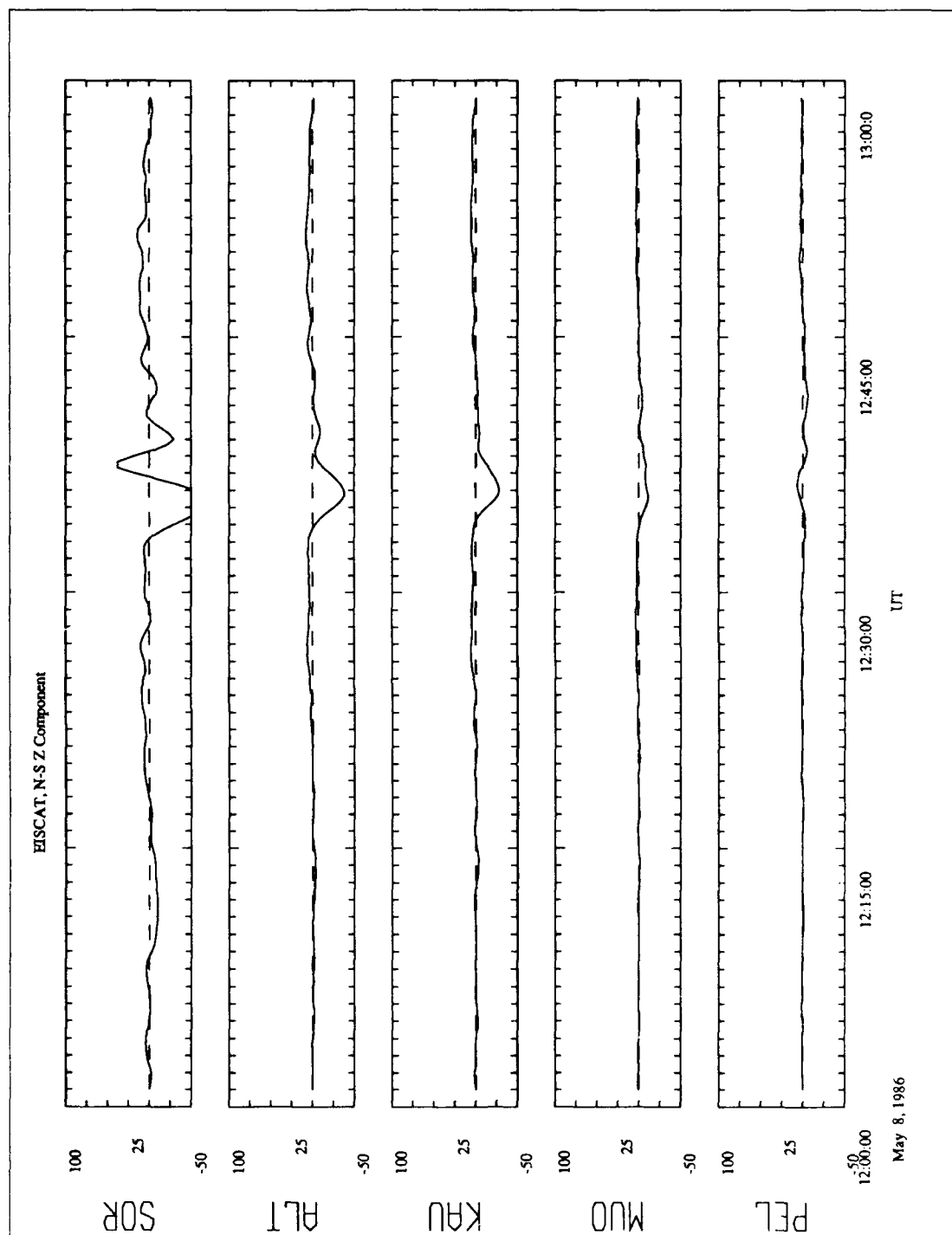


figure 3-8c

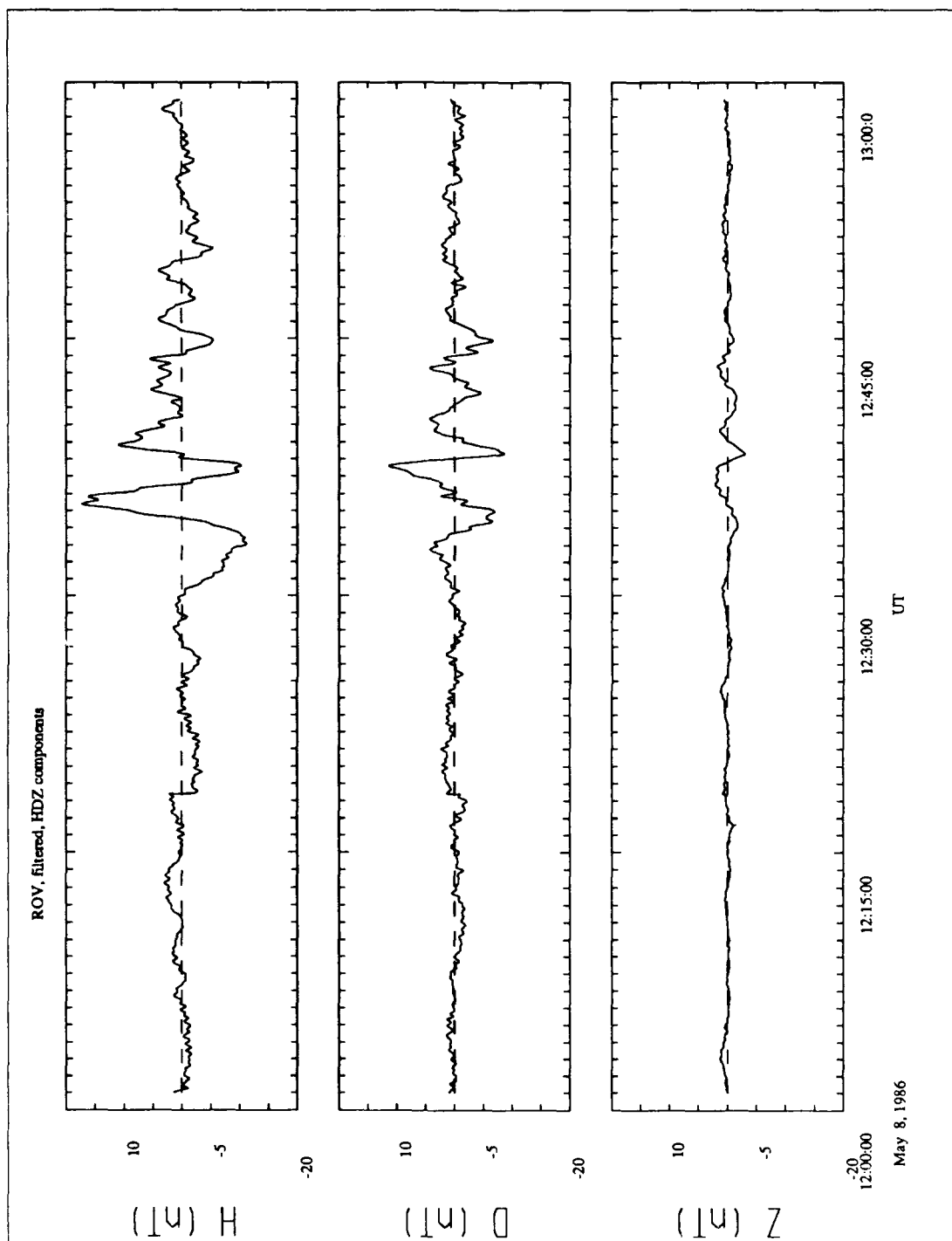


figure 3-9

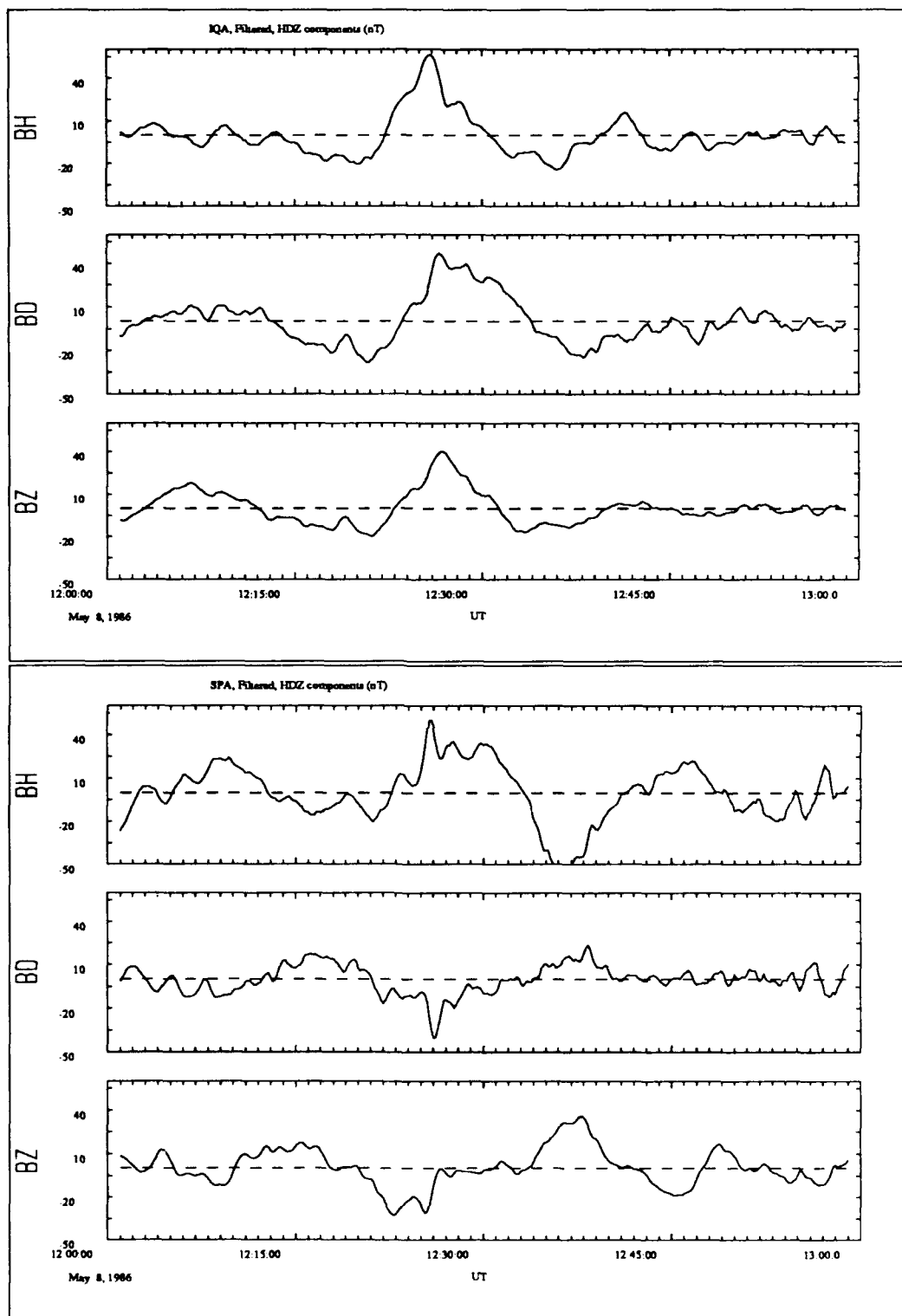


figure 3-10

general trend just described. In order to investigate the global characteristics of the event we used 22 stations from the FMI's world ground magnetometer network. These stations are widely spaced and represent the low resolution end (one minute) of the instruments used. The coordinate system for these data in the CDAW data base is XYZ coordinates.

AE Index

Figure 3-11 shows the AE index during the event studied. The substorm activity is clearly evident. There are four onsets as determined by the detection of nightside Pi2s at 1131, 1150, 1152, and 1215 UT (R. McPherron, personal communication).

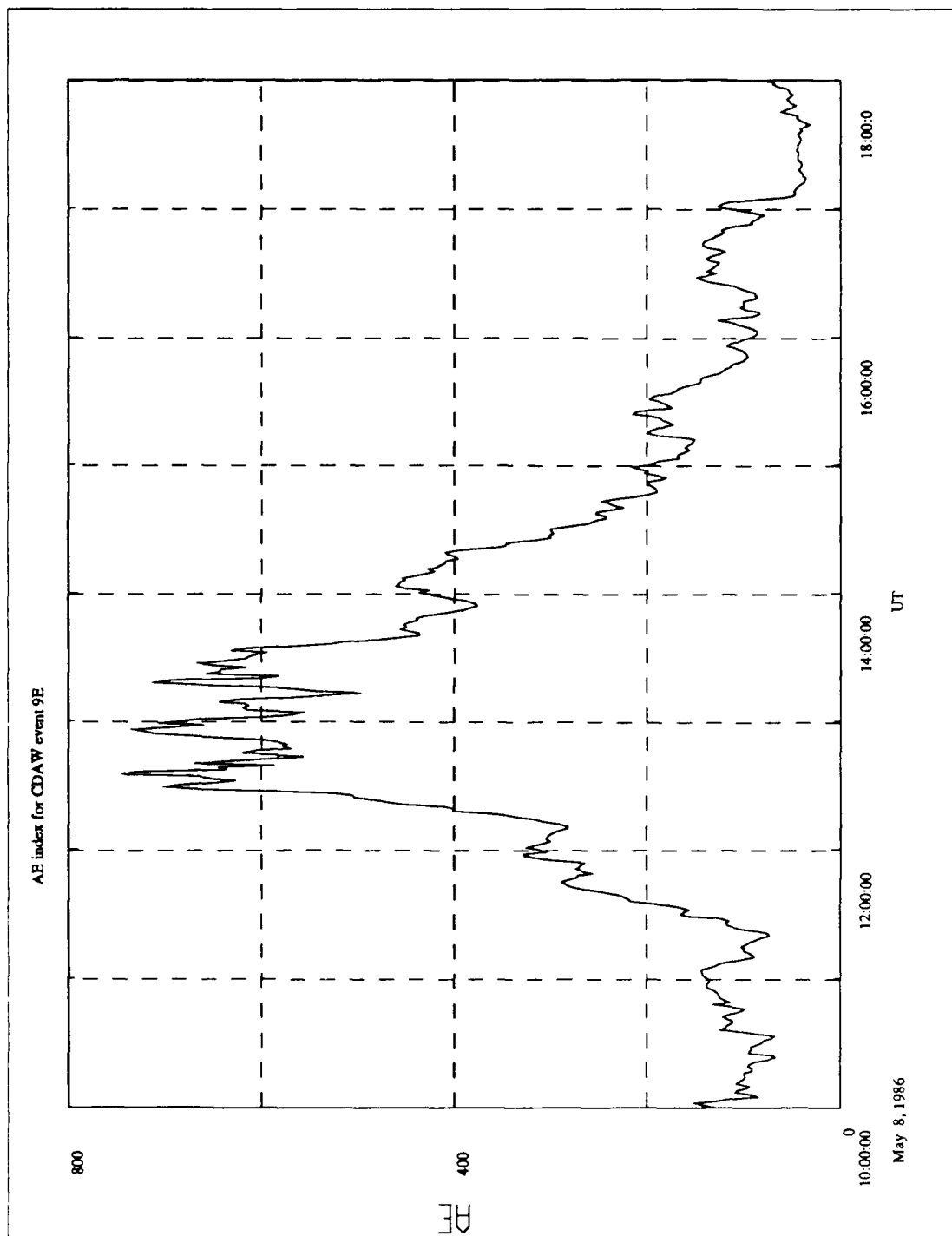


figure 3-11

Chapter 4: Analysis.

Data Preparation

To isolate the pulsations of interest we usually high pass filter the data by subtracting a 20 minute running average. This removes low frequencies and the background field. Occasionally we transform the ground data into cylindrical coordinates. From an HDZ or XYZ system Z remains the same, the rho (radial) component corresponds to the magnitude of the horizontal perturbation and an angle theta gives the phase. It is a well known result that the ionosphere rotates electromagnetic signals passing through it and that the amount of rotation depends on the ionospheric conductivity (Glaßmeier, 1988). The rho component provides a consistent measurement for comparing stations without compensating for phase differences or worrying about whether the original coordinate system is XYZ or HDZ.

Power Spectra

One of the primary goals of this analysis is to show that the ground signal is causally linked to the solar wind. As a first step we compared power spectra of solar wind and ground magnetometers to insure that there is power in the necessary frequencies to drive the ground response. Because of their high time resolution we used the stations near EISCAT for the power spectra on the ground. Figure 4-1 shows the spectra from Ivalo. There is a broad enhancement of power from 2 to 10 milliHertz (corresponding to periods from 8.3 to 1.7 minutes) and a narrower one from 20 to 30 milliHertz (50 to 30 seconds). At every frequency we can see that there is more power in the north-south (H component) than in the east-west (D component) direction. Power spectra from the other stations show similar features. In the solar wind the low resolution of the plasma

Power Spectral Density for Ivalo

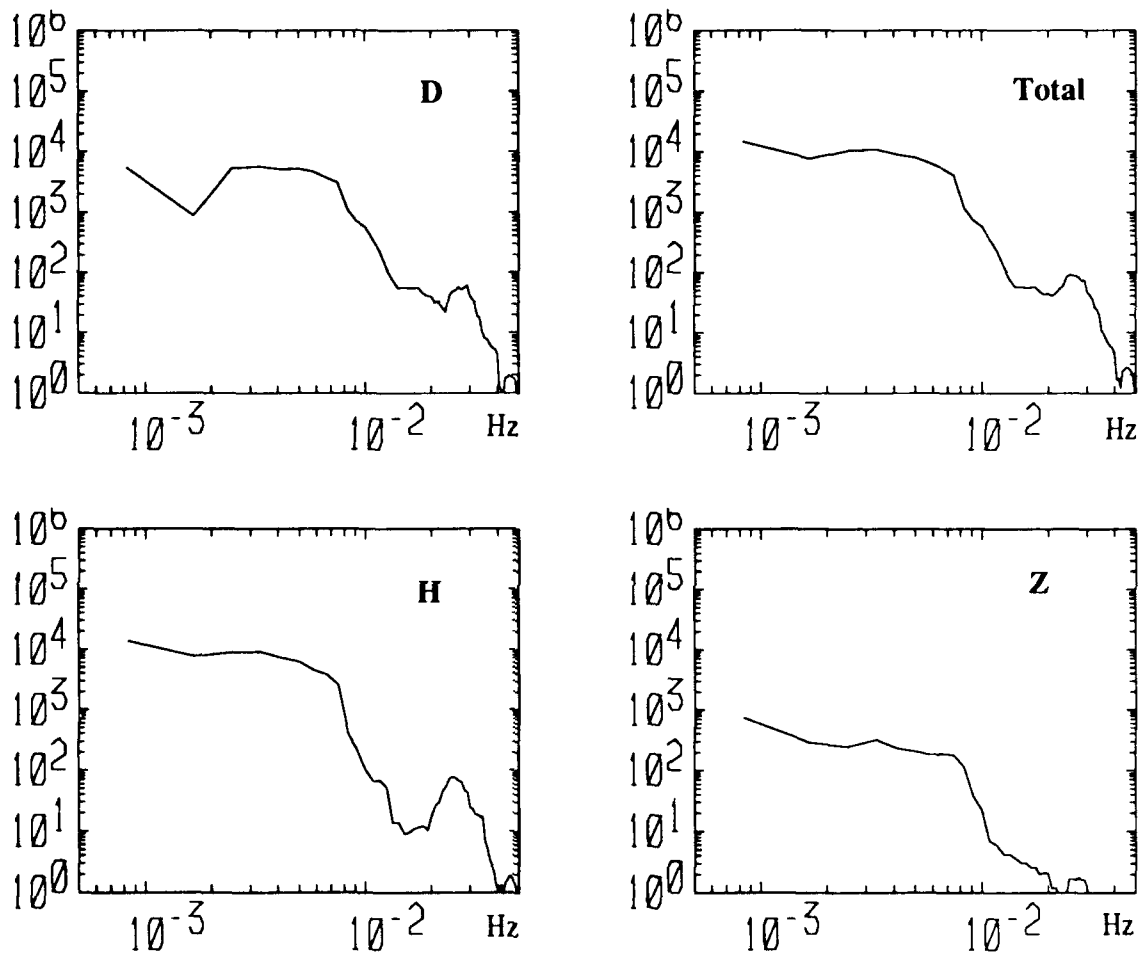


figure 4-1

data makes it difficult to produce a good spectrum. Power spectra for the IMF at IMP-8 are shown in figure 4-2. There are several peaks in each of the frequency ranges noted in the ground spectra. We can conclude that the solar wind is a reasonable source for the ground pulsations.

Timing Methods

Determining propagation times is important for linking the ground response to the solar wind and interpreting the behavior of the signal as it moves through various regimes in the geospace environment. Computing time delays from time series can be done by visual inspection, algorithmic detection, or cross-correlations. Visual inspections are fairly easy to accomplish for most events, but eliminating subjective biases can be difficult. If an algorithmic detection scheme can be implemented it can give more objective results, or at least results with systematic biases. Cross-correlations can give reasonably objective time lags between two "well-behaved" signals, but are difficult to implement for unequally spaced data or with two time series of different resolutions. In this paper we will usually use cross-correlations for determining time delays on the ground. Because of the varying formats between spaced based data, timing is done with a simple algorithm that finds the inflection point on the rising portion of the signal or by tracking peaks in the time series.

Solar Wind to Ground Timing

The solar wind does not propagate directly into the magnetosphere. An increase in the solar wind pressure displaces the magnetopause which results in increased Chapman-Ferraro currents, and a corresponding increase in the magnetospheric field. Thus in the magnetosphere we compare the solar wind signal to the magnetic field magnitude as measured by the satellite closest to the nose of the magnetopause, in this case SCATHA.

Power Spectral Density at IMP-8

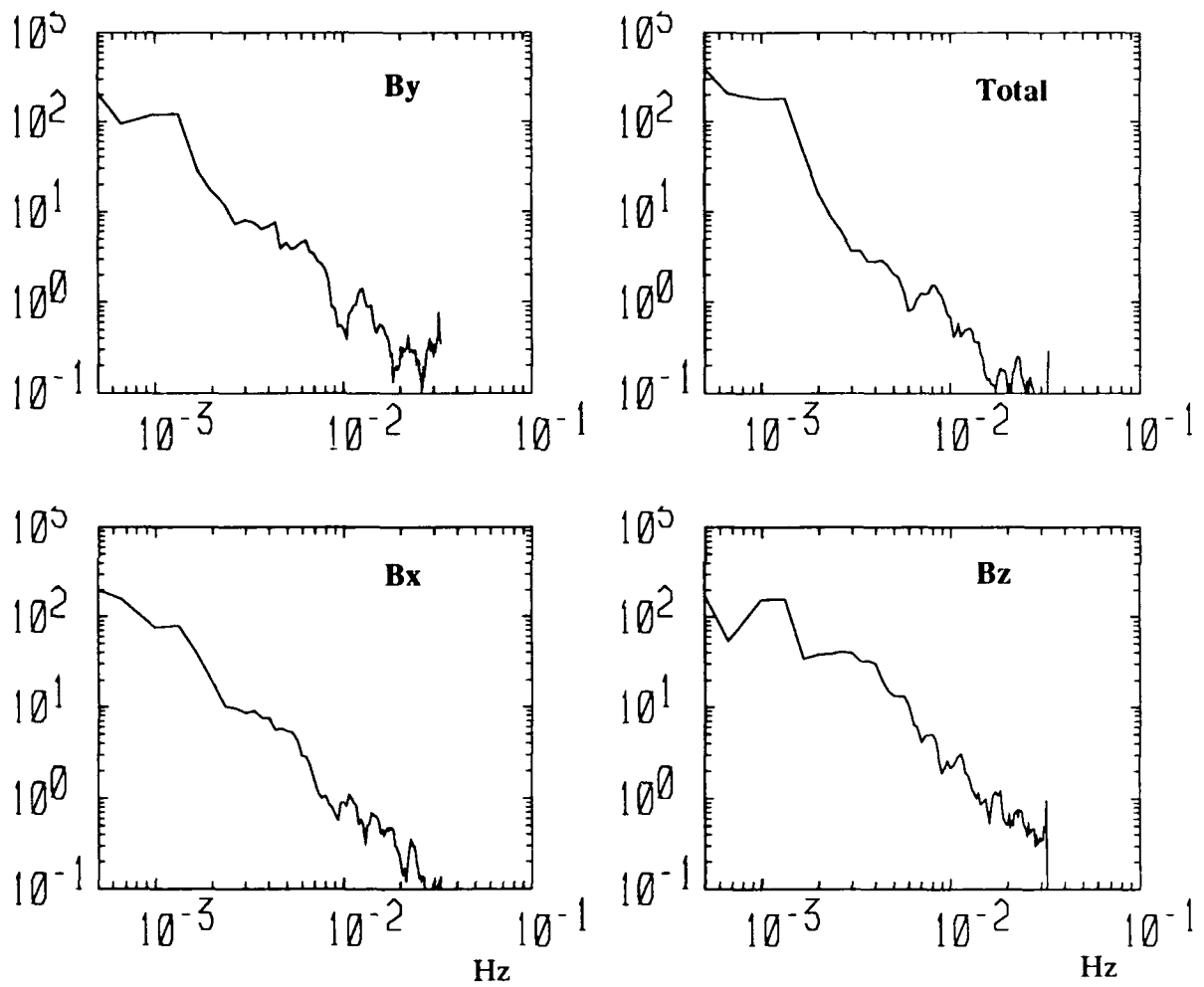


figure 4-2

Figure 4-3 shows a plot of the total solar wind pressure and SCATHA magnetic field intensity. Note that the rise time for the pressure pulse is on the order of 10 minutes. The two signals are separated by only two minutes (12:22 UT in the solar wind determined by the inflection point, 12:24 UT at SCATHA). At 425 km/sec it should take the solar wind seven minutes to flow from 37 Re at IMP-8 to 9 Re at the magnetopause. Moving at a typical fast mode velocity inside the magnetosphere of 1000 km/sec it should only take the signal 12 seconds to reach SCATHA from the nose of the magnetopause. Even if the signal does not originate at the nose, the time from the magnetopause to the satellite represents a relatively small fraction of the total transmission time. The short time delay from the solar wind monitor implies that the front associated with the density enhancement must be highly inclined to the flow. Just prior to this time the IMF is nearly radial, so assuming that the density front is aligned with the IMF can easily explain the short time delay. We will discuss some of the implications of this assumption in more detail in the next chapter. Coupling from SCATHA to the high latitude ionosphere via Alfvén waves will take about two minutes. Using the Tsyganenko 1989 magnetic field model (Tsyganenko, 1989) to map SCATHA to its northern magnetic conjugate point we find that the footpoint is within half a degree of Narssarssauq (NAQ) at 12:30 UT. Comparison of the signals at SCATHA and NAQ (figure 4-4) shows good agreement with a two minute transmission time. There is some uncertainty in this measurement because the ground data time resolution is only one minute.

Substorm Effects

As we noted earlier, there is a substorm in progress during this event. The onset of the expansion phase (12:27 UT) coincides with passage of the pressure pulse. We do not expect this to have a significant impact on the measurements made by the dayside

***Dynamic Pressure (IMP-8) and
Magnetospheric B field amplitude (SCATHA)***

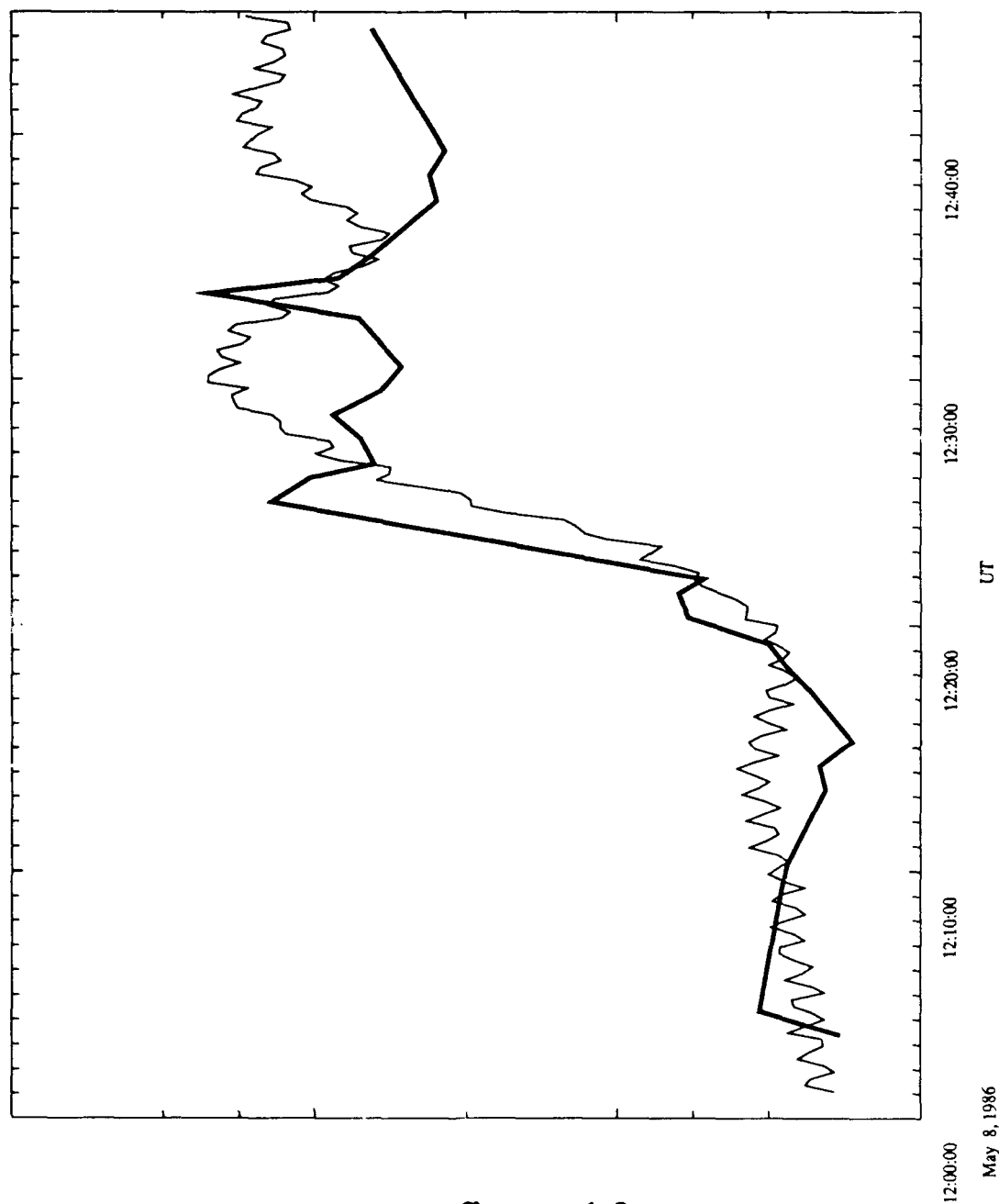


figure 4-3

NAQ versus SCATHA
Total Magnetic Field

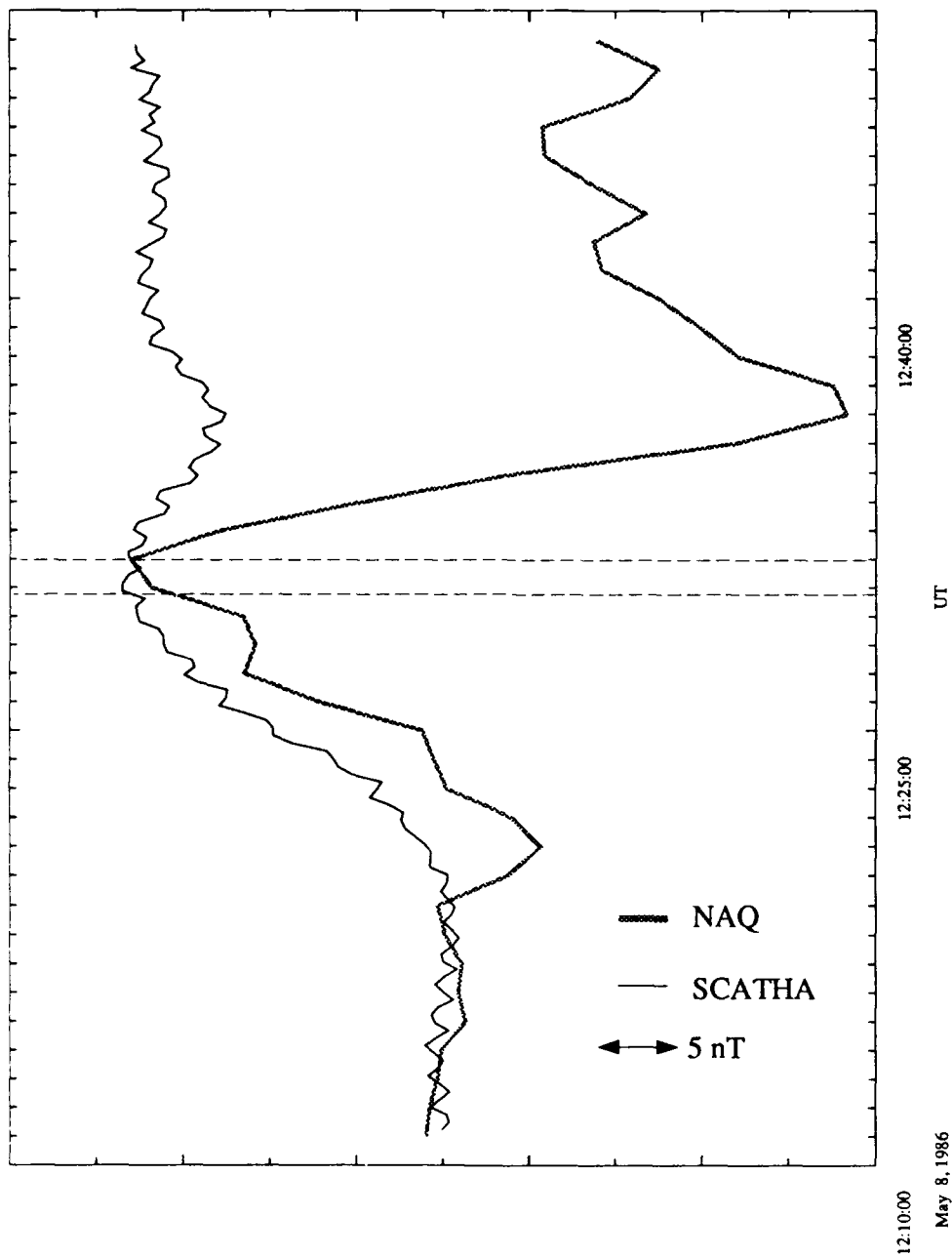


figure 4-4

satellites; however, there could be significant effects on the ground. There are three pieces of evidence which give us some assurance that the signals we are studying can be isolated from the substorm effects. In figure 4-5 we show eight hours of IMP-8 dynamic pressure and the x, y, and rho components of the ground magnetic field measured by the FMI station at Thule. The pressure increase at 12:22 UT and decrease at 14:01 UT are clearly evident in the IMP-8 data. The pressure signatures have a unique step-like character and the largest amplitudes in that time period. The ground magnetic signal shows two short periods of large amplitude waves complementary to the pressure data. The total horizontal perturbation (rho) shows a more distinct structure during these periods. This relationship helps isolate the ground response and strengthens the argument for causality. Another supporting piece of evidence is that the motion of the signal on the ground discussed in subsequent sections always shows tailward motion. If the disturbance is substorm related it would have been traveling in the opposite direction. In order to get a rough idea of the synoptic effects of the substorm, we have taken data from the FMI stations and produced several contour plots of the filtered Brho signal. We have used the horizontal perturbation component here to isolate regions of high and low signal strength without regard to polarity. Figure 4-6 shows the synoptic situation prior to the event at 12:10. Already there is a well developed magnetic signature in the nightside corresponding to the substorm. Figure 4-7 shows a series of plots during the event. There is a structured region that begins at the subsolar point and extends to the poles. The substorm signature is virtually the same as in figure 4-6 and seems well confined to the night side auroral zone regions, well away from the most critical stations.

Synoptic Evolution of the Signal

Figure 4-8 shows stack plots of the x, y, and rho components of the magnetic

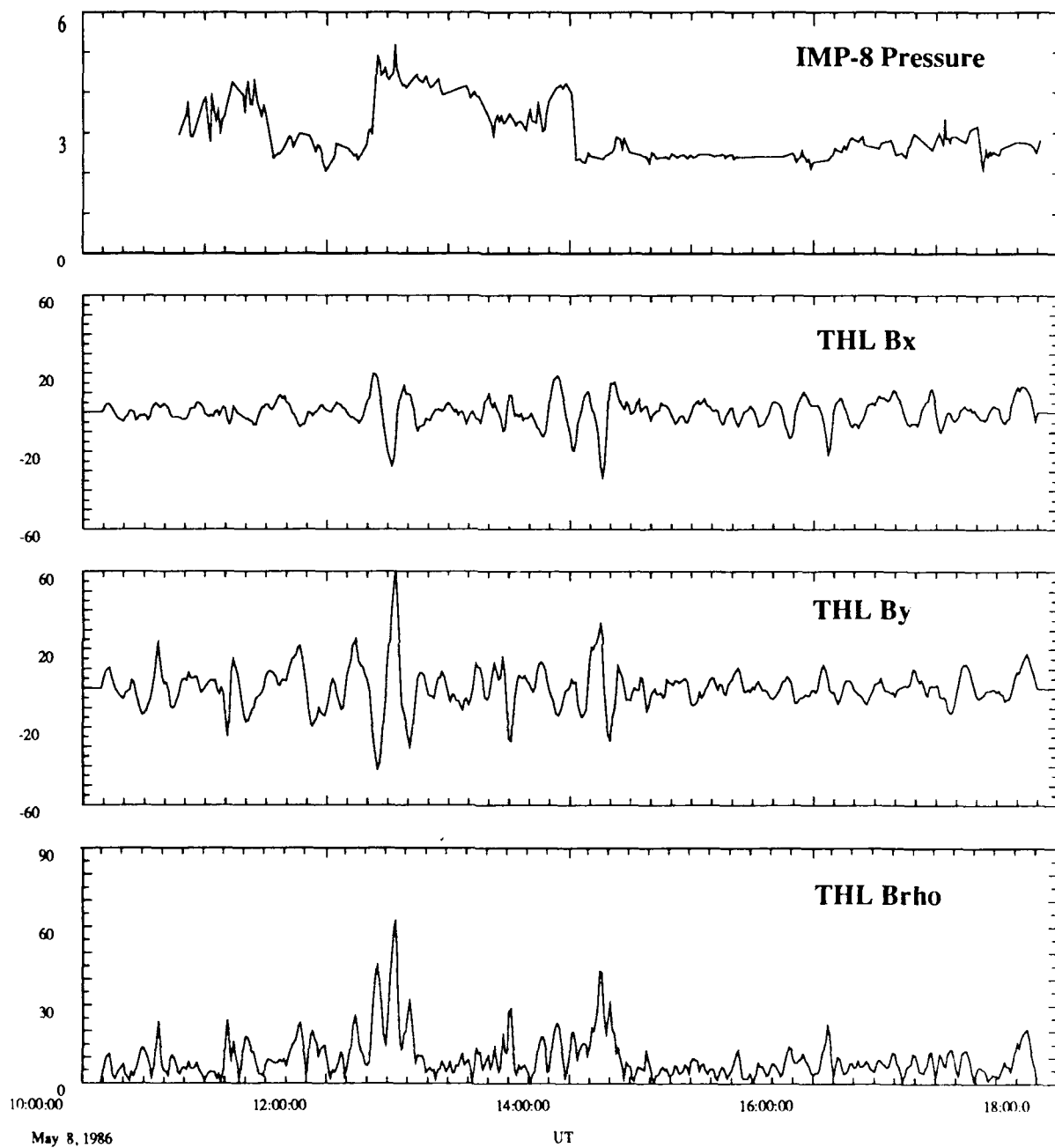


figure 4-5

Horizontal Magnetic Perturbation at 12:10 UT

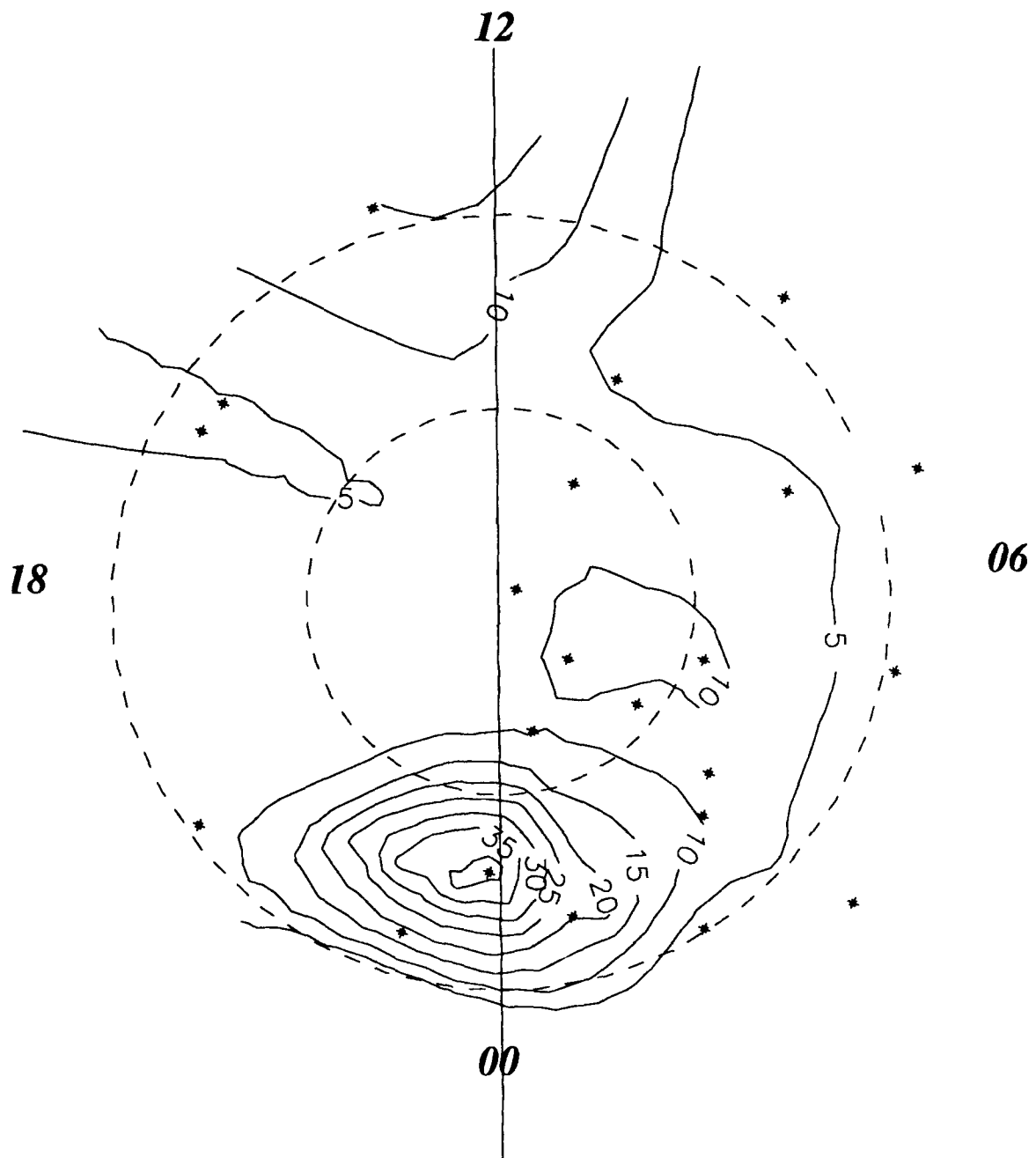


figure 4-6

Horizontal Magnetic Perturbation at 12:31 UT

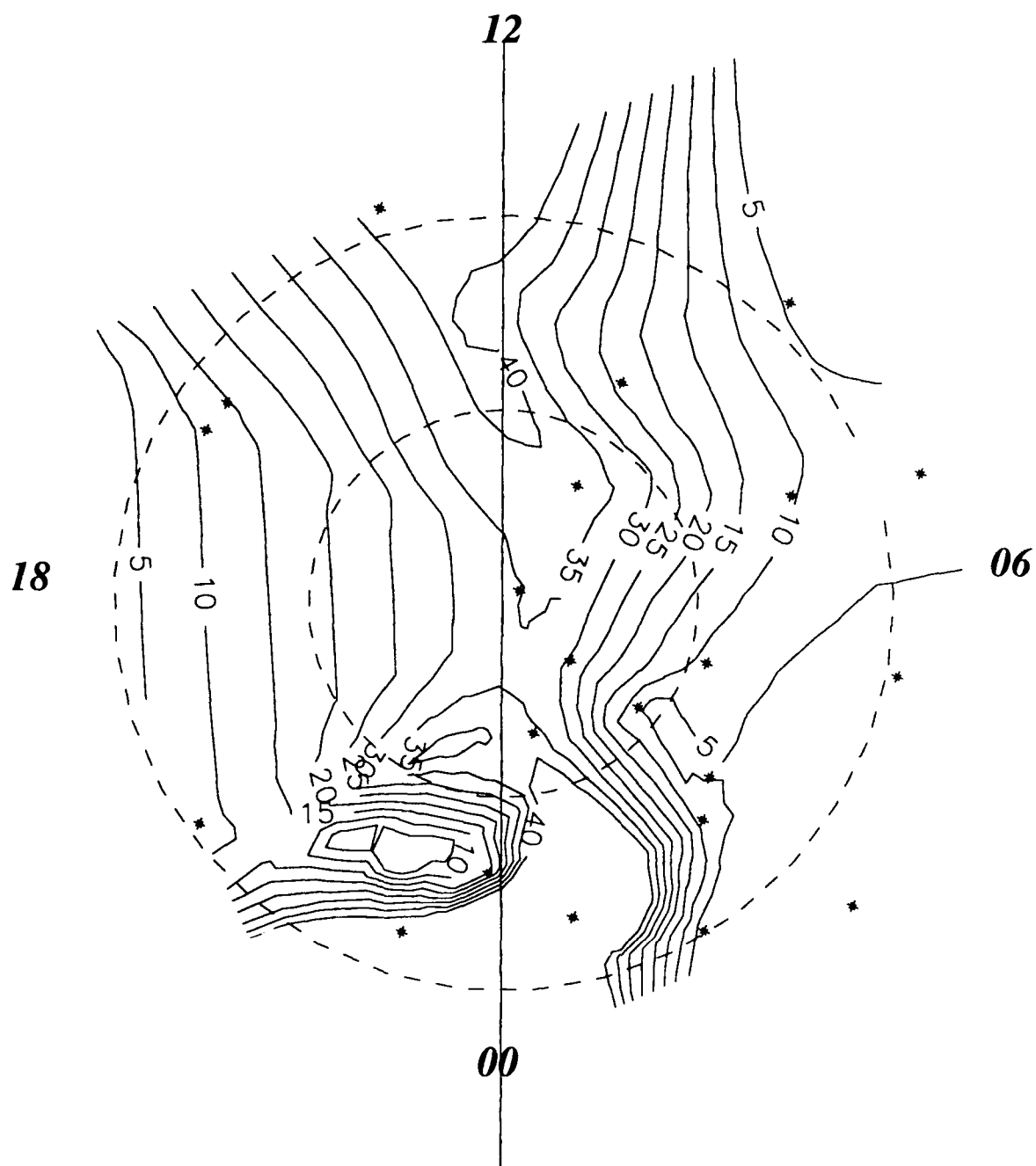


figure 4-7a

Horizontal Magnetic Perturbation at 12:32 UT

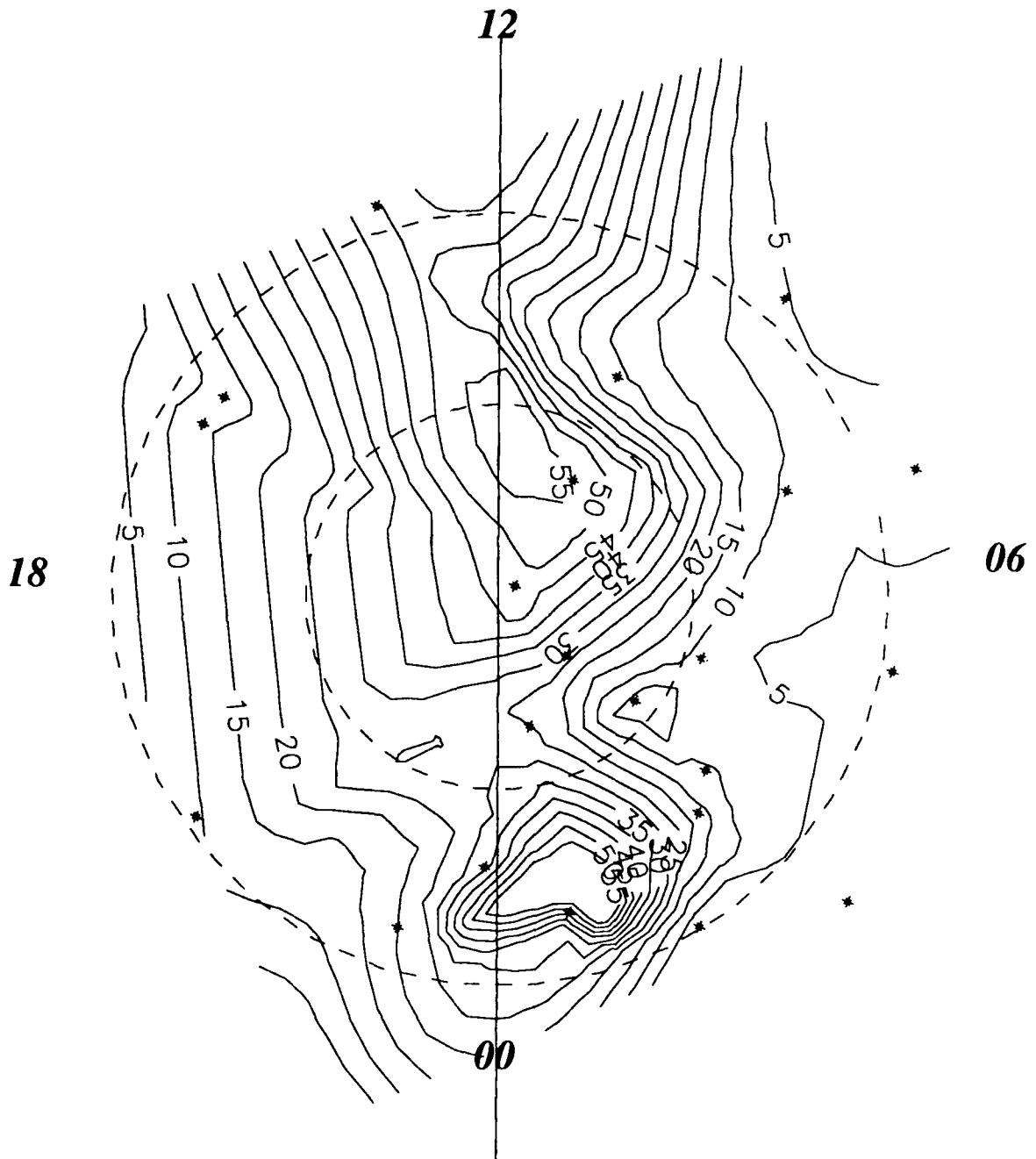


figure 4-7b

Horizontal Magnetic Perturbation at 12:33 UT

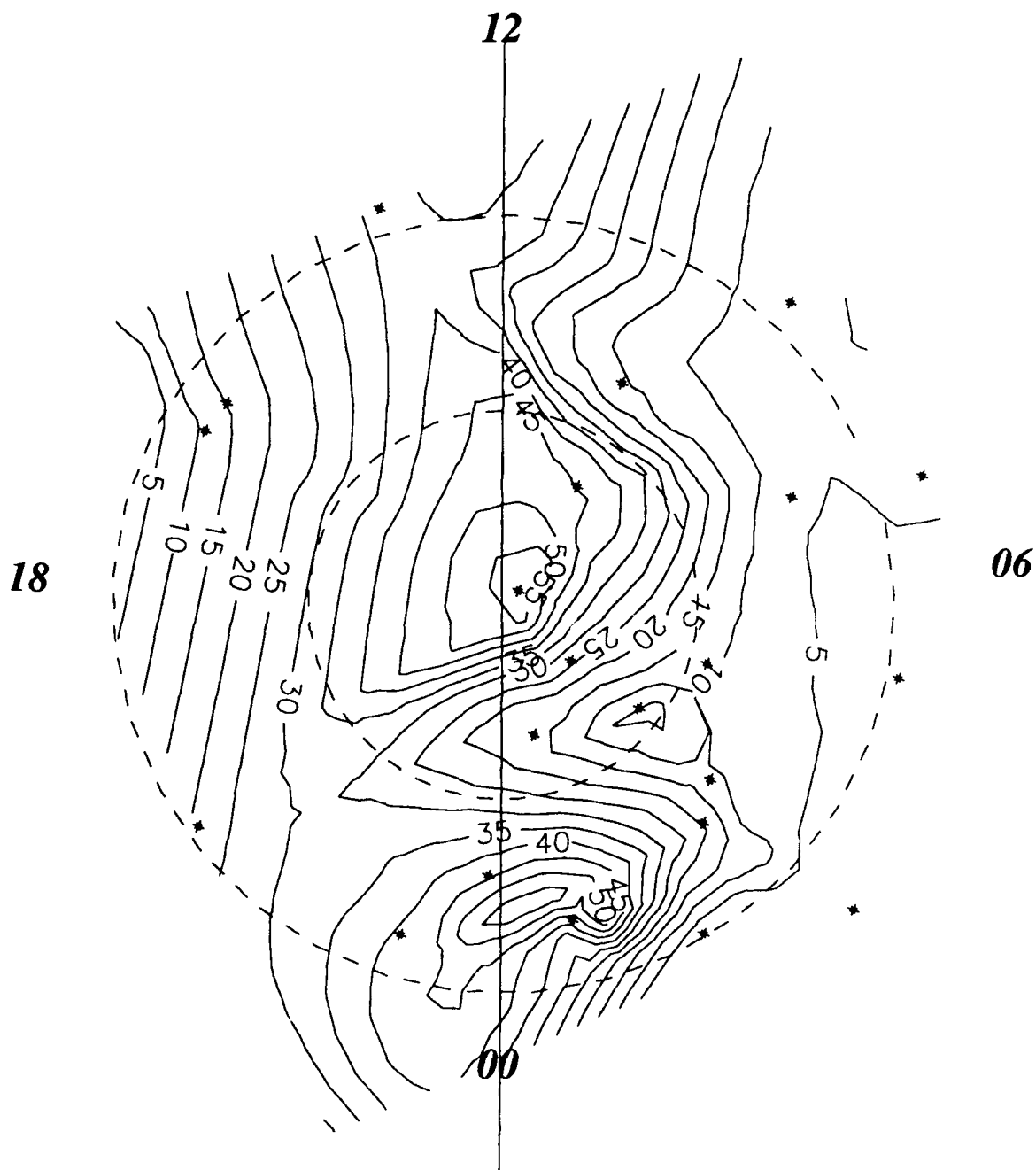


figure 4-7c

Horizontal Magnetic Perturbation at 12:34 UT

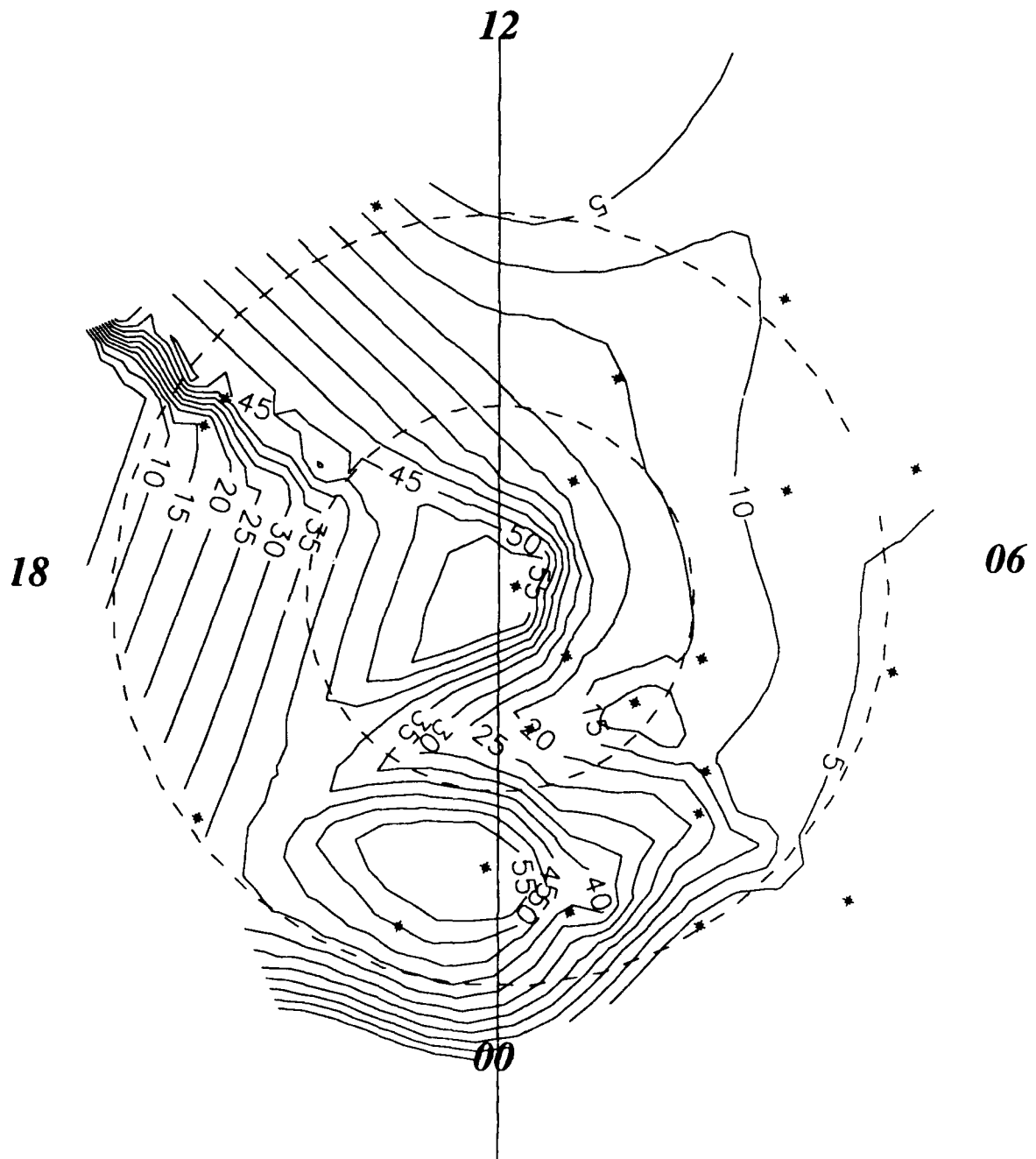


figure 4-7d

Horizontal Magnetic Perturbation at 12:35 UT

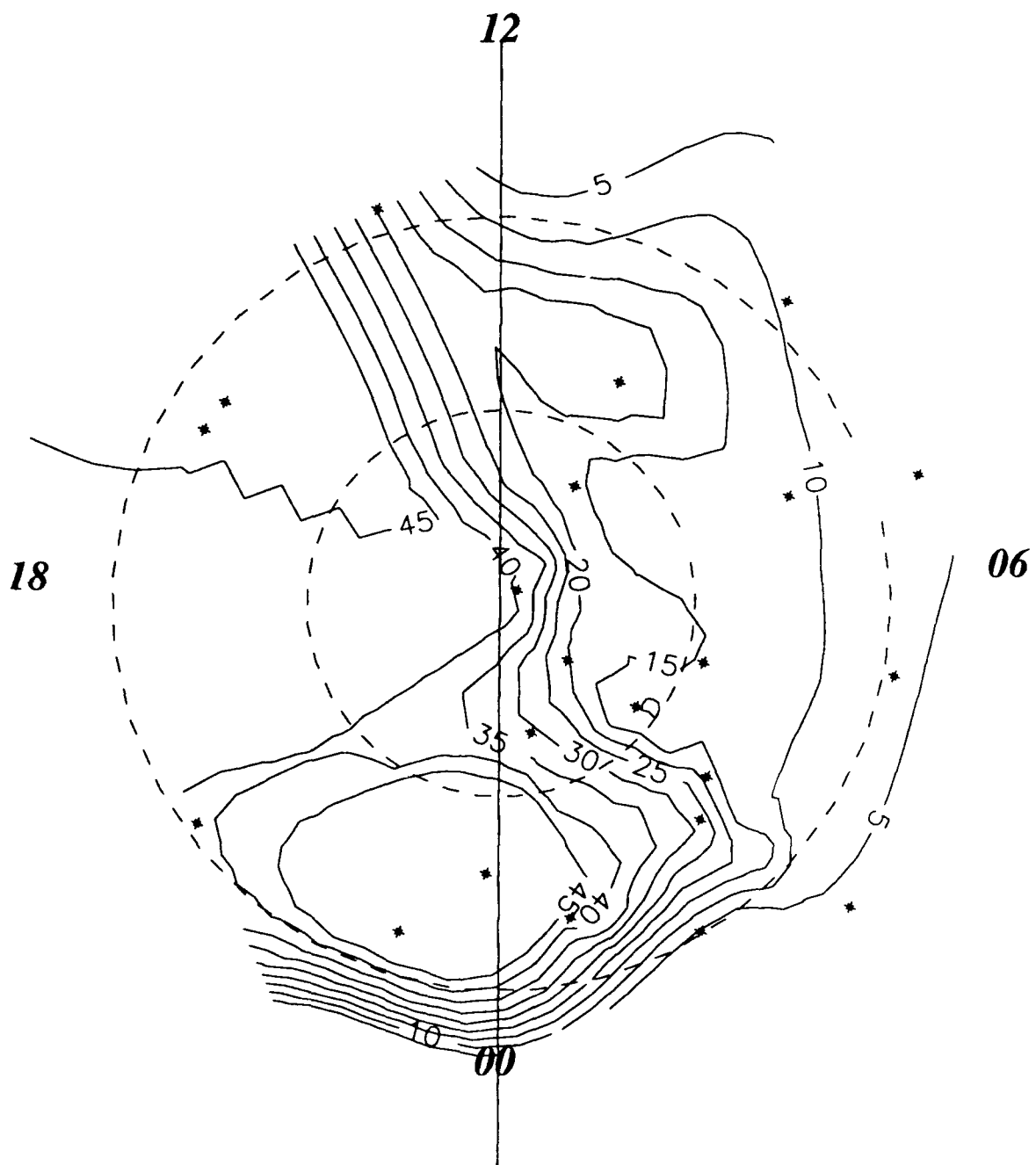


figure 4-7e

Horizontal Magnetic Perturbation at 12:36 UT

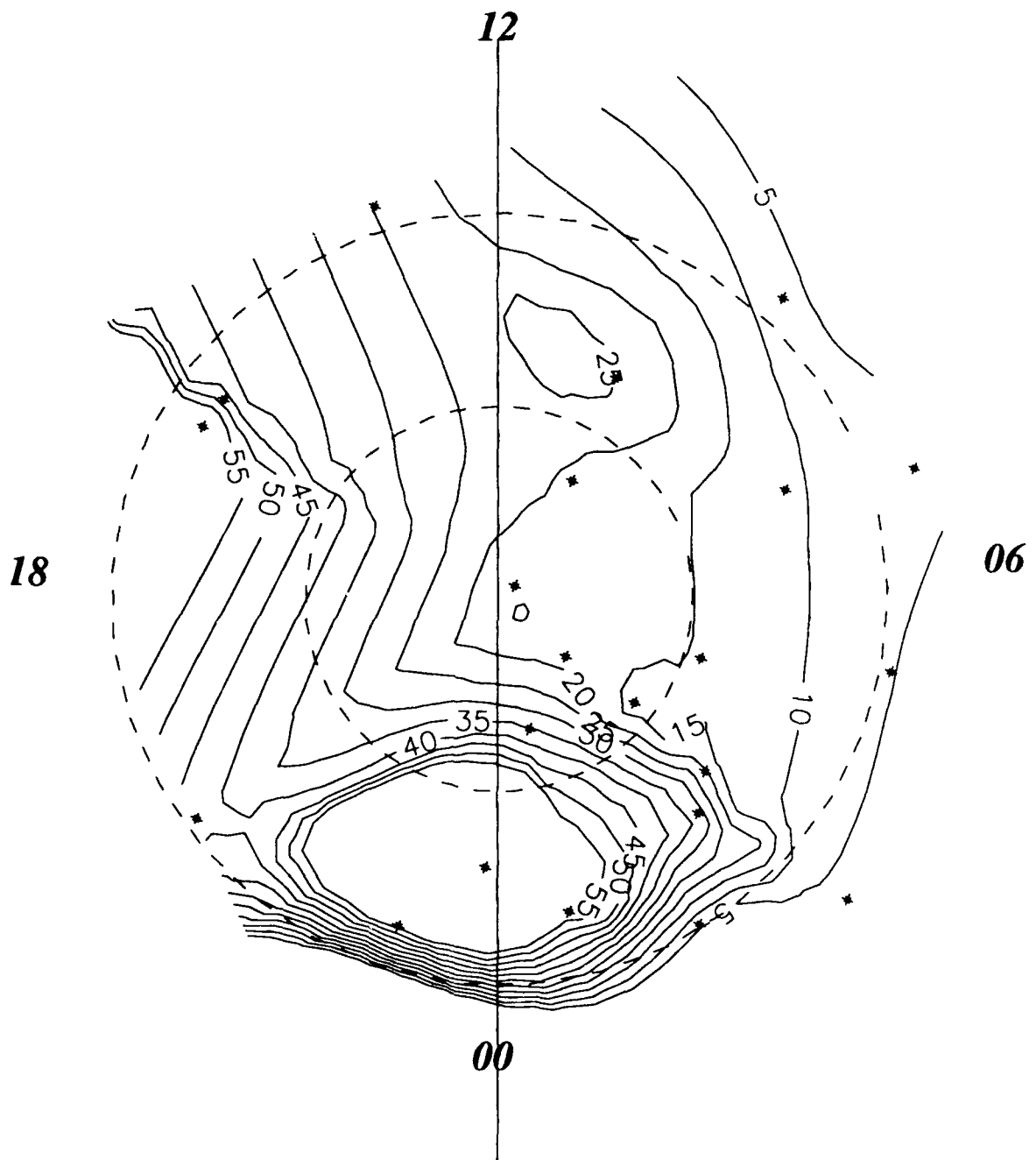


figure 4-7f

Horizontal Magnetic Perturbation at 12:37 UT

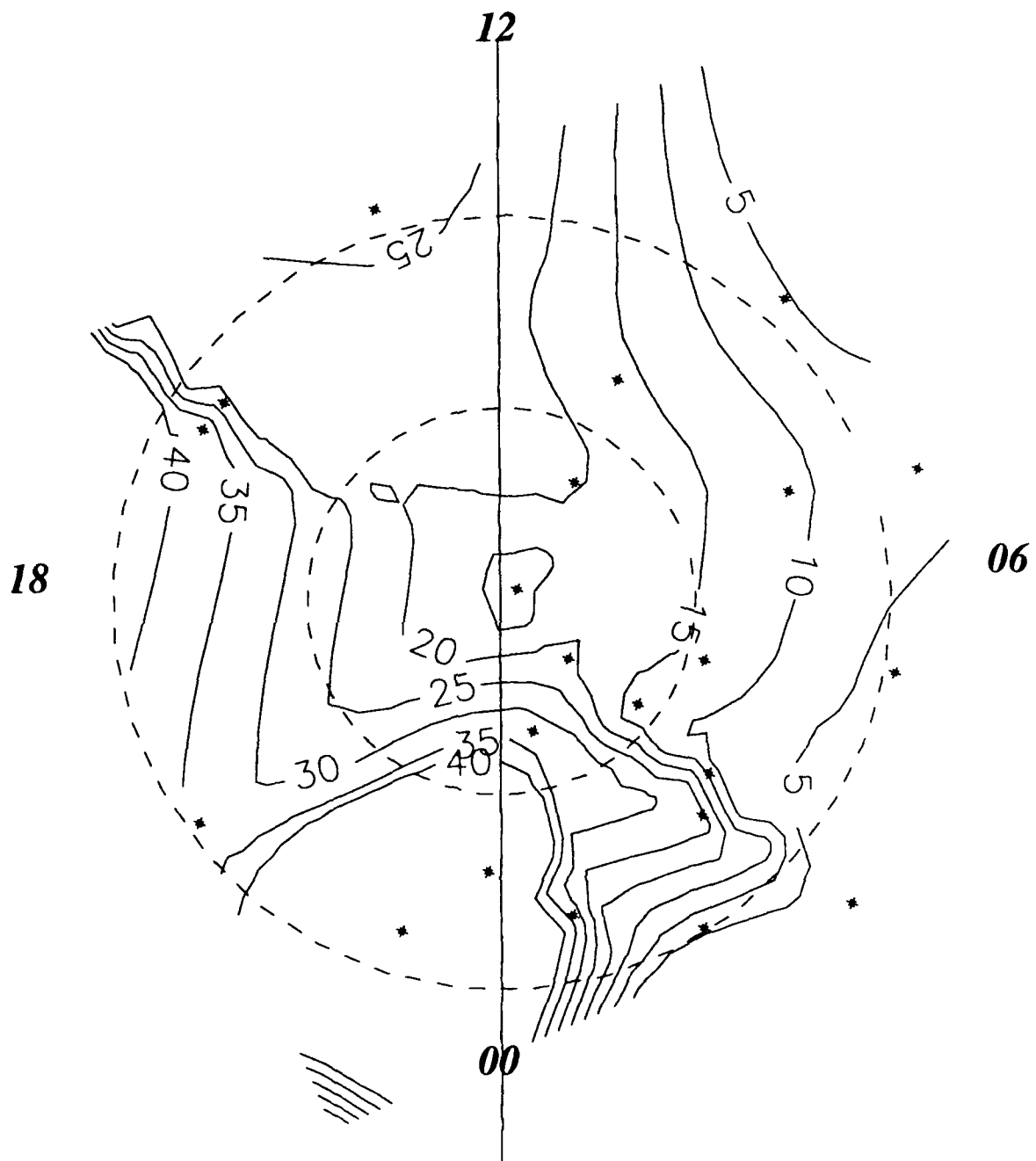


figure 4-7g

Horizontal Magnetic Perturbation at 12:38 UT

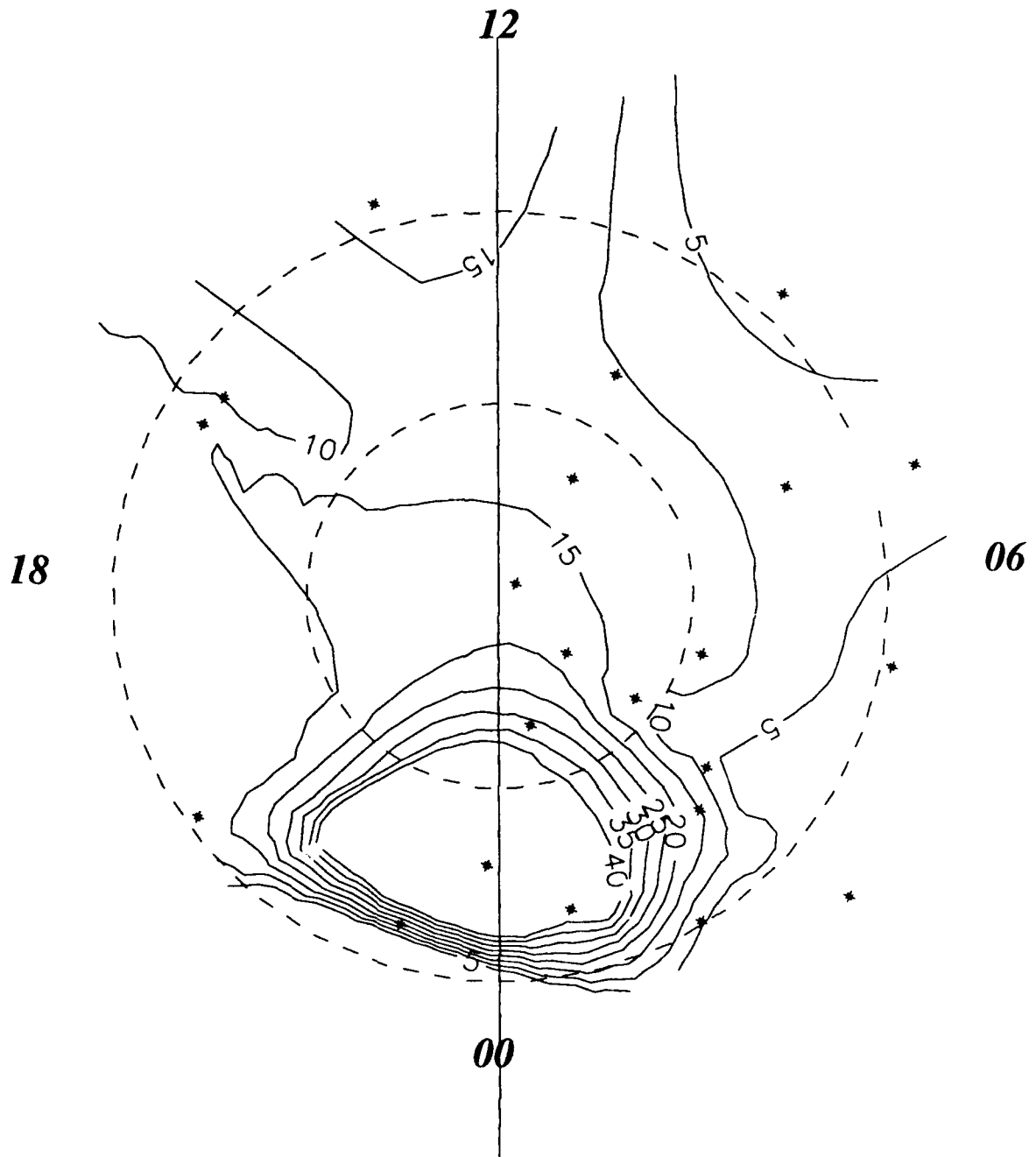


figure 4-7h

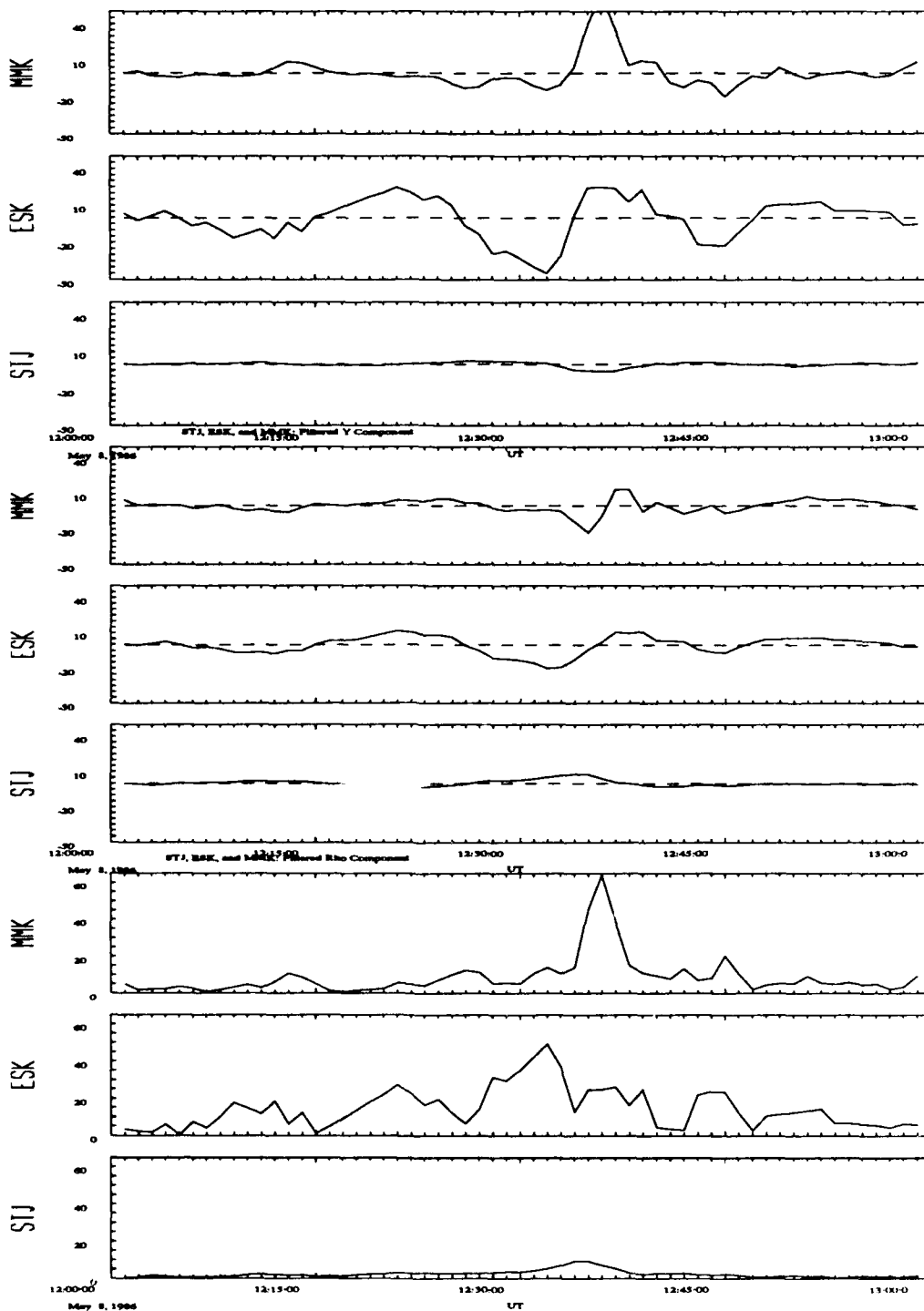


figure 4-8

field perturbations from three stations spanning the dayside hemisphere at nearly the same magnetic latitude: Murmansk (MMK), Eskdalemuir (ESK), and St. Johns (STJ). Cross-correlations of the x and y components of the signal give very different results. We attribute this to the change in phase and shape of these signals between these widely separated stations. There may be some change in the frequency content of the signal seen in the widening of the shape of the largest peaks from east to west. A cross-correlation with the rho component should avoid these problems, and does give a more reasonable result. The signal appears first at ESK, the station closest to noon, at 12:32 UT, then two minutes later 60.68 degrees westward at STJ, then another two minutes later at MMK, 42.36 degrees east of ESK. The shorter transit time (which is over a longer distance) between ESK and STJ appears to indicate that the signal propagates from a location in between these stations. This places the first impulse at noon or just dawnward of the noon meridian. Although not at the same latitude Narsarssuaq (NAQ) is in between STJ and ESK which shows an initial peak at 12:30, supporting the suggestion that the signal originates in the pre-noon sector. Using the eastern pair of stations to compute the signal velocity we get $11^\circ/\text{min}$ or 20 km/s in the ionosphere. This maps to 180 km/s on a magnetopause 9 Re away. This is on the order of typical magnetosheath velocities (200 km/s) and indicates that the magnetopause source may be convecting along the magnetosheath-magnetopause boundary. Figure 4-9 shows a similar set of stack plots from a north-south set of stations near 20° magnetic longitude. The southern most station is STJ, the station at the western end of the east-west cross analyzed above. The stations northward of STJ are Narsarssuaq (NAQ), Godhavn (GDH) and Thule (THL). We expect NAQ and GDH to bracket the polar cap boundary based on the position of the Feldstein oval location given by Whalen (1970). The picture presented by this cross

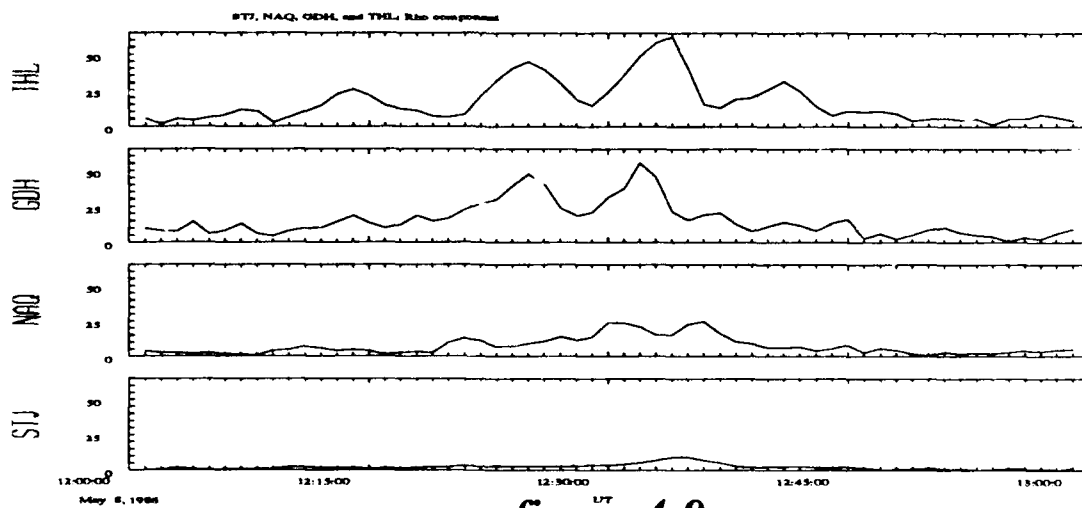
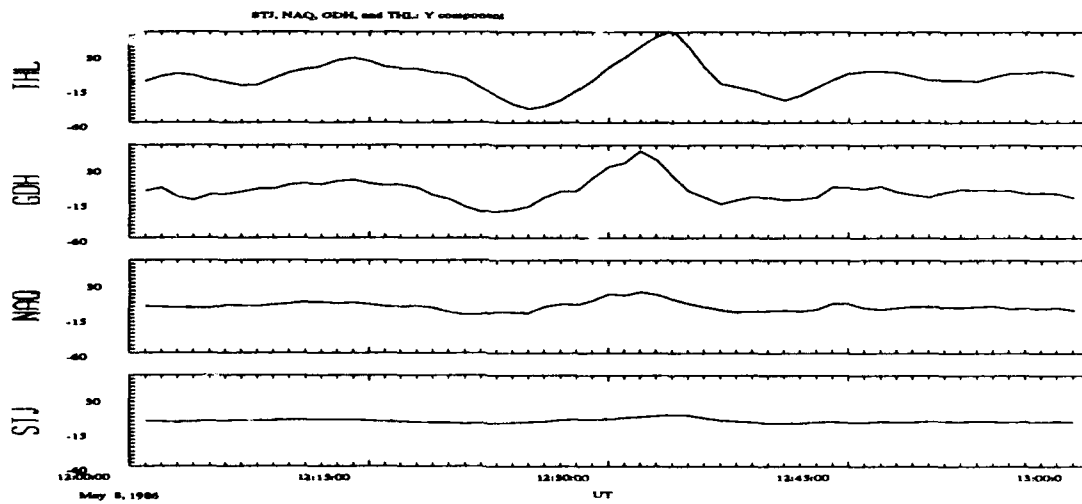
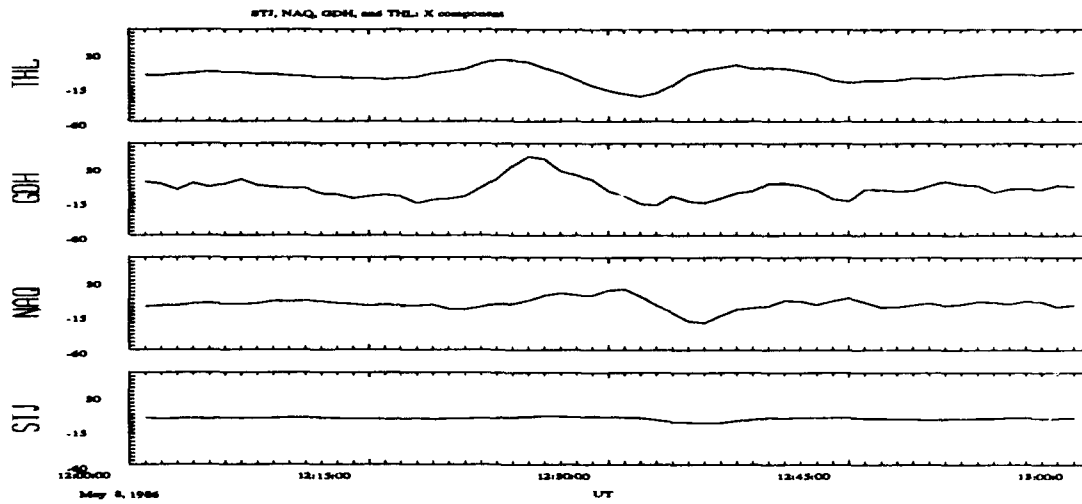


figure 4-9

section has many interesting features. The stations near and poleward of the polar cap boundary exhibit considerable wave activity even prior to the event, probably driven by the substorm in progress. There are several large amplitude peaks coincident with the arrival of the pressure pulse. Although in principle this set of stations could be used to determine the poleward movement of the signal the substorm activity, the possibility of azimuthal movement and the phase perturbations introduced by the ongoing wave activity obscure any useful timing data. It is interesting to note some of the differences between the X and Y components for the various stations. The Y component is largest at the poles, suggesting that it is influenced by the polar cap convection system. The X component amplitude appears largest near the polar cap boundary so it may be responding to a different process. The time between the X and Y peaks increases poleward, which also allows the possibility that these components are responding to different processes

Localized Signal Characteristics

At EISCAT the magnetometers are arranged to track the motions of passing current structures. However, the data in the CDAW data base barely has the resolution needed for our study. The east-west axis of the array spans 5.6° of magnetic longitude. The signal we found globally moving at $11^\circ/\text{minute}$ would pass in only 30 seconds. Correlations in this data set would show a shift of only one data point, which may not be statistically significant. We did the comparisons and found a systematic one data point shift representing 20 seconds, which may be not significant for timing, but does show a consistent tailward motion. It allows us to say that the speed measured with the widely separated stations agrees with the lower limit lower limit detectable with the array (to be confident of our results we would like shifts of at least two data points, 40 seconds, which would imply speeds of $8.4^\circ/\text{min}$ roughly equal to $11^\circ/\text{min}$). Measured delays along the

north-south portion of the array appear more significant. There is a consistent shift of 1 to 2 data points over the 3.5 degrees of latitude spanned by the stations. This does not necessarily imply that the signal source is propagating poleward. The north-south line formed by the stations is inclined to the lines of geomagnetic longitude near the stations. The northern station is 2.6° east of the southern station. If the phase front of the signal is organized as a plane source moving perpendicularly to lines of geomagnetic latitude at $11^\circ/\text{min}$ there would be a 14 second delay from south to north. This means that north-south delays imply similar propagation speeds as the east-west delays, with similar confidence. The stations near EISCAT can be used to look at signal propagation with better temporal resolution. The delay measured across this set of stations runs from 5 to 6 seconds west to east. If we simply divide the distances between stations by the delays we get much higher velocities than we expect, on the order of a degree per second. However, we can make some guesses about the geometries and motions that can reduce the observed velocity. Figure 4-10 shows the best determination of delays we have been able to make. If we assume the signal propagates as a plane source in the direction of its own normal, velocities on the order of 30 km/sec for a front inclined 20° can explain the observations. A plane geometry is an acceptable assumption for some of the largest events of this type observed, up to 2000 km (Glaßmeier, 1989). We expect that taking account of the curved geometry of the system would reduce this calculated velocity. A signal with a smaller inclination would imply a greater azimuthal velocity. There is insufficient data to characterize the orientation of the front but this analysis allows us to emphasize that it is not simple to infer structures or motions from limited observations.

Equivalent Current Signature

The classic phenomenon associated with the propagating impulse is an equivalent

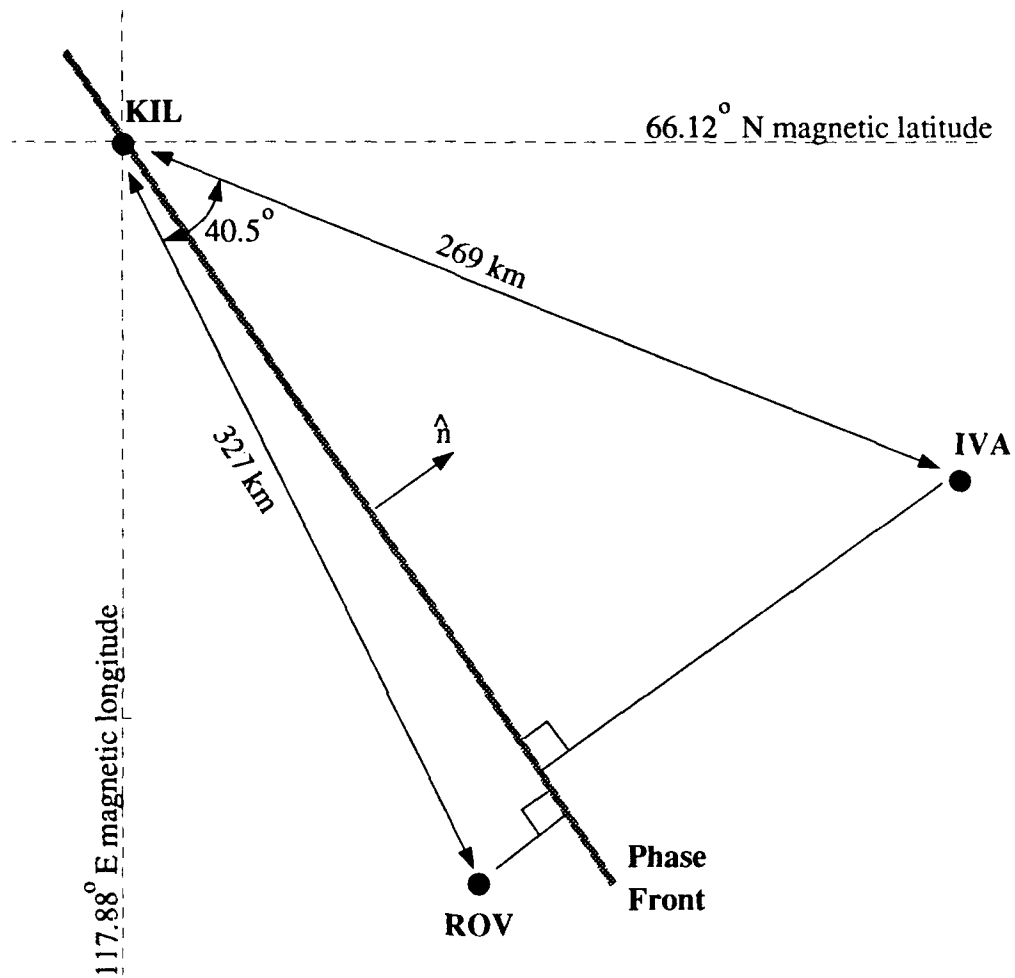


figure 4-10

current vortex. The equivalent current is the form the perturbing current would take if the signal were due solely to ionospheric currents. The equivalent current is usually found by rotating the magnetic perturbation vectors clockwise 90° as viewed from above the ionosphere. If the current structure is stable the change in the current over time can be used to infer the spatial structure of the source. A plot of the equivalent current vectors is shown in figure 4-11. Each column represents the vectors from the five north-south EISCAT stations which span 350 km. The station spacing is not quite as even as it appears in the plot. Each row of vectors is a time series with one vector every twenty seconds. Thus this plot can be viewed as a time series of equivalent current vectors for the five stations that run north-south with time decreasing to the left, or invoking the assumption that a stable structure is convecting eastward over the stations, as an instantaneous spatial distribution of the equivalent current. Having time decrease is required in order to infer the correct spatial structure for a signal *propagating tailward on the dusk hemisphere*. Using an azimuthal velocity of 20 km/s would imply a horizontal spacing between vectors of 400 km. At 12:34 there is a strong poleward current which turns equatorward, then turns poleward again. One can fit an intense counterclockwise vortex to the eastern flow vectors and possibly a more diffuse clockwise vortex to the flow vectors in the west. The signatures that follow the initial vortex could also be waves stimulated by the passage of the FAC. For a velocity of 20 km/s the vortex would have an east-west scale size of 6000 km. The leading vortex would be associated with an upward field-aligned current. The flows seem to be the most intense near the eastward edge. The fact that we are able to make this observation may be because the vortex is being imaged fairly close to noon. We intuitively expect that these sharp current gradients, if they are real, would tend to smooth themselves out as the structure evolves and moves away from noon.

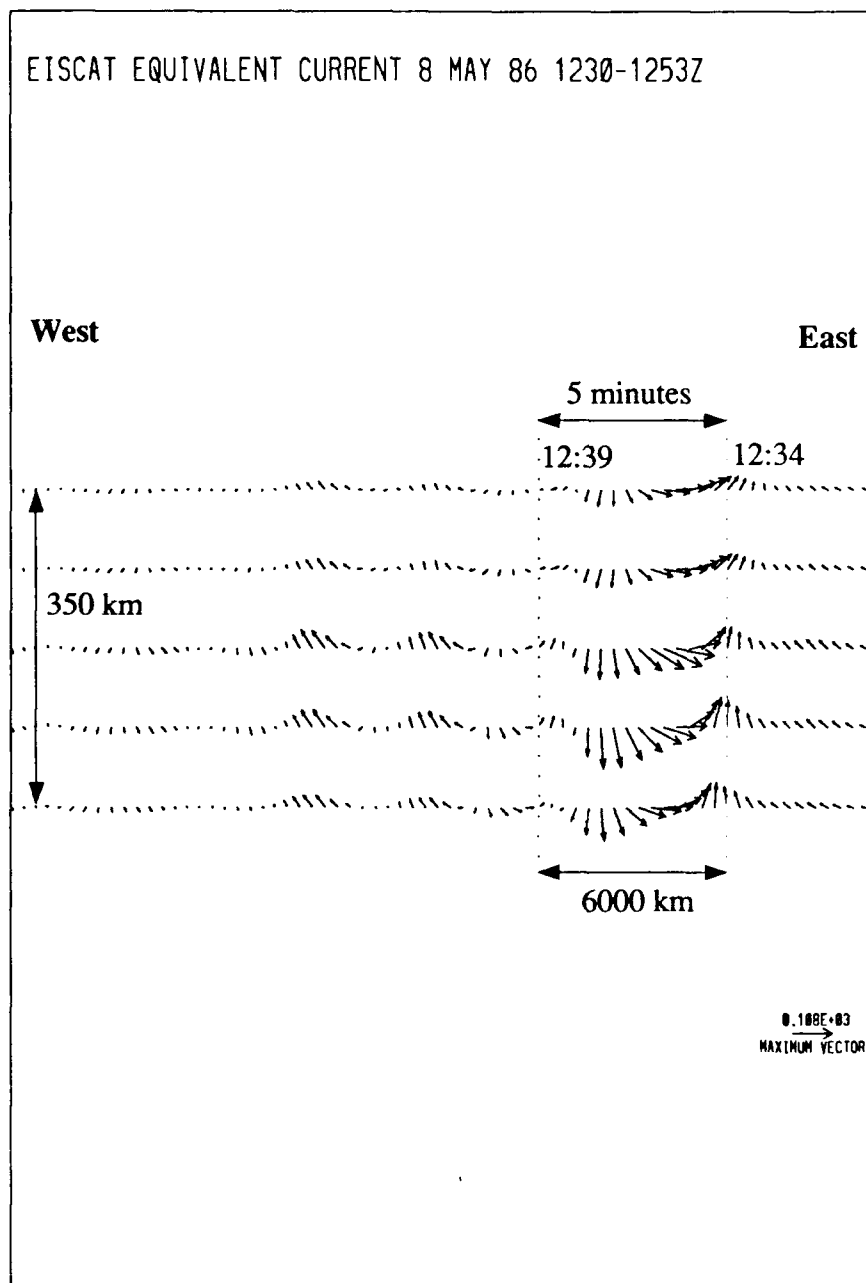


figure 4-11

Chapter 5: Discussion.

Signal Propagation in the Solar Wind

When we established the solar wind to magnetosphere timing we argued that the compressional front must have been aligned with the interplanetary magnetic field. The measured IMF field lies at an angle 165 to the GSM X axis. The first tangent field lines touch the magnetopause at 7 LT. Extrapolating back into the solar wind this field line crosses the X axis 47 Re upstream of the magnetopause nose. This implies that IMP-8 should have detected the signal after SCATHA, not before as observed. The ground data also gives initially conflicting results. In the previous section the ground signal appeared to originate between ESK and STJ, at the noon to pre-noon local times. Using the azimuthal velocity calculated from the dusk stations places the source near 11 LT. These disparities can qualitatively be explained by including the effects of the bow shock and magnetosheath. The bow shock is a fast mode hydromagnetic phenomenon which rotates the field away from the shock normal. The magnetosheath flows also serve to bend the field away from the magnetopause as well as carry the plasma that flows through the shock around the magnetopause. The plasma that flows through the shock well away from noon never reaches the magnetopause, thus it is the plasma penetrating the shock near noon which must be considered when studying the coupling to the magnetosphere. The geometry is shown in figure 5-1 which illustrates how the front may reach the magnetopause near 1100 LT. The general argument should hold for any pressure front that is aligned with the IMF field. Sibeck (1990) discussed fronts aligned with the IMF spiral angle and predicted that they would strike the post-noon magnetopause. We are

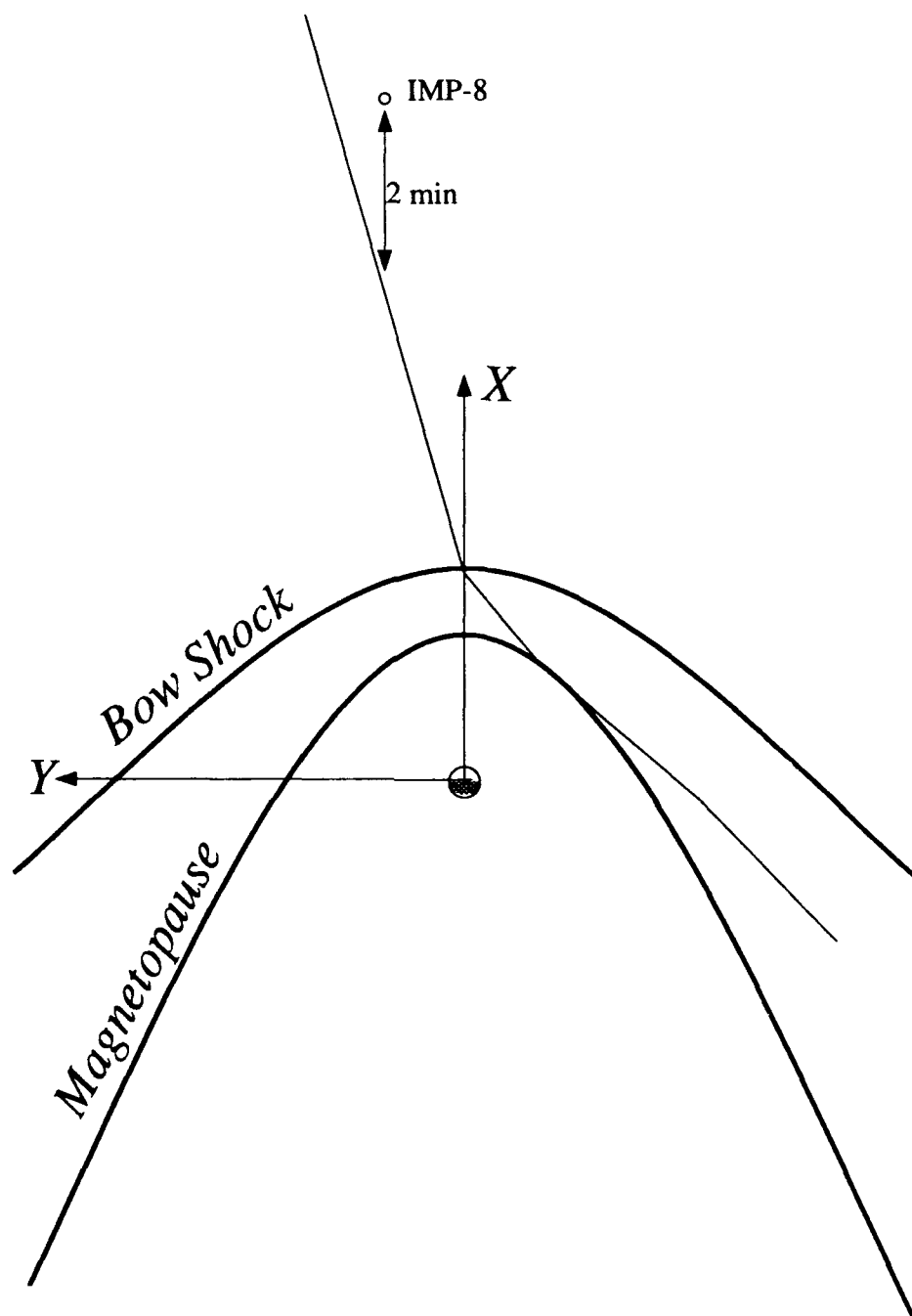


figure 5-1

extending that idea by including the bow shock and thus we predict that fronts aligned with the spiral angle would strike closer to noon than the 1500 LT implied by Sibeck.

Global Characteristics

On the ground the observations show a much greater variety than predicted by the models summarized in chapter 2. There is a wide ranging global response which may involve a variety of processes. At high latitudes the signal falls into at least two groups. The first group is dominated by a low frequency signal with a period near 10 minutes. These signals produce a nearly simultaneous positive excursion in X associated with the SI seen at Huancayo and SCATHA, followed by a reverse impulse approximately 10 minutes later. The reverse impulse in X is associated with a negative impulse in Z at dawn and a positive impulse in Z at dusk. These signals are seen primarily in the morning portion of the dayside hemisphere. The second group has a similar low frequency component but has sharper peaks which indicate that they contain more of the higher frequencies. For these signals the X component has an almost unipolar positive peak, the Y component appears like the second derivative of the X component, and the Z component has a negative peak. These signals are also followed by ringing after the primary peak. We can identify these waves only in the dayside hemisphere; if either of these types of waves extend into the nightside hemisphere they are obscured by the substorm. The dusk/dawn asymmetry noted is not new (Glaßmeier et al., 1989; Glaßmeier and Heppner, 1990; Lanzerotti, 1990b). Especially interesting is Glaßmeier and Heppner's 1990 observation of a similar morphological change in signal characteristics between morning and afternoon hemispheres; however, they observed the sharper signals in the dawn hemisphere. This is especially puzzling since many of the circumstances under which they made their observations are in some ways very similar to ours. The case they studied was associated

with a positive SI, indicating that the source was a compressional pressure pulse. The OMNI data base of one hour average solar wind properties from NSSDC indicates a negative GSM Y component to the solar wind as in the case studied here. One important difference is that the Z component of the IMF was positive in the Glaßmeier and Heppner event. The overall impression is that the sharp peaks may represent a localized enhancement or a separate process embedded in a global magnetospheric response. The long period signals appear to be part of the global response at high latitudes which sets a background pattern to the magnetic perturbations. The theories of sudden magnetic impulses (SIs) observed at low and mid latitudes associated with pressure pulses form an interesting parallel to the processes discussed so far. A positive (compressional) SI is usually observed as a main impulse (MI) in the H component of a low latitude observatory. Some SIs are accompanied by preliminary impulses (PIs) in the opposite sense of the MI, these are designated SI*. The sense of the equivalent current patterns for these signals resemble the dual vortex pattern of the Glaßmeier-Heppner model, but the scale is much larger, covering most of the dayside hemisphere. The convection pattern for a PI associated with a positive SI has the same sense as the Glameier-Heppner pattern. The MI which follows has the opposite sense (Araki, 1977; Glaßmeier and Heppner, 1990). Tamao (1964) has published a theory specifically trying to explain the PI signal in terms of dual convection vortices due to FACs coupled to the compression of the magnetopause. Changes in the polar cap electric field transmitted to low latitudes (Kituchi and Araki, 1979) has also been used to explain these current systems. The local time differences could be a result of station biases. The dusk sector stations are clustered near a small range of latitudes which are not well covered by the stations in the dawn sector. The Glameier and Heppner 1990 paper shows a concentration of stations in the

dawn sector where they located the sharper signal and very few stations in the dusk sector. The stations where they were able to resolve the convection vortices were very close to EISCAT latitudes. This suggests two explanations of the observed asymmetry. Possibly the local time variations are real and the signal differences imply that the propagation path or the source has a dusk-dawn asymmetry. Asymmetries in the propagation path could be a result of local conductivity differences or variations in the magnetospheric plasma distribution. Alternatively, the sharp perturbations are present in both dawn and dusk sectors but they are very limited in latitude and are only seen if the station locations are sufficiently close to the appropriate latitude. In this study we have not been able to examine these possibilities in detail. We will discuss these features in the context of the processes we have discussed so far and try to define the relationship between the pressure pulse and the observed signal. It is difficult to imagine a pressure pulse being structured such as to produce a significant dawn-dusk asymmetry. If an additional process is involved it is extremely likely that it is causally linked to the pressure pulse. An FTE coincident with, perhaps triggered by, the pressure pulse might be detected as an embedded signal in the background. An FTE would be associated with a smaller scale footprint in the ionosphere, and perhaps a sharper ground magnetic perturbation. An FTE would only appear at dusk in the northern hemisphere for $B_y < 0$ as shown in figure 2-9. The direction of the field-aligned current inferred from the equivalent current signature, upward, matches the direction we would expect from an FTE. However, the signal observed at EISCAT is larger, moving faster, and in the wrong direction from what we would anticipate for an FTE. The case for an FTE effect in the Glameier and Heppner report is even less likely because of the positive B_z . Also in that case the negative IMF B_y would result in a FTE on the dusk side in the northern hemisphere,

not the dawn hemisphere where the second type of signal was seen. If the dusk-dawn discrepancy is not real it follows that the high frequency signal is highly localized in latitude so that it is not detected on the dawn side. The degree to which a pressure pulse generated signal is localized in latitude should be related to the displacement of the magnetopause and its mapping to the ionosphere. For the parameters observed, the magnetopause stand-off distance moved from 9.4 to 8.6 Re when it encountered the solar wind density enhancement. If we consider the simple case of a dipole field the latitudinal range, $\Delta\theta$, for a given change in L shells (ΔL) is given by:

$$\Delta\theta \approx (\cos^3 \theta_o \Delta L) / (2 \sin \theta_o)$$

where θ_o is the invariant latitude. For EISCAT near 65° and $\Delta L \approx 0.8$, $\Delta\theta \approx 4.0^\circ$. Only one dusk side station is well positioned near EISCAT latitudes for seeing the signal, Post-de-la-Baleine (PDB), near 0730 LT, ~4.5 hours before 11 LT (where we placed the signal's origin) compared to ~4 hours after for EISCAT. However, the signal there was not like the one seen at EISCAT, supporting the idea that the dawn dusk symmetry is real. Another process for producing localized signals is field line resonances. The mechanism for FAC generation discussed by Southwood and Kivelson (1990) explicitly invokes field line resonances to produce localized signatures that are expected to move azimuthally in concert with the displacement of the magnetopause. Field line resonances are toroidal mode Alfvén waves which result in enhancements of the perturbation field on the ground primarily in the H direction as observed. It is not known if the source has sufficient power and if the coupling to field line resonances is efficient enough to produce the enhancements seen. There must be some damping mechanism to widen the resonant peak so that it can be observed over the wide range of L-shells as observed. The magnitude of damping required may not exist for field lines terminating in the highly

conducting ionosphere on the dayside hemisphere. Both of these effects on the ground would also be modulated by variations in the propagation path discussed above and in combination with these could explain the east-west asymmetries.

Measured Velocity

In light of this discussion we need to reevaluate our understanding of the velocities derived for the signal. If the signals like those at EISCAT are due to an independent source embedded in the pressure pulse then we cannot interpret the delay between ESK and MMK until we specify what the source is. If the second class of signals represents an enhancement or resonance then the timing is fairly sound. The velocities computed here are some of the highest reported for dayside magnetic impulse events.

Summary of Models versus Observations

Table 5-1 is a list of the vortex characteristics seen at EISCAT and shows how these observations compare to the models discussed. It is obvious that no one model completely satisfies the observations. The FAC associated with the EISCAT vortex has the wrong sense for a pressure pulse driven system. The scale and speed of the disturbance would seem to rule out FTEs. The fact that only a single vortex was seen does not unambiguously rule out the existence of a nearby, but unobserved second vortex of a twin vortex system. For a tailward moving FTE the Southwood theory would place a second, downward FAC poleward of the upward FAC. This could reasonably explain why the second vortex was missed. In the Kivelson-Southwood pressure pulse model a downward FAC should have proceeded the upward current. Because the trailing (upward) FAC originates in the compressed section of the magnetosphere and would map to lower latitudes in the ionosphere placing the "missing" vortex slightly poleward of the upward current (Kivelson, private communication). Because the Kivelson-Southwood picture

would place the second vortex ahead of the observed signal the correlation with the solar-wind would have to be reevaluated.

TABLE 5-1: Summary of model characteristics in the post-noon section of the northern hemisphere compared to observations.

A positive pressure pulse and negative IMF By have been assumed where relevant.

| Model - Characteristic: | <u>Observation</u> | <u>SLF</u> | <u>SF</u> | <u>GHP</u> | <u>KSP</u> |
|----------------------------|--------------------|--------------------------|--------------------------|--------------------------|------------------------|
| Speed | 20 km/s | Strongly Inconsistent | Strongly Inconsistent | Consistent | Consistent |
| Direction | Tailward | Inconsistent | Inconsistent | Strongly Consistent | Strongly Consistent |
| Scale Sizes | ~6000 km | Strongly Inconsistent | Strongly Inconsistent | Consistent | Consistent |
| Local Flow Pattern | Monopolar | Consistent | Inconsistent | Consistent | Inconsistent |
| Sense of FAC System | Upward | Strongly Inconsistent | Inconsistent | Strongly Inconsistent | Inconsistent |

Table of expected characteristics predicted for Saunders-Lee FTE model (SLF), Southwood FTE model (SF), Glaßmeier-Heppner pressure pulse (GHP), and Kivelson-Southwood pressure pulse (KSP) compared to the observations.

Chapter 6: Conclusions.

In this study we identified a magnetic impulse event seen in the CDAW-9 multipoint, multi-instrument data set. The magnetic impulse signal coincided with a large pressure increase in the solar wind which occurred during an interval of southward IMF Bz. Because of the size of the pressure change and the wide range of data available we felt we could identify the effects directly related to the solar wind, even though there was a substorm in progress at that time. In the first part of our analysis we concentrated on timing the signal as it moved from the solar wind to the magnetosphere and across the ground. Examination of the signal propagation clearly supported the idea that the pressure increase was related to the processes responsible for the ground magnetic impulse. We then used data from the EISCAT magnetometer array and nearby high-resolution stations to further clarify the signals speed, direction, and structure. The goal of the second part of the analysis was to compare these results with theoretical predictions of ground signatures produced by pressure perturbations and FTEs.

The ground observations reflect the presence of a single, fast-moving, vortical disturbance in the ionosphere associated with an upward field aligned current. This sharp signal with a timescale ≈ 3 minutes appeared to be embedded in a global signal with a rise time on the order of 10 minutes, similar to the rise time seen in the solar wind. The east-west scale of the localized disturbance was on the order of 6000 km. This picture disagrees with some aspect of every model. The scale size and speed of the disturbance rules out FTEs and the FAC associated with the EISCAT vortex has the wrong sense or structure for a pressure enhancement driven system. However, we are not willing to completely rule out any model. The literature is full of suggestions for extending

various models to more realistic magnetospheric conditions. One example is to improve the magnetic field mapping (Crooker and Siscoe, 1990; Crooker, 1990) to determine the scale sizes and shapes of the ionospheric footprints. The kind of modifications that have been suggested could explain how a Southwood FTE might produce a signature such as the one observed by elongating the footprint and sweeping it azimuthally around the polar cap.

We believe we have shown in the detailed analysis of a single event that the processes coupling the disturbances at the magnetopause to the ionosphere are more complicated than suggested by any of the models. We showed that the various signatures seem well correlated with a single cause, a change in the solar wind dynamic pressure. However, we were unable to prove that the ground signature was due solely to the pressure perturbation despite the clear signature of a step like dynamic pressure increase in the solar wind. The ground response may have been obscured by reconnection driven processes associated with the southward IMF B_z . Another possibility is that our understanding of these signals or the analysis may need careful revision. Although the observations are inconsistent with the models, the two which produce dipolar signatures could conceivably explain the results if we assume we missed part of the signature because of the extended spatial structure of the FAC system and the limited station coverage.

We feel that this study contributes to the motivation to pursue a better theoretical framework and to collect more detailed observations in order to understand the nature of magnetic impulse events and in turn learn more about the nature of solar-wind to magnetospheric coupling. In particular we see a strong need to understand the mapping of various field aligned current sources to the ionosphere and the dynamics and evolution of the ionospheric flows. In particular, it would be worthwhile to assemble a data set

for a similar study that occurs during northward IMF Bz. Such data, coupled with more comprehensive spatial and temporal data on the global distribution of the perturbations may, enable us to develop theories which would allow us to link these signals to specific driving mechanisms.

BIBLIOGRAPHY

Araki, T., "Global structure of geomagnetic sudden commencements," Planetary and Space Science, vol. 25, pp. 373-384, 1977.

Bering, E., J. R. Benbrook, G. J. Byrne, B. Liao, J. R. Theall, L. J. Lanzerotti, C. G. MacLennan, A. Wolfe, and G. L. Siscoe, "Impulsive electric and magnetic field perturbations observed over South Pole: Flux Transfer Events?", Geophysical Research Letters, vol. 15, pp. 1545-1548, 1988.

Bering, E. A., L. J. Lanzerotti, J. R. Benbrook, Z. M. Lin, C. G. MacLennan, A. Wolfe, R. E. Lopez, and E. Friis-Christensen, "Solar wind properties observed during high-latitude impulsive perturbation events," Geophysical Research Letters, vol. 17, pp. 579-582, 1990.

Cowley, S. W. H., "The causes of convection in the Earth's magnetosphere: A review of developments during the IMS," Reviews of Geophysics and Space Physics, vol. 20, pp. 531-565, 1982.

Cowley, S. W. H., "Evidence for the occurrence and importance of reconnection between the Earth's magnetic field and the interplanetary magnetic field," in Magnetic Reconnection in Space and Laboratory Plasmas, ed. E. W. Hones, Jr., Geophysical Monograph Series, vol. 30, pp. 375-378, AGU, Washington, D. C., 1984.

Crooker, N. U., "Flux Transfer Event footprint patterns and implications for convection," Journal of Geophysical Research, vol. 95, pp. 10567-10573, 1990.

Crooker, N. U. and G. L. Siscoe, "On mapping flux transfer events to the ionosphere," Journal of Geophysical Research, vol. 95, pp. 3795-3799, 1990.

Dungey, J. W., "Interplanetary magnetic field and the auroral zones," Physics Review Letters, vol. 6, p. 47, 1961.

Elphic, R., "Multipoint observation of the magnetopause: Results from ISEE and AMPTE," Advances in Space Research, vol. 8, no. 9, pp. 223-238, 1988.

Baumjohann, W., G. Paschmann, H. Luhr, and D. Sibeck, "Upstream pressure variations associated with the bow shock and their effects on the magnetosphere," Journal

of Geophysical Research, vol. 95, pp. 3773-3786, 1990.

Farrugia, C., R. Rijnbeek, M. Saunders, D. Southwood, D. Rodgers, M. Smith, C. Chaloner, D. Hall, P. Christiansen, and L. Woolliscroft, "A multi-instrument study of Flux Transfer Event structure," Journal of Geophysical Research, vol. 93, pp. 14465-14477, 1988.

Farrugia, C., M. Freeman, S. Cowley, D. Southwood, M. Lockwood, and A. Etemadi, "Pressure-driven magnetopause motions and attendant response on the ground," Planetary Space Science, vol. 37, pp. 589-607, 1989.

Friis-Christensen, E., M. McHenry, C. Clauer, and S. Vennerstrom, "Ionospheric traveling convection vortices observed near the polar cleft: A triggered response to sudden changes in the solar wind," Geophysical Research Letters, vol. 15, pp. 253-256, 1988a.

Friis-Christensen, E., S. Vennerstrom, C. Clauer, and M. McHenry, "Irregular magnetic pulsations in the polar cleft caused by traveling ionospheric convection vortices," Adv. Space Research, vol. 8, pp. 311-314, 1988b.

Glaßmeier, K. H., "Reconstruction of the ionospheric influence on ground-based observations of a short-duration ULF pulsation event," Planetary and Space Sciences, vol. 36, pp. 801-817, 1988.

Glaßmeier, K., M. Honisch, and J. Untiedt, "Ground-based and satellite observations of traveling magnetospheric convection twin vortices," Journal of Geophysical Research, vol. 94, pp. 2520-2528, 1989.

Glaßmeier, K. and C. Heppner, "Traveling magnetospheric convection twin-vortices: Another case study, global characteristics, and a model," Journal of Geophysical Research, 1990. in press

Goertz, C. K., E. Nielsen, A. Korth, K. H. Glaßmeier, C. Haldoupis, P. Hoeg, and D. Hayward, "Observations of a possible ground signature of Flux Transfer Events," Journal of Geophysical Research, vol. 90, pp. 4069-4078, 1985.

Hargraves, J. K., The Upper Atmosphere and Solar-Terrestrial Relations, p. 48, Van Nostrand Reinhold Company Ltd, New York, 1979.

Kikuchi, T. and T. Araki, "Horizontal transmission of the polar electric field to the equator," Journal of Atmospheric and Terrestrial Physics, vol. 41, pp. 927-936, 1979.

Kivelson, M. and D. Southwood, "Ionospheric traveling vortex generation by solar wind buffeting of the magnetosphere," Journal of Geophysical Research, vol. 96, pp. 1661-1667, 1991a.

Kivelson, M. and D. Southwood, "Ionospheric signatures of localized magnetospheric perturbations," Journal of Geomagnetism and Geoelectricity, in press, 1991b..

Kivelson, M. G., Pulsations and magnetohydrodynamic waves, chapter 13 of the 1990 Rubey Colloquium, unpublished manuscript, 1991.

Lanzerotti, L., L. Lee, C. MacLennan, A. Wolfe, and L. Medford, "Possible evidence of Flux Transfer Events in the polar ionosphere," Geophysical Research Letters, vol. 13, pp. 1089-1092, 1986.

Lanzerotti, L., "Ionosphere and ground-based response to field aligned currents near the magnetospheric cusp regions," Journal of Geophysical Research, vol. 92, pp. 7739-7743, 1987.

Lanzerotti, L., "Conjugate spacecraft and ground-based studies of hydromagnetic phenomenon near the magnetopause," Adv. Space Research, vol. 8, pp. 301-310, 1988.

Lanzerotti, L. J., "Comment on 'Solar wind dynamic pressure variations and transient magnetospheric signatures'", Geophysical Research Letters, vol. 16, pp. 1197-1199, 1989.

Lanzerotti, L. J. and C. G. MacLennan, "Hydromagnetic waves associated with possible Flux Transfer Events," Astrophysics and Space Science, vol. 144, pp. 279-290, 1988.

Lanzerotti, L. J., R. M. Konik, A. Wolfe, D. Venkatesan, and C. G. MacLennan, "Cusp-Latitude Magnetic Impulse Events, 1. Occurrence Statistics," unpublished manuscript, 1990.

Lee, L., "Magnetic flux transfer at the Earth's magnetopause," in Solar Wind-Magnetosphere Coupling, pp. 297-314, 1986.

Lee, L. C. and Z. F. Fu, "Simulation of multiple X-line reconnection at the dayside magnetopause," Geophysical Research Letters, 1985.

Lockwood, M. and S. Cowley, "Observations at the magnetopause and in the auroral ionosphere of momentum transfer from the solar wind," Adv. Space Research, vol. 8, pp. 281-299, 1988.

Lockwood, M., P. E. Sandholt, and S. W. H. Cowley, "Dayside auroral activity and magnetic flux transfer from the solar wind," Geophysical Research Letters, vol. 16, pp. 33-36, 1989.

McHenry, M. and C. Clauer, "Modeled ground magnetic signatures of Flux Transfer Events," Journal of Geophysical Research, vol. 92, pp. 11231-11240, 1987.

McHenry, M., C. Clauer, E. Friis-Christensen, and J. Kelly, "Observations of ionospheric convection vortices: Signatures of momentum transfer," Adv. Space Research, vol. 8, pp. 315-320, 1988.

McHenry, M. A., C. R. Clauer, E. Friis-Christensen, P. T. Newell, and J. D. Kelly, "Ground Observations of Magnetospheric Boundary Layer Phenomena," Journal of Geophysical Research, vol. 95, pp. 14995-15005, 1990.

Mende, S. and R. Rairden, "Magnetic impulses and associated optical signatures in the dayside aurora," Geophysical Research Letters, vol. 17, pp. 131-134, 1990.

Moore, T. E., D. L. Gallagher, J. L. Horwitz, and R. H. Comfort, "MHD wave breaking in the outer plasmasphere," Geophysical Research Letters, vol. 14, pp. 1007-1010, 1987.

Nishida, A., Geomagnetic Diagnosis of the Magnetosphere, Springer Verlag, New York, 1979.

Russell, C. T. and R. C. Elphic, "Initial ISEE magnetometer results: Magnetopause observations," Space Science Reviews, vol. 22, pp. 681-715, 1978.

Russell, C. T. and R. C. Elphic, "ISEE observations of Flux Transfer Events at the dayside magnetopause," Geophysical Research Letters, vol. 6, pp. 33-36, 1979.

Russell, C. T., "Reconnection at the Earth's magnetopause: Magnetic field observations and Flux Transfer Events," in Magnetic Reconnection in Space and Laboratory

Plasmas, ed. E. W. Hones, Jr., Geophysical Monograph Series, vol. 30, pp. 124-138, AGU, Washington, D. C., 1984.

Sandholt, P. E., C. S. Deehr, A. Egeland, B. Lybekk, R. Viereck, and G. J. Romick, "Signatures in the dayside aurora of plasma transfer from the magnetosheath," Journal of Geophysical Research, vol. 91, pp. 10063-10079, 1986.

Saunders, M. A., C. T. Russell, and N. Sckopke, "Flux Transfer Events: Scale size and interior structure," Geophysical Research Letters, vol. 11, pp. 131-134, 1984.

Scholer, Manfred, "Magnetic flux transfer at the magnetopause based on single x line bursty reconnection," Geophysical Research Letters, vol. 15, pp. 291-294, 1988.

Sibeck, D., W. Baumjohann, and R. Lopez, "Solar wind dynamic pressure variations and transient magnetospheric signatures," Geophysical Research Letters, vol. 16, pp. 13-16, 1989a.

Sibeck, D., W. Baumjohann, and R. Lopez, "Reply," Geophysical Research Letters, vol. 16, pp. 1200-1202, 1989b.

Sibeck, D., W. Baumjohann, R. Elphic, D. Fairfield, J. Fennel, W. Gail, L. Lanzerotti, R. Lopez, H. Luehr, A. Lui, C. MacLennan, R. McEntire, T. Potemera, T. Rosenberg, K. Takhashi, "The magnetospheric response to 8-minute period strong-amplitude upstream pressure variations," Journal of Geophysical Research, vol. 94, pp. 2505-2519, 1989c.

Sibeck, D. G., "A model for the transient magnetospheric response to sudden solar wind dynamic pressure variations," Journal of Geophysical Research, vol. 95, pp. 3755-3771, 1990.

Sonnerup, B. U. O., "On the stress balance in Flux Transfer Events," Journal of Geophysical Research, vol. 92, pp. 8613-8620, 1987.

Southwood, D. J., "Theoretical aspects of ionosphere-magnetosphere-solar wind coupling," Advances in Space Research, vol. 5, no. 4, pp. 7-14, 1985.

Southwood, D. J., "The ionospheric signature of Flux Transfer Events," Journal of Geophysical Research, vol. 92, pp. 3207-3213, 1987.

Southwood, D. and M. Kivelson, "The magnetohydrodynamic response of the magnetospheric cavity to changes in solar wind pressure," Journal of Geophysical Research,

vol. 95, pp. 2301-2309, 1990.

Southwood, D. J. and W. J. Hughes, "Theory of hydromagnetic waves in the magnetosphere," Space Science Reviews, vol. 30, pp. 301-366, 1983.

Southwood, D. J., C. J. Farrugia, and M. A. Saunders, "What are Flux Transfer Events?," Planetary and Space Sciences, vol. 36, pp. 503-508, 1988.

Tamao, T., "A hydromagnetic interpretation of a geomagnetic SSC," Rep. Ionospheric and Space Res. Japan, vol. 18, pp. 16-31, 1964.

Todd, H., B. J. I. Bromage, S. W. H. Cowley, M. Lockwood, A. P. van Eyken, and D. M. Willis, "EISCAT observations of bursts of rapid flow in the high latitude dayside ionosphere," Geophysical Research Letters, vol. 13, pp. 909-912, 1986.

Tsyganenko, N. A., "A magnetospheric magnetic field model with a warped tail current sheet," Planetary and Space Science, vol. 37, pp. 5-20, 1989.

Whalen, J. A., Auroral oval plotter and Nomagram for determining corrected geomagnetic local time, latitude, and longitude for high latitudes in the northern hemisphere, AFCRL-70-0422, 1970.

From: Capt Michael D. Krajnak
8065 Trefoil Ct.
Colorado Springs, CO 80920

14 March 1991

Reply to
attn of: Capt Krajnak

Subject: Thesis

To: AFIT/CIR

IAW AFITR 53-1 para 7-8, I am forwarding one unbound copy of my thesis to your office. If you have any questions I can be reached at my new home phone number (719) 598-4405 or by contacting Maj Kernigan at Det 7, 4WW.



MICHAEL D. KRAJNAK, Capt, USAF

1 Attch.
Thesis